FILLING OUT MISSING DAILY STREAMFLOW DATA USING FUZZY RULE-BASED MODELS

A THESIS SUBMITTED TO
THE GRADUATE SCHOOL OF NATURAL AND APPLIED SCIENCES
OF
MIDDLE EAST TECHNICAL UNIVERSITY

BY

ÖMER BURAK AKGÜN

IN PARTIAL FULFILLMENT OF THE REQUIREMENTS
FOR
THE DEGREE OF MASTER OF SCIENCE
IN
CIVIL ENGINEERING

JUNE 2020

Approval of the thesis:

FILLING OUT MISSING DAILY STREAMFLOW DATA USING FUZZY RULE-BASED MODELS

submitted by **ÖMER BURAK AKGÜN** in partial fulfillment of the requirements for the degree of **Master of Science** i**n Civil Engineering, Middle East Technical University** by,

Prof. Dr. Halil Kalıpçılar
Dean, Graduate School of **Natural and Applied Sciences** _____

Prof. Dr. Ahmet Türer
Head of the Department, **Civil Engineering** _____

Prof. Dr. Elçin Kentel Erdoğan
Supervisor, **Civil Engineering, METU** _____

Examining Committee Members:

Prof. Dr. İsmail Yücel
Civil Engineering, METU _____

Prof. Dr. Elçin Kentel Erdoğan
Civil Engineering, METU _____

Prof. Dr. Mustafa Tamer Ayvaz
Civil Engineering, Pamukkale University _____

Asst. Prof. Dr. Gülizar Özyurt Tarakcıoğlu
Civil Engineering, METU _____

Assoc. Prof. Dr. M. Tuğrul Yılmaz
Civil Engineering, METU _____

Date: 29.06.2020

I hereby declare that all information in this document has been obtained and presented in accordance with academic rules and ethical conduct. I also declare that, as required by these rules and conduct, I have fully cited and referenced all material and results that are not original to this work.

Name, Last name : Ömer Burak Akgün

Signature :

ABSTRACT

FILLING OUT MISSING DAILY STREAMFLOW DATA USING FUZZY RULE-BASED MODELS

Akgün, Ömer Burak
Master of Science, Civil Engineering
Supervisor : Prof. Dr. Elçin Kentel Erdoğan

June 2020, 118 pages

Daily streamflow observations are used for many purposes including analysis of current water-resources conditions in a basin, development of water-resources planning and management strategies and climate change adaptation measures. Streamgages are used to collect streamflow data; however, many streamgages suffer from a common problem: data-gaps. In this study, a Takagi-Sugeno Fuzzy Rule-Based (TS_FRB) Model that uses Subtractive Clustering (SC) for rule generation is developed to fill out missing daily streamflow data due to a streamgage becoming inoperative for a long period. Fuzzy Rule-Based (FRB) model uses only daily streamflow data of neighboring streamgages, thus is very advantageous in terms of data requirement. Ergene Basin, Turkey is used as the case study and FRB models are developed to fill out missing daily streamflow data at four streamgages found in this basin. Numerous models are built to investigate the effect of the SC parameters (i.e., the number of cluster centers and the cluster radius) by which the rule-base of the FRB is identified, and the number of input variables on the performance of the models. Small cluster radius results in similar fuzzy rules to be devised, which

reveals the needs for more rules. On the other hand, as the number of cluster centers increases, the risk of overfitting increases. Thus, selection of the best cluster radius and number of cluster centers combination is a challenging task and requires a trial-and-error procedure. FRB models developed in this study provides good and robust (NSE values around 0.67) estimations for the closely spaced streamgages located on the same tributary. On the other hand, FRB model performance is poor for the streamgage that is located far away from its neighboring streamgages and for the streamgage that is located on a different tributary than its neighbors. Moreover, anthropogenic effects in the Ergene Basin, makes the training of the FRB challenging and influences the model performance negatively.

Keywords: Subtractive Clustering, Takagi-Sugeno Fuzzy Rule-Based Models, Missing Data, Infilling, Daily Streamflow

ÖZ

GÜNLÜK AKIM VERİLERİNDEKİ EKSİKLİKLERİ KURAL TEMELLİ BULANIK MANTIK MODELLERİ KULLANARAK TAMAMLAMA

Akgün, Ömer Burak
Yüksek Lisans, İnşaat Mühendisliği
Tez Yöneticisi: Prof. Dr. Elçin Kentel Erdoğan

Haziran 2020, 118 sayfa

Günlük akım tahminleri, havzalardaki su kaynaklarının mevcut durumlarının analizinde, su kaynakları planlama ve yönetim stratejileri geliştirilmesinde ve iklim değişikliği ile mücadele çalışmaları gibi birçok alanda kullanılır. Akım verilerindeki eksiklikler birçok akım gözlem istasyonunda (AGİ) karşılaşılan genel bir problemdir. Bu çalışmada, günlük akım verilerinde, AGİ'lerin aktif olmaması nedeniyle oluşan uzun boşlukları tamamlamak için, Eksiltmeli Kümeleme (EK) ile kuralları belirlenmiş Takagi-Sugeno tipi Kural Temelli Bulanık Mantık (TS_KTBM) modelleri geliştirilmiştir. Kural Temelli Bulanık Mantık (KTBM) modeli yalnızca komşu AGİ'lerde ölçülen günlük akım değerlerini kullandığı için veri gereksinimi açısından oldukça avantajlıdır. Çalışma sahası olarak Ergene Havzası seçilmiştir ve bu havzada bulunan dört AGİ için verilerdeki boşluklar doldurulmuştur. Girdi parametrelerinin miktarının ve EK parametrelerinin (küme merkezi sayısı ve küme yarıçapı) – KTBM modelinin kural temeli bu parametreler kullanılarak oluşturulur- model performansındaki etkilerini araştırmak amacıyla pek çok model kurulmuştur. Küçük küme yarıçapları birbirine yakın küme merkezlerinin seçilmesine sebep olacağı için, ihtiyaç duyulan bulanık kural sayısını artırır. Öte yandan küme merkezi sayısı arttıkça, modelin fazla eğitilme riski de artar. Bu yüzden en iyi küme merkezi

sayısı ve küme yarıçapı kombinasyonunun seçilimi zorlu bir işlemdir ve deneme-yanılma yöntemi gerektirir. Birbirine yakın ve aynı kollardaki AGİ'lerde KTBM modeli iyi ve tutarlı tahminler (0.67 civarında NSE değerleri) sağlarken, komşularıyla farklı kollarda ve birbirinden uzakta bulunan AGİ'ler için KTBM modeli kötü performans sergilemiştir. Bunun yanısıra, Ergene Havzası'ndaki insan kaynaklı etkiler, KTBM modelinin eğitilmesini zorlaştırmış ve modelin performansını kötü etkilemiştir.

Anahtar Kelimeler: Eksiltmeli Kümeleme, Takagi-Sugeno Tipi Kural Temeli Bulanık Mantık Modelleri, Eksik Veri, Tamamlama, Günlük Akım

To the Mother Earth,

ACKNOWLEDGEMENTS

I would like to express my deepest gratitude to my supervisor Dr. Elçin Kentel for her wisdom and patience. She taught me a lot. The main reason that I stayed motivated throughout this thesis study is her endless support.

I would like to thank my mother Safiye Akgün, my father Atalay Akgün and my sister Firdevs Elif Akgün for their unconditional love and endless support through my entire life.

I would like to thank to Özge Akkoç Hanım for her presence, to Enis Oğuzhan Eren for our "happy" breakfast, to Merve Aygenç for standing by me, to Serhat Bayram for his no-judgement-space, to Mustafa Kemal Atik for his wisdom, to Göksu Taşçeviren for her advices and last but not least Okan Yılmaz for his mental support.

The streamflow data used in this study is obtained within the scope of TÜBİTAK (Scientific and Technological Research Council of Turkey) project numbered 115Y064.

TABLE OF CONTENTS

LIST OF TABLES

LIST OF FIGURES

LIST OF ABBREVIATIONS

AGİ	:	Akım Gözlem İstasyonu
ANN	:	Artificial Neural Networks
ARIMA	:	Autoregressive Integrated Moving Average
EK	:	Eksiltmeli Kümeleme
FIS	:	Fuzzy Inference System
FRB	:	Fuzzy Rule-Based
FRB-Extreme	:	Fuzzy Rule-Based Extreme
KTBM	:	Kural Temelli Bulanık Mantık
mASL	:	Meters Above Sea Level
OT	:	Overtrained
RCC	:	The models with repeated cluster centers
SC	:	Subtractive Clustering
TS	:	Takagi-Sugeno
TS_FRB	:	Takagi-Sugeno Fuzzy Rule-Based
TS_KTBM	:	Takagi-Sugeno tipi Kural Temelli Bulanık Mantık
Und	:	Undefined models
VL	:	The models with very low NSE

LIST OF SYMBOLS

μ	:	Membership
$\tilde{A}$	:	Fuzzy set A
c	:	Cluster centers
r_a	:	Cluster radius
P_i	:	Potential of the normalized data point i
P_k^*	:	Potential of the cluster center k
r_b	:	User-defined positive number
R	:	Correlation
R^2	:	Coefficient of Determination
NSE	:	Nash Sutcliffe Efficiency
$PBIAS$ (%)	:	Percent Bias
$Q_{i,j}$	:	Discharge measured at streamgage i at time j
MX_A	:	Xth model of subbasin A
Y	:	Yenicegoruce
I	:	Inanli
L	:	Luleburgaz
H	:	Hayrabolu

CHAPTER 1

INTRODUCTION

Rapid population growth brings along increases in water demand for municipal, agricultural, commercial, and industrial purposes. Therefore, water resources planning and management should be carried out effectively to meet existing and future demands. Complete data sets of hydrological variables are required for water resources planning and management; however, missing data is one of the problems that hydrologists are often faced with (Aissia et al., 2017). Especially in developing countries, inoperative streamgages due to various reasons such as maintenance or budget cuts cause data gaps, which can compromise data series' utility (Harvey et al., 2012). Being a developing country, Turkey experiences this problem as well.

High industrialization and agricultural activities in Meric-Ergene Basin threaten the sustainability of water resources in the basin. Realizing the existing threats such as extensive use and deterioration in water quality, the Republic of Turkey Ministry of Agriculture and Forestry – General Directorate of Water Management initiated many projects in the Meric-Ergene Basin (MoEU, 2020). However, data availability problems limit both assessment of the current status of water resources and the development of management strategies for the basin. Similar to the rest of Turkey, a dense network of streamgages is not found in the Meric-Ergene basin, and data of most of the streamgages are not complete. Thus, filling long gaps of missing streamflow data is an essential prerequisite in developing sustainable water resources management strategies for the basin.

In this thesis, we dealt with a special type of infilling problem, where the goal is forecasting a long period of missing daily streamflow data, such as a year or two in the presence of historical records both for the streamgage with missing data and

neighboring gages. SC-based TS_FRB model is trained, validated, and used to predict streamflow for the long period of missing records. The models are built by using the training period, which contains streamflow records of neighboring stations together with those of streamgage that later became inoperative (from hereafter will be referred to as "subsequently ungaged"). FRB models have two parameters to be set by the developer, the number of clusters and cluster radius. In order to determine best combination of the number of clusters and cluster radius, the trained models are evaluated for the validation period. Afterward, the trained and validated models are used to predict the streamflow at subsequently ungauged locations for the testing period. The method is applied at the Meric-Ergene Basin of Turkey. To the best of our knowledge, the application of the SC-based TS_FRB model is limited in hydrology, and this is its first application in long-term forecasting of daily streamflow data by solely using neighboring streamgage observations.

The FRB model provides good estimation for the streamgages located in the same tributary and closely spaced sub catchments, while it fails to provide satisfactory performance for streamgages located far away from the gages whose data is used as inputs or located in a different tributary. The lagged streamflow input enhances the model performances for some basins but introduces the risk of overfitting. The robust predictions by the FRB model are obtained for different periods for the streamgages having close neighboring gages. However, unmonitored anthropogenic effects in the basin worsen the performance of the FRB.

The organization of this study is as follows. In Chapter 2, a literature review about Fuzzy Set Theory, FRB systems, TS_FRB, Clustering, SC, SC-based TS_FRB and Filling Missing Streamflow Data is provided. In Chapter 3, the development of the SC-based TS_FRB Model is explained in detail. In Chapter 4, information about the study area (i.e., Meric-Ergene Basin) and statistical measures about the dataset used in this study are provided. In Chapter 5, first the results of the FRB models for Yenicegoruce, Inanli, Luleburgaz and Hayrabolu streamgages are given and discussion about the results and performances of these model are provided. Then, effect of clustering parameters selection, lagged inputs, utilization of different

validation periods on FRB model performances are investigated. In addition to these, the FRB model trained using data points corresponding to extreme events (FRB-Extreme) is introduced and its results are given in this section. In Chapter 6, major findings are highlighted, and remarks for future research are provided.

CHAPTER 2

LITERATURE REVIEW

2.1. Fuzzy Set Theory

A fuzzy set, which is introduced by Zadeh (1965), is a class of elements with a continuum of grades of membership. Such a set is characterized by a membership function that assigns to each element a grade of belongingness ranging between zero and one. A classical (nonfuzzy or crisp) set is defined by crisp boundaries, i.e., there is no uncertainty in the prescription or location of the boundaries of the set, as shown in Figure 2.1(a). Thus, the boundary of a crisp set A is unambiguously defined. On the other hand, a fuzzy set has ambiguously defined boundaries, as shown for fuzzy set $\tilde{A}$ in Figure 2.1(b). Hence, the boundary of a fuzzy set is fuzzily defined.

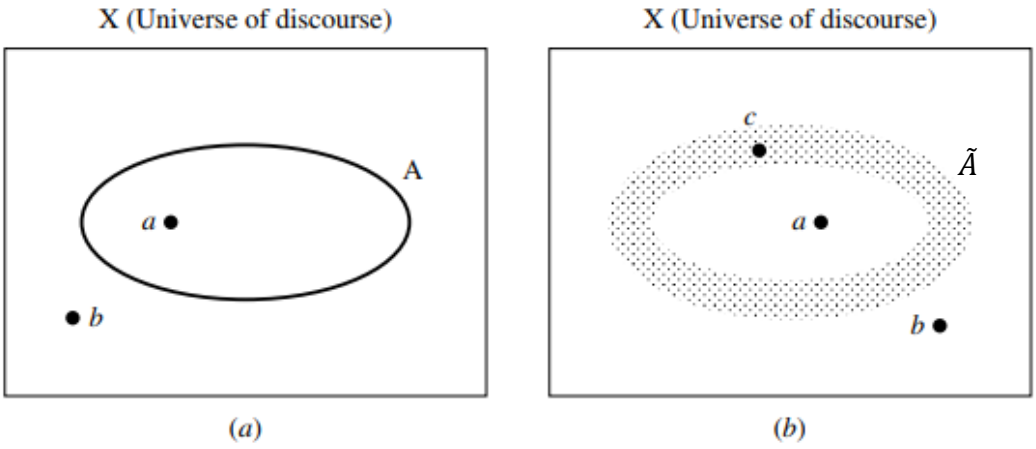

Figure 2.1. Diagrams for (a) crisp set boundary and (b) fuzzy set boundary (Ross, 2004)

Point a in Figure 2.1(a) is definitely a member of the crisp set A while point b is unambiguously not a member of the set A. However in Figure 2.1(b), the boundary

of the fuzzy set $\tilde{A}$ which is represented by the shaded area is ambiguous. Point a which is located in the central (unshaded) area of the fuzzy set $\tilde{A}$ is a *full* member of the set. In other words, point a fully belongs to $\tilde{A}$. Likewise, point b, which is located outside the boundary region of the fuzzy set is clearly not a member of the fuzzy set. On the other hand, point c, which is located in the fuzzy boundary region, partially belongs to the fuzzy set $\tilde{A}$. If full membership to a fuzzy set, such as point a in Figure 2.1(b), is represented by the number 1 and no-membership to a fuzzy set, such as point b in Figure 2.1(b) is represented by the number 0, the point c has an intermediate value of membership (partial membership) for the fuzzy set $\tilde{A}$ in the interval [0,1]. Furthermore, linguistic variables representing human cognitive patterns primarily on conceptual basis rather than numerical quantities are simple and vague; thus, they can be interpreted by fuzzy sets owing to their ambiguous and vague definitions (Ross, 2004). For instance, "age" is a linguistic variable when its values are represented linguistically rather than numerically, such as young, middle-aged, old rather than crisp numbers like 20, 35, 75. In fuzzy logic, the statement "Burak is young" indicates that Burak belongs to the fuzzy set of "young" with a certain degree. For instance, let's assume that Burak is 30 years old. Considering the fuzzy set "young," which is shown in Figure 2.2, Burak belongs to the fuzzy set "young" with a membership value of 0.4. If there is another fuzzy set called "middle-aged", Burak also belongs to the fuzzy set "middle-aged" with a membership value of 0.8, as seen in Figure 2.2. The membership values indicate how compatible the age of the Burak is to the fuzzily defined sets "young" and "middle-aged" (Zadeh, 1975). Building blocks of Fuzzy Inference Systems (FISs) or FRB Models, which are explained in the following sections, use fuzzy sets in their premises.

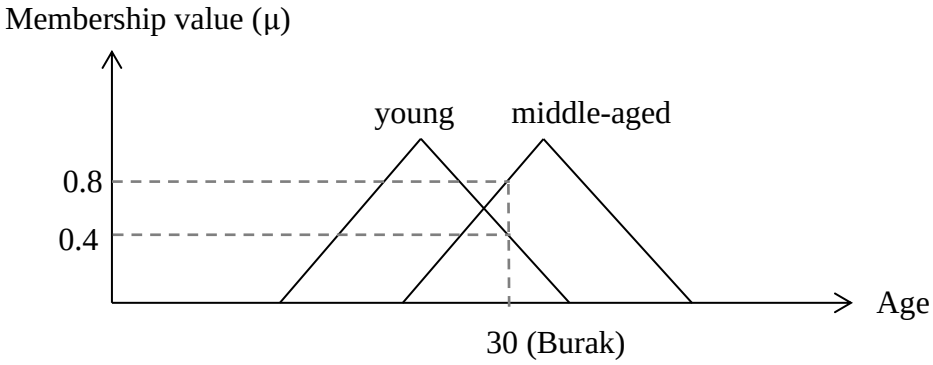

Figure 2.2. The membership functions for fuzzy sets "young" and "middle-aged"

2.1.1. Fuzzy Rule-Based (FRB) Systems

One of the most common ways to represent human knowledge is to express it in the following form:

IF premise (antecedent), THEN conclusion (consequent) (2.1)

The form in Equation (2.1) is referred to as the IF-THEN rule-based form. It typically expresses an inference such that if a fact (premise, antecedent) is known, then another fact called conclusion (consequent) can be inferred. An example of an IF-THEN rule may be as follows:

IF an apple is red, THEN it is delicious (2.2)

Equation (2.2) expresses human empirical and heuristic knowledge in the language of communication (Ross, 2004). Human knowledge expressed in Equation (2.2) can be mathematically expressed by fuzzy sets. The element apple can be defined by adjectives red and delicious which are ambiguous concepts, so can be represented by fuzzy sets. Then each apple will belong to these fuzzy sets with varying degrees.

A fuzzy rule does not necessarily compose of a single antecedent. Multiple antecedents of a rule can be connected by logical connectors such as "AND" or "OR"

which refer to conjunction and disjunction, respectively (Ross, 2004). For example, Equation (2.2) can be modified with multiple antecedents to the following form:

IF an apple is red AND shiny, THEN it is delicious (2.3)

In general, a fuzzy rule with multiple antecedents connected with "AND" operators looks like:

IF x_1 is $\tilde{A}_1$ AND x_2 is $\tilde{A}_2$ AND… AND x_n is $\tilde{A}_n$, THEN y is $\tilde{B}$ (2.4)

where $\tilde{A}_i$ is the fuzzy set representing the ith antecedent pair, $\tilde{B}$ is the fuzzy set representing the consequent, x_i is the element defined by fuzzy set $\tilde{A}_i$ and y is the element defined by fuzzy set $\tilde{B}$. The models which use fuzzy rules to make inferences are referred to as FRB models. A typical FRB model is shown in Figure 2.3 where x and y are the inputs, z is the output, x^* and y^* are the crisp values of the inputs, and Z^* is the crisp output of the system. The membership functions of the fuzzy sets employed in the fuzzy rules are determined and stored in the data-base while fuzzy rules are stored in the rule-base (see Figure 2.4). Inputs to the system, commonly as crisp numbers, are fuzzified using these fuzzy sets (i.e., membership function values of each input are determined using the corresponding fuzzy sets). This process is called fuzzification. The degree of match between crisp quantities and linguistic variables is obtained as a result of the fuzzification process, which is indicated by membership values, as mentioned in Section 2.1. For example, the membership value of the input Burak (30 years old) for the fuzzy sets "young" and "middle-aged" are 0.8 and 0.4, respectively, as shown in Figure 2.2. This shows that Burak satisfies the fuzzy set "young at a grade of 0.4, whereas he satisfies the fuzzy set "middle-aged" at a grade of 0.8.

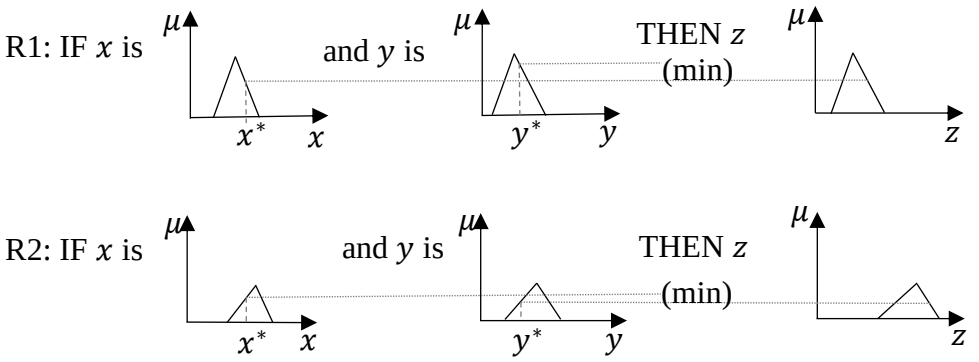

Output $\mu_{Z_{res}}$ is obtained by max membership principle

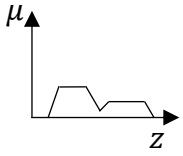

Output Z^* is obtained by mean max membership defuzzification principle: $Z^* = \frac{a+b}{2}$

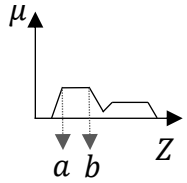

OR

Output Z^* is obtained by a centoriod defuzzification method:

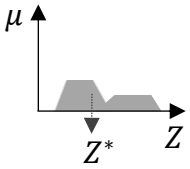

Figure 2.3. Mean max membership principle and centroid method (Modified from Ross, 2004)

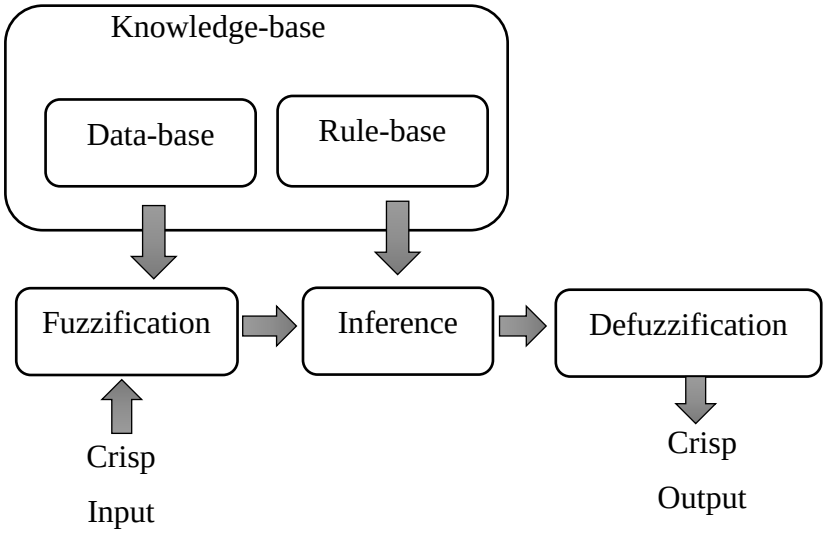

Figure 2.4. Typical FRB system (Modified from Ross, 2004; Jang, 1993)

The antecedent parts of the fuzzy rules are built based on the governing processes/rules of the system that is being modeled. A fuzzy rule can have a single or multiple antecedent part which is connected by logical operators. When there is a fuzzy rule with multiple antecedents connected with the "AND" operator, the membership values obtained from each antecedent part should be combined, which is usually carried out by the minimum or multiplication operations to obtain the firing degree for the corresponding fuzzy rule (Jang, 1993). On the other hand, to obtain the firing degree of a rule where "OR" operator is used to connect its antecedents, the maximum of membership values is commonly used (Ross, 2004). Detailed information about other operators that can be used to execute the "AND" and "OR" operators can be found in Ross (2004). The firing degree is used to evaluate how strongly the consequence of that rule will affect the overall output. Fuzzy rules stored in the rule-base are logical rules that describe the behavior of the modeled system for different conditions. The consequent of the fuzzy rule can be a fuzzy set as in the Mamdani type FRB models or a function as in the Takagi-Sugeno (TS) type FRB (Takagi and Sugeno, 1985) models (Ross, 2004).

The fuzzy rules are used to make inferences. The output of the model is determined by combining all the consequences of all the fuzzy rules. In the inference phase, firing degrees are used to weigh the impact of each fuzzy rule on the final output (Ross, 2004; Jang, 1993). A crisp or a fuzzy output is generated for each rule in correspondence of their firing degrees (Jang, 1993). Then the outputs of each fuzzy rule are aggregated into a single output. For the Mamdani type model, the aggregation can be carried out using the union operation, as shown in Figure 2.3. Then the resulting fuzzy output is converted into a single number using a defuzzification method such as the centroid method where the output is obtained by taking the centroid of the area or by taking the mean of the crisp numbers corresponding to the maximum membership value of the resulting fuzzy output, as shown in the last two rows of Figure 2.3 (Ross, 2004). When a TS_FRB model is used, the crisp outputs of each fuzzy rule are aggregated to obtain the overall output (Ross, 2004) (see Figure 2.5). Since TS_FRB models are used in this study, its details are given in the following section.

Different FRB models that have been proposed in the literature can be classified into three main types based on the inference used and the rule structure (Jang, 1993). For a two-rule fuzzy system with two antecedents connected with the logical connector "AND" three main types of inferences (i.e., Type 1, Type 2, and Type 3) are explained in Figure 2.5. According to Jang (1993), for Type 1, the firing degree of a fuzzy rule (i.e., R1 of Type 1 in Figure 2.5) is obtained by taking the minimum of the firing degrees from each premise. Using the firing degree found in the premise part (i.e., w1 of Type 1 in Figure 2.5), the crisp output (i.e., z1 of Type 1 in Figure 2.5) is obtained by using the monotonic membership function for the rule. Then the output of the FRB model is calculated by weighing the crisp output of each rule corresponding to their firing degrees. Mamdani Type FRB model is presented as Type 2. The fuzzy output is obtained by using the max membership principle on the membership functions of the consequent parts for each fuzzy rule according to the membership values obtained in the antecedent part by taking the minimum of each premise. After the fuzzy output is obtained, the defuzzification is carried out using

the centroid method to get the crisp output. TS_FRB model is shown as Type 3. The output of each rule is computed as a linear function of the input variables. The output of the system is calculated as the weighted average of the output of each rule. Since crisp outputs are obtained, time-consuming defuzzification methods necessary for the Mamdani type FRB (Type 2) is not required for TS_FRB models (Jang, 1993; Ross, 2004). TS_FRB models are developed in this thesis to estimate daily streamflows; thus, this method is explained in detail in the next sections.

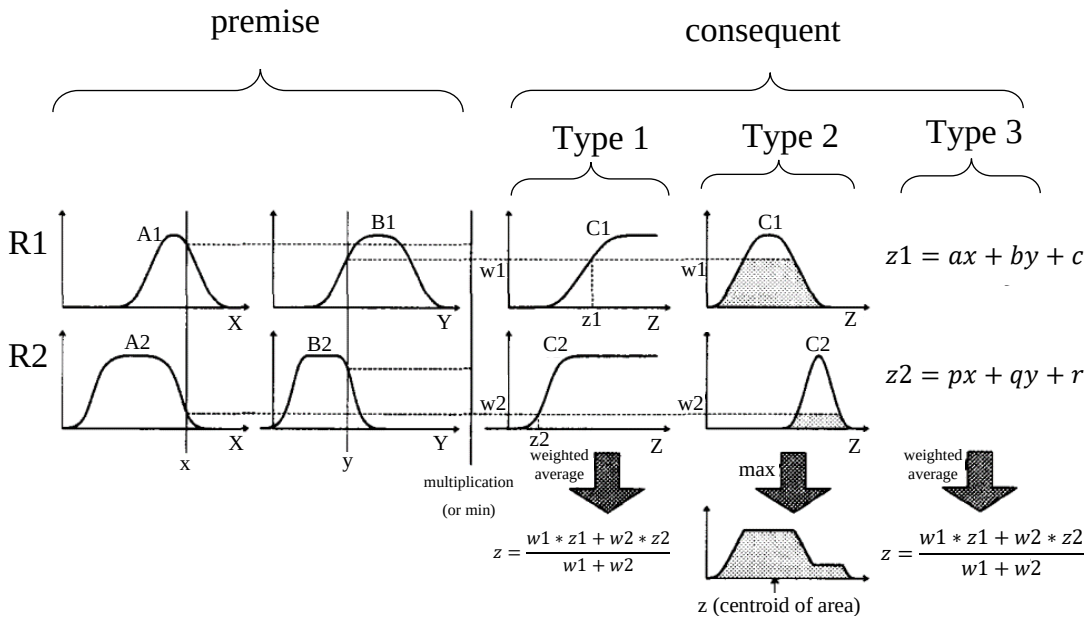

Figure 2.5. Commonly used FRB systems (Modified from Jang, 1993)

2.1.2. Takagi-Sugeno Fuzzy Rule-Based System

Owing to their efficiency, transparency, and flexibility, TS_FRB models have been widely used in the analysis of complex systems. Since TS_FRB models are capable of simulating non-linear behavior, they are suitable for complex systems (Angelov, 2004). The fields of application of TS_FRB has wide implications for many fields, including adaptive non-linear control, knowledge extraction, robotics, forecasting (Angelov and Filev, 2004). Recently, TS_FRB model applications in the field of hydrology started appearing in the literature as well as other soft computing

techniques like Artificial Neural Networks (ANN), genetic programming, etc. For example, Vernieuwe et al. (2005) compared TS_FRB models for rainfall-discharge dynamics, Kisi et al. (2012) carried out hybrid TS_FRB model to predict daily lake levels, Xiong et al. (2001) applied TS_FRB to analyze rainfall-runoff dynamics and, Jacquin and Shamseldin (2009) reviewed the application of FRB models including TS for flow forecasting. In this thesis, TS_FRB models are developed to predict streamflow at ungaged catchments. The behavior of the system, relations between the responses of neighboring catchments to the ungaged one are represented using a number of fuzzy rules, which are formulated utilizing the SC algorithm.

2.2.Clustering

As explained in Jain et al. (1999), cluster analysis is the organization of a collection of patterns (usually represented as a vector of measurements, or a point in multidimensional space) into clusters based on similarity. Intuitively, patterns within a valid cluster are more similar to each other than they are to a pattern belonging to a different cluster. An example of clustered data is shown in Figure 2.6.

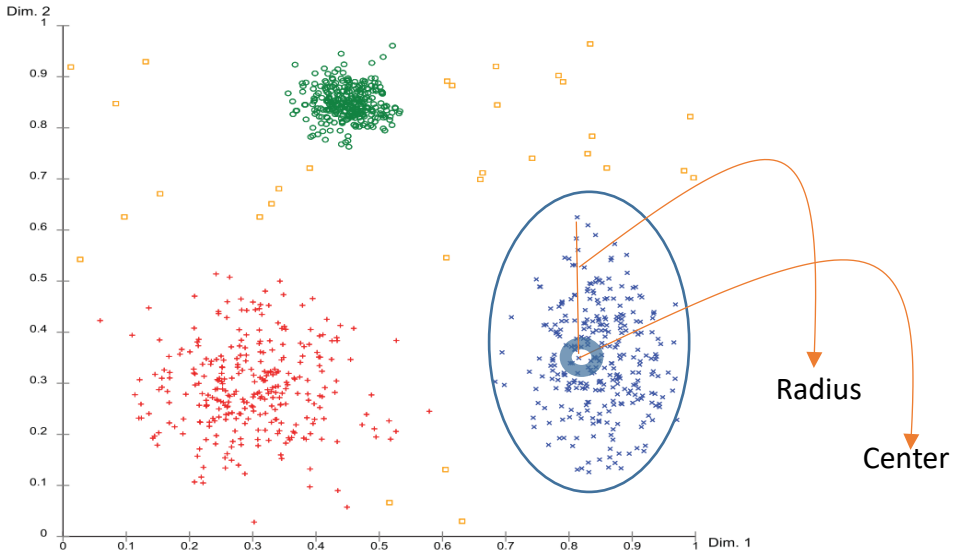

Figure 2.6. Clustered Data (Kriegel et al., 2011)

Clustering is one of the most effective approaches used in the data mining process for discovering groups and identifying distributions and patterns in the underlying data (Jain et al., 1999). Clustering methods are used for pattern-analysis, decision-making, data mining, image segmentation, document retrieval, and pattern classification (Jain et al., 1999). Each cluster can be defined by its cluster center and its radius. The focal point of a cluster is called its cluster center. The cluster center represents the cluster's behavior at most. The cluster radius defines the distance between the cluster center and the outermost data in that cluster. This outermost data is the last one that represents that cluster's behavior, maybe to the least extent (Batistakis et al., 2001).

In the field of hydrology, various clustering algorithms have been used in the literature, e.g., partitional clustering, hierarchical clustering, fuzzy c-means clustering and SC. Kentel (2009) applied fuzzy c-means clustering in the analysis of river flow, Nayak and Sudheer (2008) applied SC to forecast reservoir inflow and Dogulu and Kentel (2017) provided an overview of clustering methods for runoff predictions in ungauged basins. In this study, SC is used in developing fuzzy rules; thus, it is explained in detail in the following section.

2.2.1. Subtractive Clustering

SC, which is one of the first density-based clustering algorithms, is proposed by Chiu (1994). In density-based approaches, clusters are formed based on the density concept. In SC, density is referred to as the potential. In other words, the data points are grouped into a cluster based on their potentials. Each data point is considered as a candidate to be a cluster center, and the potential of each data is reversely proportional to the distance between that data point and all other data points as shown in Figure 2.7. In other words, as the centrality of a data point increases the potential of it to be a cluster center increases as well (Angelov and Yager, 2013). Besides the distance, the potential also depends on the cluster radius that defines the neighborhood between cluster centers. As the cluster radius decreases, cluster centers

get closer to each other. SC is one of the clustering algorithms proposed by Chiu (1994) to generated fuzzy rules since each cluster center is, in essence, a prototypical data point that exemplifies a characteristic behavior of the dataset. Therefore, each cluster center can be used as the basis of a rule that describes the system behavior. In this thesis, SC is used in formulating rules of the fuzzy models.

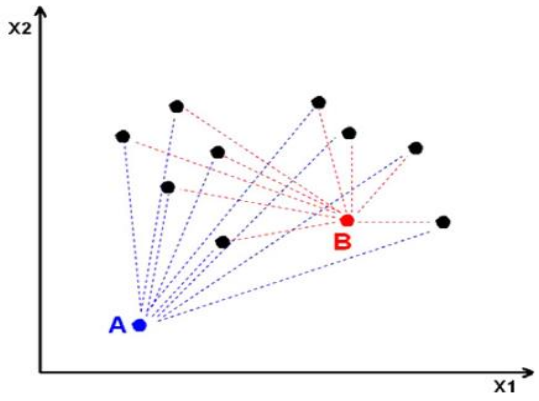

Figure 2.7. Distances from data point A and B to all other data (Adapted from Angelov and Yager, 2013)

2.3. Takagi-Sugeno Fuzzy Rule-Based Model that uses Subtractive Clustering

The simultaneous application of a set of fuzzy rules enables the simulation of non-linear processes by TS_FRB models. Although, the consequent part of each rule is a constant or a linear combination of the inputs used in the antecedent part, the simultaneous firing of multiple rules to generate the output allows modeling complex, non-linear phenomena. The simplicity of the consequent parts of the fuzzy rules increases the computational efficiency of TS_FRB models. TS_FRB model can be developed via the formulation of the structure (rule-base), firing degrees (membership functions), and estimation of parameters, which can be solved as a least square problem for fixed antecedent parameters (Angelov, 2004).

TS_FRB models are formulated by using SC in this thesis. Similar to the other clustering methods, a cluster can be defined by its clustering parameters, which are the center and the radius in the SC algorithm, as explained earlier. Therefore, clustering parameters affect the rule-base (see Figure 2.4) of the TS_FRB. While the number of cluster centers set the number of fuzzy rules, the cluster radius affects the satisfaction degree (or degree of belongingness) of crisp inputs in the fuzzy sets used in the antecedent part of the fuzzy rules. A large or small number of cluster centers might result in too many or not enough fuzzy rules than required, to adequately represent the system. In other words, a large cluster radius might lead to a coarse model which usually lacks the ability to fit highly nonstationary phenomenon and might result in underfitting, whereas a small radius might cause an overcomplicated model which learn from noise and leads to overfitting (Demirli et al., 2003; Ge and Zeng, 2018). Chiu (1994) suggested to assign a constant value for the cluster radius and set a threshold for the number of cluster centers based on the centrality of the generated cluster center at the latest. Akgun and Kentel (2018) investigated the impact of the number of rules on model performance. They concluded that increasing the number of cluster centers improves the performance up to a point, and this point should be determined based on an extensive trial-and-error procedure. After this point, the performance of the model decreases due to the increased dimension of the search space. Banakar and Azeem (2006) applied the Genetic Algorithm to determine the cluster radius used for SC-based TS_FRB. In this thesis, a trial and error procedure is used to select the cluster radii and the number of cluster centers.

2.4. Filling Missing Streamflow Data

In the literature, the filling of missing streamflow data often refers to the estimation of streamflow data where there is no record or only a short record of record (Hirsch, 1979). The drainage-area ratio method, which is based on the linearity assumption between drainage-area and streamflow, is commonly used for the reconstruction of streamflow, where there is no record (Asquith et al., 2006). Besides, tree-ring

information-based methods are widely used for reconstruction of historical streamflow records for long periods (Akkemik et al., 2008; Shah et al., 2013; Young 1994; Lara et al. 2005; Strachan et al., 2011; Bekker et al., 2014; Allen et al., 2013; Woodhouse and Lukas, 2006; Meko et al., 2001).

When there is enough data, various statistical methods have been used for infilling missing streamflow records (Beauchamp et al., 1989; Boakye and Schultz, 1994), including ANN approaches (Ayvaz et al., 2018; Khalil et al., 2001; Cigizoglu, 2003) and chaos theory principles (Elshorbagy et al., 2002). The model choice is influenced by the length and the season of the missing data, availability of hydro-meteorological data, corresponding climatic region, and the length of the available data from the past observations (Mwale et al., 2012). One of the most straightforward approaches for infilling daily streamflow data is replacing the missing values by the sample mean or mean of the subgroup. However, replacing a missing value with the sample mean might cause underestimation of the variance, and improper identification of subgroup might mislead the results (Kamwaga et al., 2018; Yozgatligil et al., 2012). Similar to the mean substitution method, Autoregressive Integrated Moving Average (ARIMA) (Lettenmaier, 1980) and interpolation (Boakye and Schultz, 1994) are two methods that use historical records of the streamgage with missing data for infilling. On the other hand, a large group of infilling techniques relies upon functions for transferring data from donor gauging stations (Harvey et al., 2012). These methods vary from simple regression (Harvey et al., 2012) to complex ANN (Dastrorani et al., 2010) and dynamic regression models, which include seasonal ARIMA with regression (Tencaliec et al., 2015). For both cases, numerous reviews and studies on the comparison of methods are conducted (Aissia et al., 2017; Boakye and Schultz 1994; Khalil et al. 2001; Harvey et al. 2012; Ng et al. 2009). More recently, geospatial methods such as Map-Correlation Method are proposed (Archfield and Vogel, 2010) and used in predicting daily streamflows at ungaged locations as well (Ergen and Kentel, 2016; Krasnogorskaya et al., 2019).

In this thesis study, the infilling problem where the aim is to forecast a long period of missing daily streamflow data, such as a year or two, is solved using the TS_FRB

model. Similar studies using heuristic methods have appeared in the literature, but they generally focused on the infilling of a short period of streamflow data. Valipour et al. (2013) compared the performance of ARIMA models and dynamic autoregressive ANN models in forecasting monthly inflows to a dam reservoir. As a result, ARIMA provides better performance in the short term (12 months) forecasting while dynamic autoregressive ANN shows better performance in the long term (60 months) forecasting. Kentel (2009) developed a tool for a one-step-ahead forecast of daily streamflow using ANN and evaluated the efficiency of the estimation with fuzzy clustering. Shiau and Hsu (2016) used ANN in their study to extend daily streamflow records and concluded that ANN is suitable for it. For long-term and short-term flow forecasting, numerous comparisons of methods and reviews have been carried out (Aissia et al., 2017; Boakye and Schultz, 1994; Khalil et al., 2001; Harvey et al., 2012; Ng et al., 2009).

In this thesis, we developed TS_FRB models based on SC to estimate missing daily streamflow data for long periods. TS_FRB based on SC was previously applied by Akgun and Kentel (2018) for one-step-ahead forecasting of monthly streamflow, by Vernieuwe et al. (2005) for rainfall-runoff modeling, by Nayak and Sudheer (2008) for inflow forecasting of the reservoir and by Nayak et al. (2005) and Lohani et al. (2014) for flood forecasting. To the best of our knowledge, the application of the TS_FRB model based on SC is limited in hydrology, and this is its first application in long-term forecasting of daily streamflow data by solely using neighboring streamgage observations.

CHAPTER 3

METHODOLOGY

3.1.Subtractive Clustering-Based Takagi-Sugeno Fuzzy Rule-Based Model

The framework of the SC-based TS_FRB model is given in Figure 3.1. First, the SC-based TS_FRB model is developed, trained, and validated; then, it is used to make predictions. The first step is clustering daily streamflow data obtained from all the streamgages used in this study. Each cluster center is then used to develop a rule that represents the behavior of the system (i.e., in this study, the relations between hydrologic responses of sub-catchments represented by streamgages at their outlets).

As the case study, it is assumed that all streamgages collected daily streamflow data between 1996 and 2003. Then one of the streamgages became inoperative (i.e. subsequently ungaged) and stopped collecting daily streamflow data while the remaining gages continued to collect data. SC-based TS_FRB models are developed for the subsequently ungaged locations to predict its daily streamflows. Input to SC are vectors of streamflow measurements of all the streamgages that are used in the study for each day of the observation period (i.e., the period used for training). Thus, the observation period is the period along which daily streamflow measurements are collected from all the neighboring streamgages and the subsequently ungaged one.

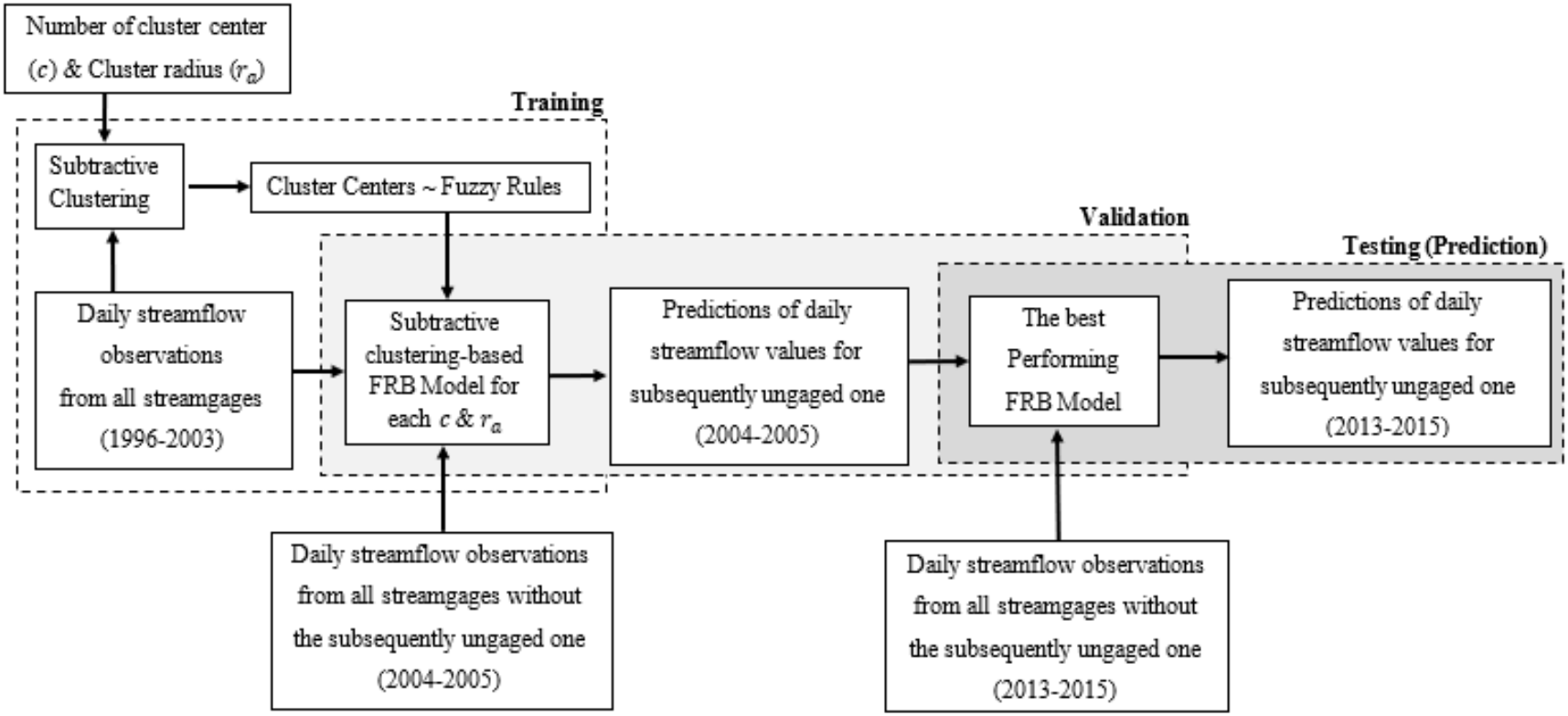

Figure 3.1. SC-based TS_FRB model

SC-based TS_FRB models are developed based on user-defined parameters of SC, namely the number of cluster centers (c) and cluster radius (r_a). Effect of different number of cluster centers and cluster radii is investigated in this study. In other words, for each c and r_a pair, a SC-based TS_FRB is trained using data of the training period. Then the trained model is used to make predictions for the validation period. This analysis is carried out to avoid overfitting. The model with the best validation performance is then used to test the robustness of the FRB model. The testing is carried out with the test data set which is different from training and validation data sets.

3.1.1. Subtractive Clustering

Formulation of the SC-based TS_FRB model that estimates the discharge at the subsequently ungaged location in day t, using discharges measured at the surrounding $(m-1)$ streamgages in day t, $Q_{subsequently\ ungaged}(t) = f\big(Q_1(t), Q_2(t), \dots, Q_{m-1}(t)\big)$, is explained below. For an observation period of n days and m streamgages, there will be n data points $\{V_1, V_2, V_3 \dots, V_n\}$ (i.e., samples or patterns), where V_i is a vector with m elements. Daily streamflow observations at each streamgage form the m-dimensional feature space, which includes $m-1$ dimensional input space (i.e. surrounding streamgages that collect daily streamflow data) and 1-dimensional output space (i.e. subsequently ungaged location). Prior to clustering log-transformation is applied to the dataset and the feature space is normalized so that all data are bounded by a unit hypercube.

In SC, each data point is treated as a candidate to be a cluster center and potential of each data point to be a cluster center is calculated using the following equation (Chiu, 1994):

$$P_i = \sum_{j=1}^{n} e^{-\left(\frac{4}{r_a^2}\right)\|X_i - X_j\|^2} \quad (i = 1,2,3, \dots, n) \tag{3.1}$$

where X_i is the normalized data point i, P_i is the potential of normalized data point i, r_a is a user-defined positive constant representing cluster radius of the first cluster center and n is the number of data points.

The potential of a data point decays exponentially (see Equation 3.1) with the square of the distance between that data point and all other data points, which ensures that a data point with many closeby neighbors has a high potential. The constant, r_a, is the radius defining the neighborhood. At the end of the potential calculation process, the data with the highest potential is selected as the first cluster center. Afterward, the potentials are updated using the following equation (Chiu, 1994):

$$P_i \leftarrow P_i - P_k^* \, e^{-(4/r_b^2)\|X_i - X_k^*\|^2} \quad (i = 1,2,3,\dots,n) \tag{3.2}$$

where X_k^* is the cluster center k, P_k^* is the potential of cluster center k and r_b is a user-defined positive constant. When r_b is chosen to be a small number, closer cluster centers are formulate.

The updated potential decays exponentially with the square of the distance from each data point to the previous cluster center as well. In this way, the potential of the data point located near the previous cluster center drops significantly compared to the other data points that are far away from the previous cluster center. After the updating process, the data point with the highest potential is chosen as the next cluster center. Note that, while updating potentials, predecessor cluster center is used. This procedure continues until the user-defined number of cluster centers are identified. Each cluster center is in essence a prototypical data point that exemplifies a characteristic behavior of the dataset. Therefore, each cluster center can be used as the basis of a fuzzy rule that describes the system behavior (Chiu, 1994).

3.1.2. TS_FRB Model Development

Each cluster center is obtained in the m-dimensional space. In order to convert cluster centers into fuzzy rules, each cluster center is decomposed into two vectors. For example, cluster center c is decomposed into Y_c^* and Z_c^* vectors, where Y_c^* is

composed of $(m-1)$ dimensions which is the total number of input variables and Z_c^* is composed of 1-dimension which represents the output (i.e. the discharge at the streamgage assumed to be the subsequently ungaged location for the validation and testing periods). In this study, each fuzzy rule is designed to have the following form:

$$\text{Rule } r\text{: IF } y_1 \text{ is } A_1^r \text{ \& } y_2 \text{ is } A_2^r \text{ \& ... \& } y_{m-1} \text{ is } A_{m-1}^r \text{ , THEN } z = G_1^r y_1 + \cdots + G_{m-1}^r y_{m-1} + H^r \quad (3.3)$$

where $y_1, y_2, \ldots y_{m-1}$ are the input variables and z is the output variable; $A_1^r, A_2^r, \ldots, A_{m-1}^r$ are antecedent fuzzy sets for rule r which are defined by Gaussian membership functions, $G_1^r, G_2^r, \ldots, G_{m-1}^r$ and H^r are the coefficients of the linear function for rule r and they need to be estimated using the training data points.

The cluster centers are used as the mean values of the membership functions. For example, if $Y_1^* = (y_{1,1}^*, y_{1,2}^*, \ldots, y_{1,m-1}^*)$ is identified as the first cluster center (used to generate the first fuzzy rule), then the membership functions for $A_1^1, A_2^1, \ldots, A_{m-1}^1$ are given in Figure (3.2). In this study, a linear function of the input variables is used to calculate the output according to Takagi and Sugeno (1985a) inference mechanism as given in Equation (3.3). Moreover, multiplication is used to carry out the AND operation. Thus, for an input vector of $Y_k = (y_{k,1}, y_{k,2}, \ldots, y_{k,m-1})$ the firing degree (or fulfillment degree) of the first fuzzy rule (represented by the first cluster center, Y_1^*) is calculated using the following equaiton (Chiu, 1994):

$$\mu_{k,1} = e^{-(4/r_a^2)\|Y_k - Y_1^*\|^2} \quad (3.4)$$

and the output (of the input vector Y_k for the first rule) is calculated using:

$$z_k^1 = G_1^1 y_{k,1} + \cdots + G_{m-1}^1 y_{k,m-1} + H^1 \quad (3.5)$$

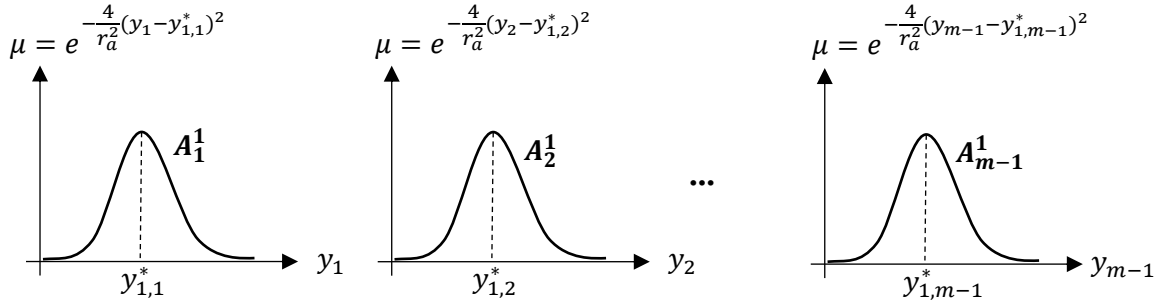

Figure 3.2. Membership functions for antecedent fuzzy sets

Equation (3.4) is used to calculate firing degrees of all fuzzy rules for each input vector and Equation (3.5) is used to calculate the output of each input vector for all the rules. For each input vector, i there will be one firing degree for each rule and the output of this input vector, z_i for a fuzzy inference system with c rules is calculated using:

$$z_i = \frac{\mu_{i,1} z_i^1 + \mu_{i,2} z_i^2 + \cdots + \mu_{i,c} z_i^c}{\sum_{p=1}^{c} \mu_{i,p}} \tag{3.6}$$

Therefore if there are n observation points (i.e., each observation point has m dimensions of which $(m-1)$ is for inputs and one is for the output in this study) then there will be n linear equations generated by aggregating results of c rules using Equation (3.5). Each of these linear equations has unknown parameters (i.e. G_r^p and $H^p,\ r = 1,2,\dots,m-1$ and $p = 1,2,\dots,c$) that need to be estimated/calibrated using the outputs of the observation points. This results in a system of linear equations of the form $A\underline{x} = \underline{R}$, where A is $n \times [(m-1)c + c]$ dimensional coefficient matrix, $\underline{x}$ is the unknown column vector with $[(m-1)c + c]$ elements and the right hand side vector $\underline{R}$ is composed of the output values of the n observation points (i.e. $n \times 1$ column vector). In this study, the unknown parameters of the system of linear

equations are estimated using computationally efficient and well-behaved recursive least square estimation to avoid singularity problem caused by the ordinary least square estimation.

3.1.3. Parameter Estimation with Recursive Least Square Method

For an equation in the form $A\underline{x} = \underline{R}$, the parameters are estimated iteratively by the Recursive Least Square Method as follows (Chiu, 1994):

$$X_{j+1} = X_j + S_{j+1}a_{j+1}\left(r_j - a_{j+1}^T X_j\right) \tag{3.7}$$

$$S_{j+1} = S_j - \frac{S_j a_{j+1} a_{j+1}^T S_j}{1 + a_{j+1}^T S_j a_{j+1}} \quad (j = 0,1,2, \ldots . n-1) \tag{3.8}$$

where X_j is the estimate of $\underline{x}$ obtained at iteration j, S_j is the covariance matrix, a_j^T is the ith row vector of A and r_j is the jth element of vector R. S_j is a $cm \times cm$ dimensional square matrix. Initial conditions for iteration are $X_0 = 0$ and $S_0 = \gamma I$, where γ is the large positive number and I is the identity matrix having the same dimensions with S. The least-square estimate of $\underline{x}$ corresponds to X_n (Chiu, 1994).

CHAPTER 4

CASE STUDY: MERIC-ERGENE BASIN

The proposed method is applied for four streamgages, D01A020 – Inanli, D01A008 – Luleburgaz, E01A006 – Hayrabolu and E01A012 – Yenicegoruce located in Meric-Ergene Basin (see Figure 4.1). Meric – Ergene River drains a surface area of 12,438 km^2 (MoEF, 2008) within the boundaries of North-Western Turkey in the Thrace Region. Yenicegoruce streamgage is located upstream of the conjunction of the Ergene River with the main stream of the Meric River (Mesta et al., 2018; Mesta et al., 2019).

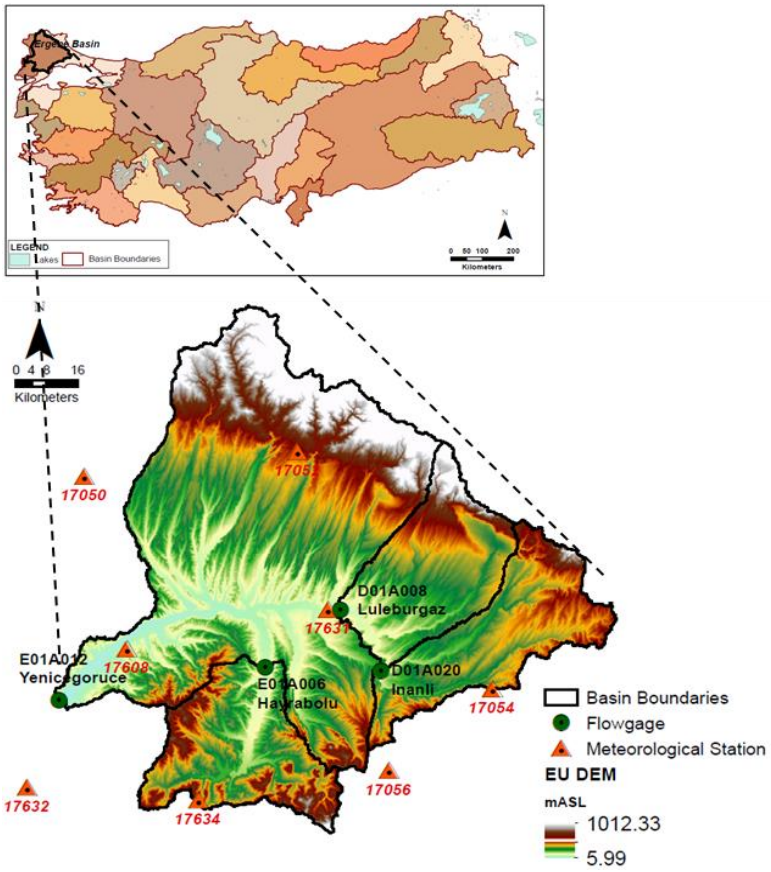

Figure 4.1. The topography of the Meric-Ergene Basin (Tezel et al., 2019)

The elevation of the study area ranges between 6 mASL and 1012 mASL. Historical daily temperatures recorded at the Luleburgaz (Station No: 17631 as shown in Figure 4.1) meteorological station within the catchment for the period between 1997 and 2017 indicate that the mean annual temperature is 14.4°C and the mean annual precipitation is 570 mm. Monthly mean values for 21 years average (1997-2017) show that December and August are the wettest (65.5 mm average) and driest (10.3 mm average) months, respectively. The highest and lowest mean temperatures recorded in this period are 35.7°C (July 2000) and -13.7°C (January 2010), respectively. Agricultural lands in Meric-Ergene Basin form the most dominant land covering around 65% of the entire basin. Other main land cover types are forests and shrubbery (27%), and meadows and pastures (5.7%). Water bodies cover 0.5% of the entire Meric-Ergene Basin (MoEF, 2008). Surface runoff forms the main source of water potential in the basin. Groundwater contribution is around 20% of the basin's water potential (MoEF, 2008).

SC-based TS_FRB models are built for Yenicegoruce station located at the outlet of the basin, for Hayrabolu station located at the upstream of the Yenicegoruce located on Ergene river, for Luleburgaz station located at the upstream of the Yenicegoruce and Inanli station located at the upstream of the Luleburgaz station as shown in Figure 4.1 (Mesta et al., 2018). Only daily streamflow records are used to build SC-based TS_FRB models. Based on the availability of data, training and validation periods are selected as 1997-2003 and 2004-2005, respectively. Monthly mean flows, monthly maximum flows, monthly standard deviation values and some basic statistical measures of all streamgages for the training and validation periods are given in Table 4.1, Table 4.2, Table 4.3 and Table 4.4, respectively.

Table 4.1. Monthly mean values for training, validation, and testing periods for all streamgages

	Monthly means in m^3/s	Jan	Feb	Mar	Apr	May	Jun	Jul	Aug	Sep	Oct	Nov	Dec
Training	Inanli (D01A020)	10.45	18.99	11.98	9	4.29	3.29	2.32	2.28	2.32	4.52	5.55	18.81
	Hayrabolu (E01A006)	8.3	15.36	10.52	7.13	3.07	2.26	1.92	1.86	1.78	1.99	3.54	13.19
	Yenicegorece (E01A012)	52.71	96.41	56.11	44.64	23.47	12.57	7.96	8.44	9.74	13.56	23.55	67.3
	Luleburgaz (D01A008)	15.56	31.95	17.64	13.52	7.44	5.38	3.83	3.59	4.01	6.18	8.43	29.28
Validation	Inanli (D01A020)	15.1	15.16	14.77	9.15	8.93	8.67	7.4	5.45	5.03	3.69	4.1	4.02
	Hayrabolu (E01A006)	6.93	9.63	5.2	1.43	1.41	1.87	2.02	3.15	1.64	0.64	0.38	0.43
	Yenicegorece (E01A012)	28.04	52.18	36.09	16.57	13.06	11.87	11.08	11.29	10.19	10.25	10.44	13.01
	Luleburgaz (D01A008)	16.57	11.87	12.01	6.7	6.27	6.59	5.64	5.59	5.59	5.77	6.01	6.04
Testing	Inanli (D01A020)	33.43	39.07	25.91	17.00	9.03	17.23	6.36	5.30	11.78	20.24	13.02	38.17
	Hayrabolu (E01A006)	21.75	24.44	11.16	11.29	6.27	10.53	6.28	4.78	11.30	16.74	9.75	23.19
	Yenicegorece (E01A012)	11.98	19.08	7.07	7.94	4.35	7.40	5.01	5.04	3.06	5.72	2.51	7.47
	Luleburgaz (D01A008)	90.12	147.04	99.80	90.94	22.51	41.92	30.11	18.91	27.13	42.92	46.45	134.96

Table 4.2. Monthly maximums for training, validation, and testing periods for all streamgages

	Monthly maximums in m^3/s	Jan	Feb	Mar	Apr	May	Jun	Jul	Aug	Sep	Oct	Nov	Dec
Training	Inanli (D01A020)	60	195	115	165	61	16.5	3.6	6.82	12	210	133	280
	Hayrabolu (E01A006)	79.2	122	127	82.8	21.3	12.1	6.1	4.59	7.28	38.1	45.4	116
	Yenicegorece (E01A012)	327	909	344	164	113	52.6	22.5	19.1	25.1	91.4	126	857
	Luleburgaz (D01A008)	67.9	800	107	260	70.4	18.4	6.77	8.97	15.2	107	126	572
Validation	Inanli (D01A020)	153	86.8	66.5	19	18.7	27.3	12.4	11.5	6.46	17.7	20.7	16
	Hayrabolu (E01A006)	143	103	21.8	2.33	4.11	5.77	15.7	14.1	3.95	1.71	1.37	2.65
	Yenicegorece (E01A012)	66.5	184	71.7	23.1	44.9	23.7	47.2	19.4	18.2	19.2	20.6	48.7
	Luleburgaz (D01A008)	211	60.9	53	9.33	9.18	13.1	6.34	6.4	6.21	15.6	17.2	14
Testing	Inanli (D01A020)	204	365	204	241	17.5	249	33.7	6.99	159	299	77.7	376
	Hayrabolu (E01A006)	166	204	61.7	188	19.9	129	113	9.02	144	307	75.1	293
	Yenicegorece (E01A012)	147	325	54.9	284	17.7	101	8.62	43.5	10.5	138	13.2	99
	Luleburgaz (D01A008)	443	701	265	391	60.7	187	325	77.8	128	451	239	481

Table 4.3. Monthly standard deviations for training, validation, and testing periods for all streamgages

	Monthly standard deviations in m^3/s	Jan	Feb	Mar	Apr	May	Jun	Jul	Aug	Sep	Oct	Nov	Dec
Training	Inanli (D01A020)	8.99	31.3	13.53	14.96	4.66	1.38	0.73	0.77	1	14.97	11.33	36.91
	Hayrabolu (E01A006)	10.76	23.11	16.68	9.5	2.7	1.66	0.97	1	1.34	5.45	8.2	23.04
	Yenicegorece (E01A012)	44.88	135.5	53.1	32.85	23.96	7.86	3.94	3.51	4.52	14.54	31.74	117.85
	Luleburgaz (D01A008)	12.75	77.28	17.58	19.78	5.78	2.31	0.87	0.85	1.43	9.04	12.23	68.61
Validation	Inanli (D01A020)	31.62	12.44	11.39	4.93	4.46	5.23	3.56	1.73	1.01	2.16	3.39	2.26
	Hayrabolu (E01A006)	22.01	19.19	4.94	0.35	0.96	1.24	2.5	2.1	0.7	0.33	0.24	0.34
	Yenicegorece (E01A012)	15.41	40.57	15.18	3.1	7.43	3.93	7.59	2.83	2.29	2.02	2.54	8.33
	Luleburgaz (D01A008)	32.53	8.34	8.34	0.64	0.95	1.44	0.26	0.31	0.22	1.65	2.19	1.35
Testing	Inanli (D01A020)	41.46	51.40	34.89	30.01	2.17	33.17	3.75	0.78	19.74	47.33	10.41	56.37
	Hayrabolu (E01A006)	29.25	31.74	8.55	21.98	1.81	17.92	11.29	0.92	20.13	44.41	9.18	36.53
	Yenicegorece (E01A012)	21.70	41.33	6.94	29.69	2.66	10.88	1.67	4.70	2.34	17.29	2.06	13.81
	Luleburgaz (D01A008)	84.23	131.58	67.88	79.89	10.49	44.65	51.75	8.13	25.82	68.96	54.62	125.84

Table 4.4. Basic statistical measures for training, validation, and testing periods for all streamgages

	Values in m^3/s	Inanli (D01A020)	Hayrabolu (E01A006)	Yenicegorece (E01A012)	Luleburgaz (D01A008)
Training	Minimum	0.89	0.11	0.18	2.17
	First Quantile	2.2	0.87	8.36	4.05
	Median	3.4	1.86	13.6	5.41
	Mean	7.76	5.86	34.36	12.13
	Standard Deviation	17.22	12.54	62.97	32.2
	Third Quantile	6.8	4.46	33	9.76
	Maximum	280	127	909	800
Validation	Minimum	1.59	0.11	5.61	3.42
	First Quantile	3.75	0.55	9.64	5.56
	Median	4.7	1.25	11.6	5.97
	Mean	8.43	2.87	18.51	7.88
	Standard Deviation	11.53	8.91	18.49	10.61
	Third Quantile	11	2.41	19.4	7.02
	Maximum	153	143	184	211
Testing	Minimum	2.64	0.502	8.25	3.39
	First Quantile	5.21	1.78	15.6	6.18
	Median	6.32	4.1	23.5	8.67
	Mean	13.06	7.144	65.56	19.61
	Standard Deviation	24.31	17.81	84.03	35.17
	Third Quantile	10.15	6.38	84.15	16.5
	Maximum	307	325	701	376

Irrigation water demand is supplied from reservoirs and ponds in the basin and from Ergene River and its tributaries through direct water abstraction (Tezel et al., 2019). Upper tributaries of Ergene River (streams in Inanli and Luleburgaz subbasins) are under high pollution stress due to heavy industrialization at the East of the basin as shown in Figure 4.2 (Tezel et al., 2019). Industrial water demand is mainly met by groundwater abstraction (Kahraman and Ozkul, 2018). Flowrate in the Ergene River is significantly affected by industrial effluent discharges (Gunes and Taninli, 2013; Sungur et al., 2014; Tezyapar et al., 2018). Turkish Ministry of Environment and Urbanization reports that industrial effluent discharges contribution to the streamflow in the basin may reach up to three times higher than the natural surface runoff during the low flow season (MoEU, 2015). Most of the industrial discharges are intermittent and irregular. The volumes of irrigational and industrial water extractions and discharges, particularly from industrial establishments, are not continuously monitored and hence not available to researchers. In fact, as reported by the chair of a local irrigation union during one of the site visits, especially during heavy rainfall events, the industrial establishments discharge their effluents to Ergene River in an uncontrolled manner (Tezel et al., 2019). Unmonitored anthropogenic effect on basin may affect the prediction skills of SC-based TS_FRB being data-driven method.

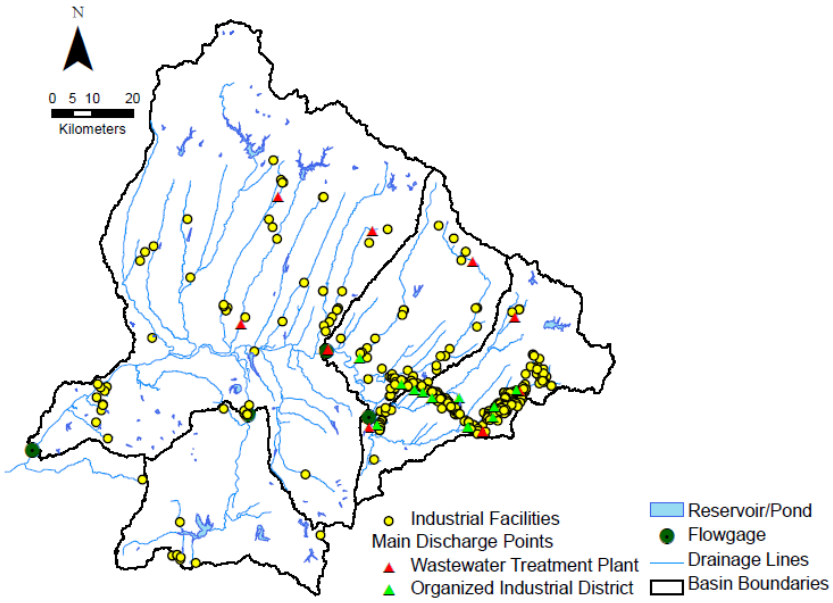

Figure 4.2. Industrial facilities found on the study area (Tezet et al., 2019)

CHAPTER 5

RESULTS AND DISCUSSIONS

SC-based TS_FRB models are developed using R computer language in this study. The code runs in approximately 20 seconds in a computer with i9-9900K processor and 32GB RAM for one simulation with three input parameter and eight cluster centers (i.e., training, validation and testing of a single model). In the developed code "openxlsx" R package is used to read data from excel files (Walker and Bragliga, 2018). The rest of the model is self-coded.

Streamflow predictions obtained by using SC-based TS_FRB (from hereafter will be referred to as FRB models) within the study catchment are given and analyzed in this section. The study catchment has four streamgages, Yenicegoruce (E01A012), Inanli (D01A020), Luleburgaz (D01A008), and Hayrabolu (E01A006). A total of 22 different type of models (i.e., different sets of inputs are used) are built, six FRB models each for Yenicegoruce and Inanli, five models each for Luleburgaz and Hayrabolu using different sets of input. To determine the best parameter set (i.e., cluster radius and number of cluster centers) of each type of FRB model, 150 variations (from here after they will be referred to as sub-models) of each type is developed. These sub-models are built based on different fuzzy rules generated using a different number of cluster centers and cluster radii. In other words, 3300 models are built..

Streamflow data is divided into three parts for training, validation and testing. Training data set is used to train FRB models while the validation data set is used to identify the best parameter set. Then testing data set is used to evaluate the performance of the trained model. For four streamgages, the models which provide the best estimates and analysis with respect to cluster centers and cluster radii are

presented in this section. The results of the remaining models are given in the Appendices.

To test robustness of the models, same procedure is applied (i.e., 3300 models are built) by interchanging the datasets of the validation and testing periods (i.e., these runs are referred to as Case 2). Thus, 6600 models are built in total in this study.

5.1. Estimation of Streamflow Using Subtractive Clustering-based Takagi Sugeno Fuzzy Rule-Based Model

Within the study catchment, each of the streamgages is assumed to be subsequently ungaged and SC-based TS_FRB models are developed to estimate its daily streamflow values. FRB model used to predict streamflow at the subsequently ungaged location, Q_{su} using streamflow observations at three neighboring streamgages, Q_{n1}, Q_{n2}, Q_{n3}, can be expressed mathematically as follows:

$$Q_{su} = f(Q_{n1}, Q_{n2}, Q_{n3}) \tag{5.1}$$

Statistical model performance measures used in this study to evaluate the efficiency of the FRB models are R, R^2, NSE and $PBIAS$:

$$R = \frac{\sum_{t=1}^{n_t}[(Q_t^o - \bar{Q}^o)\times(Q_t^s - \bar{Q}^s)]}{\sqrt{\sum_{t=1}^{n_t}(Q_t^o - \bar{Q}^o)^2 \times \sum_{t=1}^{n_t}(Q_t^s - \bar{Q}^s)^2}} \tag{5.2}$$

$$R^2 = Corr^2 \tag{5.3}$$

$$NSE = 1 - \frac{\sum_{t=1}^{n_t}(Q_t^s - Q_t^o)^2}{\sum_{t=1}^{n_t}(Q_t^o - \bar{Q}^o)^2} \tag{5.4}$$

$$PBIAS = \frac{\sum_{t=1}^{n_t}(Q_t^o - Q_t^s)}{\sum_{t=1}^{n_t}(Q_t^o)} \times 100 \quad (5.5)$$

where t stands for the time steps, Q_t^s and Q_t^o are simulated and observed streamflows at time t, $\bar{Q}^s$ and $\bar{Q}^o$ are the corresponding mean values of simulated and observed streamflows throughout the entire duration of the simulation/observation, respectively and n_t is the total number of streamflow data. The mean and instantaneous streamflows are expressed in m^3/s in the equations. Performance of FRB models evaluated using Table 5.1.

Table 5.1. Performance evaluation criteria for evaluating statistical measures, namely R^2, NSE and $PBIAS$ (%), for daily, monthly, and yearly flow predictions of basin-scale models (adapted from Moriasi et al., 2015)

Statistical Measure	**Performance Evaluation Criteria**			
	Very Good	*Good*	*Satisfactory*	*Unsatisfactory*
R^2	$R^2 > 0.85$	$0.75 < R^2 \leq 0.85$	$0.60 < R^2 \leq 0.75$	$R^2 \leq 0.60$
NSE	$NSE > 0.8$	$0.7 < NSE \leq 0.8$	$0.5 < NSE \leq 0.7$	$NSE \leq 0.5$
$PB(PBIAS)$ (%)	$PB < \pm 5$	$\pm 5 \leq PB < \pm 10$	$\pm 10 \leq PB < \pm 15$	$PB \geq \pm 15$

5.1.1. Yenicegoruce Streamgage

5.1.1.1. Analysis of the number of cluster center and the cluster radius

First, Yenicegoruce streamgage is assumed to be the subsequently ungaged location and Inanli, Luleburgaz and Hayrabolu streamgages are used to predict its streamflow. Initially, the first type of the model, the base model, $M1_Y$ is developed where streamflow observations at time t at Inanli ($Q_{I,t}$), Luleburgaz ($Q_{L,t}$) and Hayrabolu ($Q_{H,t}$) are used to predict streamflow at time t at Yenicegoruce ($Q_{Y,t}$) (see

Table 5.2). Then, five other types of FRB models where the effect of travel time is considered are developed. Yenicegoruce streamgage is located at the outlet of the basin (see Figure 4.1). Since the basin has a drainage area of 10,402 km^2, it takes a few days for the peak of the hydrograph to travel from Inanli streamgage to Yenicegoruce streamgage. As demonstrated in Figure 5.1, the travel time changes, while it took around six days in October 1997 for the peak of the hydrograph to travel from Inanli to Yenicegoruce streamgage; it only took around three days in January 2004. Considering different travel times, six types of FRB models using streamflow measurements at t, $(t-1)$, $(t-2)$, $(t-3)$, $(t-4)$ and $(t-5)$ at Inanli, Luleburgaz, and Hayrabolu streamgages are developed and trained to estimate streamflow at t at Yenicegoruce streamgage. The architectures of these models are shown

in Table 5.2. In Table 5.2, $Q_{i,j}$ is the discharge measured at streamgage i at time j. To predict streamflow at Yenicegoruce (Y) at t, $Q_{Y,t}$, Luleburgaz (L), Inanli (I), and Hayrabolu (H) are used as the neighboring streamgages (i.e., $i = Y, L, I, H$).

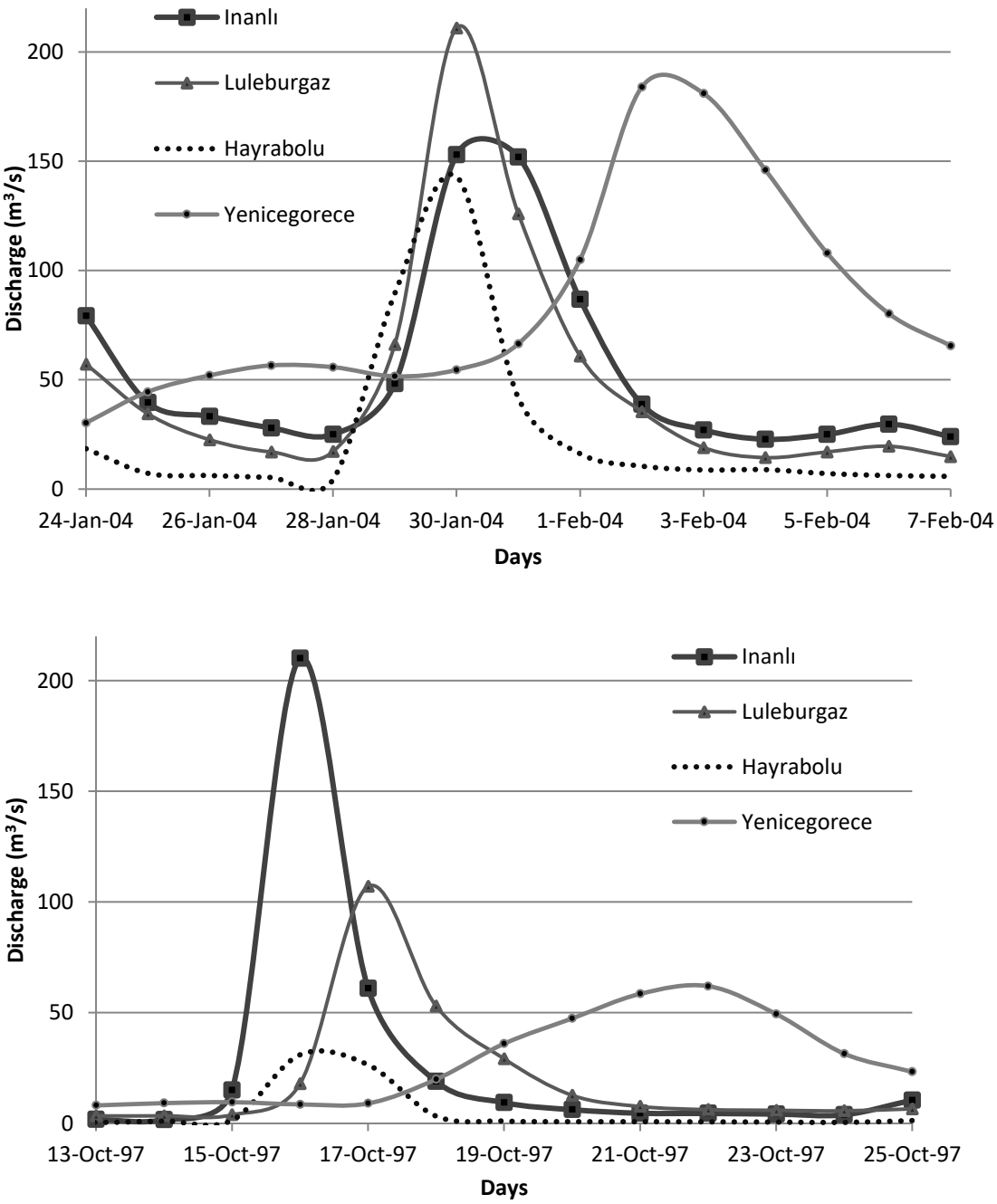

Figure 5.1. Hydrographs of Inanli, Luleburgaz, Hayrabolu and Yenicegoruce streamgages in two different periods: February and October

Table 5.2. FRB model architectures used for Yenicegoruce streamflow predictions

Type of Model	Input Parameters	Output
$M1_Y$	$Q_{I,t}, Q_{L,t}, Q_{H,t}$	$Q_{Y,t}$
$M2_Y$	$Q_{I,t-1}, Q_{I,t}, Q_{L,t-1}, Q_{L,t}, Q_{H,t-1}, Q_{H,t}$	$Q_{Y,t}$
$M3_Y$	$Q_{I,t-2}, Q_{I,t-1}, Q_{I,t}, Q_{L,t-2}, Q_{L,t-1}, Q_{L,t}, Q_{H,t-2}, Q_{H,t-1}, Q_{H,t}$	$Q_{Y,t}$
$M4_Y$	$Q_{I,t-3}, Q_{I,t-2}, Q_{I,t-1}, Q_{I,t}, Q_{L,t-3}, Q_{L,t-2}, Q_{L,t-1},$ $Q_{L,t}, Q_{H,t-3}, Q_{H,t-2}, Q_{H,t-1}, Q_{H,t}$	$Q_{Y,t}$
$M5_Y$	$Q_{I,t-4}, Q_{I,t-3}, Q_{I,t-2}, Q_{I,t-1}, Q_{I,t}, Q_{L,t-4}, Q_{L,t-3}, Q_{L,t-2}, Q_{L,t-1},$ $Q_{L,t}, Q_{H,t-4}, Q_{H,t-3}, Q_{H,t-2}, Q_{H,t-1}, Q_{H,t}$	$Q_{Y,t}$
$M6_Y$	$Q_{I,t-5}, Q_{I,t-4}, Q_{I,t-3}, Q_{I,t-2}, Q_{I,t-1}, Q_{I,t}, Q_{L,t-5},, Q_{L,t-4}, Q_{L,t-3},$ $Q_{L,t-2}, Q_{L,t-1}, Q_{L,t}, Q_{H,t-5}, Q_{H,t-4}, Q_{H,t-3}, Q_{H,t-2}, Q_{H,t-1}, Q_{H,t}$	$Q_{Y,t}$

First, all the sub-models of all six types of models are trained using daily streamflow data of Inanli, Luleburgaz, Hayrabolu and Yenicegoruce streamgages for the duration of October 1996 to November 2003 (1997-2003 water years). Then for each type of model, the best sub-model is selected based on the highest NSE value for the validation phase, which is from October 2003 to November 2005 (2004-2005 water years). These sub-models are referred to as the selected models of each type. Then the best model of the selected models is used to predict daily streamflow at Yenicegoruce streamgage for the testing period, which is from October 2012 to November 2015 (2013-2015 water years).

For each type of model (i.e., models with different inputs), the results of only the selected model are presented in this section. The performances of the selected FRB models of each type for both training and validation periods for Yenicegoruce streamgage are given in Table 5.3. The number of cluster centers, c and cluster radius, r_a are user-defined parameters of an FRB model. In this study, to limit the search space, up to 15 cluster centers and maximum r_a of 0.5 are assumed, and 150 sub-models are developed and evaluated to identify the best c and r_a combination for each type of model. The parameter, r_b is taken as $1.5r_a$ for all models in this thesis (Chiu, 1994). Based on the validation period's performance, the best model is selected for each type. In evaluating the model performance NSE values are used; however, the stability of the model with respect to the increase in the number of cluster centers is also assessed. The model with 1 cluster center is equivalent to multiple linear regression (MLR); therefore, in this study performances of the linear model (i.e., MLR) and non-linear models (FRB) are compared as well.

The best type of model is selected as $M6_Y$ (i.e., $c = 8$ and $r_a = 0.25$) based on the performance indicators given in Table 5.3; so results of all of its sub-models for training and validation periods are given in Tables 5.4 and 5.5, respectively. Although, $M6_Y$ with 13 cluster center and cluster radius of 0.5 provides slightly higher performance in terms of NSE in the validation period, $M6_Y$ with 8 cluster center and cluster radius of 0.25 (see the last row of Table 5.3) is selected, because the model performance for the radius of 0.25 is more stable than that of the model with radius 0.5. On the other hand, $M5_Y$ with 12 cluster centers and cluster radius of 0.2 (see Table 5.3) providing similar performance in terms of NSE and better performance in terms of $PBIAS$ compared to $M6_Y$ with 8 cluster centers and cluster radius of 0.25, can be a another good candidate to be the best model. But having slightly better performance in terms of NSE in the validation period (see Table 5.3), the best model for Yenicegoruce Streamgage is selected to be $M6_Y$. According to Table 5.1, the $M6_y$ has "Satisfactory" performance in terms of R^2 and NSE, and "Good" performance in terms of $PBIAS(\%)$ for the validation period. On the other

hand, for the training period the performance of $M6_y$ is "Very Good" in terms of all goodness of fit measures. The details of $M6_y$ is presented here, and all the sub-models of other types of models are given in Appendix A.

Table 5.3. Model performances of selected models for daily streamflow predictions of Yenicegoruce Streamgage for training and validation periods

	Training				**Validation**			
Yenicegoruce	R	R^2	NSE	$PBIAS$	R	R^2	NSE	$PBIAS$
Selected Model								
$M1_Y$ $(c = 7, r_a = 0.35)$	0.77	0.59	0.57	12.68	0.66	0.44	0.40	-4.53
$M2_Y$ $(c = 12, r_a = 0.25)$	0.83	0.69	0.68	8.43	0.71	0.51	0.38	-6.59
$M3_Y$ $(c = 9, r_a = 0.50)$	0.89	0.80	0.80	5.63	0.80	0.63	0.53	-3.13
$M4_Y$ $(c = 12, r_a = 0.50)$	0.92	0.85	0.85	4.32	0.80	0.63	0.59	0.31
$M5_Y$ $(c = 12, r_a = 0.20)$	0.88	0.77	0.76	5.70	0.83	0.69	0.63	-0.87
$M6_Y$ $(c = 8, r_a = 0.25)$	0.88	0.77	0.76	5.84	0.83	0.68	0.64	-5.41

Table 5.4. NSE values of $M6_Y$ for training phase computed with different number of c and r_a

$M6_Y$ (Training)	r_a									
number of c	**0.05**	**0.10**	**0.15**	**0.20**	**0.25**	**0.30**	**0.35**	**0.40**	**0.45**	**0.50**
1	Und	Und	Und	Und	0.63	0.63	0.63	0.63	0.63	0.63
2	Und	Und	Und	0.64	0.64	0.64	0.65	0.66	0.75	0.76
3	Und	Und	Und	0.69	0.67	0.73	0.74	0.76	0.76	0.76
4	Und	Und	Und	0.72	0.74	0.77	0.77	0.77	0.77	0.77
5	Und	Und	Und	0.73	0.74	0.77	0.77	0.77	0.77	0.77
6	Und	Und	Und	0.72	0.76	0.77	0.78	0.78	0.77	0.77
7	Und	Und	Und	0.75	0.76	0.78	0.78	0.79	0.79	0.79
8	Und	Und	Und	0.75	**0.76**	0.77	0.78	0.79	0.79	0.80
9	Und	Und	Und	0.76	0.76	0.78	0.78	0.79	0.80	0.80
10	Und	Und	Und	0.76	0.78	0.78	0.79	0.81	0.82	0.82
11	Und	Und	Und	0.76	0.78	0.79	0.81	0.81	0.82	0.89
12	Und	Und	Und	0.78	0.77	0.79	0.81	0.81	0.82	0.89
13	Und	Und	Und	0.78	0.77	0.80	0.81	0.84	0.83	0.90
14	Und	Und	Und	0.78	0.79	0.80	0.81	0.84	0.89	0.91
15	Und	Und	Und	0.77	0.79	0.80	0.81	0.85	0.90	0.95

Und: Undefined Model

Table 5.5. NSE values of $M6_Y$ for validation phase computed with different number of c and r_a

$M6_Y$ (Validation)	r_a									
number of c	**0.05**	**0.10**	**0.15**	**0.20**	**0.25**	**0.30**	**0.35**	**0.40**	**0.45**	**0.50**
1	Und	Und	Und	Und	0.52	0.52	0.52	0.52	0.52	0.52
2	Und	Und	Und	0.51	0.52	0.52	0.53	0.54	0.58	0.58
3	Und	Und	Und	0.60	0.52	0.51	0.50	0.58	0.59	0.60
4	Und	Und	Und	0.61	0.57	0.61	0.61	0.61	0.62	0.63
5	Und	Und	Und	0.61	0.57	0.61	0.61	0.61	0.60	0.60
6	Und	Und	Und	0.61	0.64	0.61	0.59	0.59	0.61	0.62
7	Und	Und	Und	0.58	0.64	0.61	0.59	0.58	0.52	0.53
8	Und	Und	Und	0.59	**0.64**	0.61	0.59	0.55	0.52	0.52
9	Und	Und	Und	0.64	0.64	0.62	0.58	0.55	0.45	0.44
10	Und	Und	Und	0.64	0.61	0.62	0.54	0.55	0.55	0.55
11	Und	Und	Und	0.64	0.61	0.57	0.53	0.51	0.54	0.48
12	Und	Und	Und	0.62	0.63	0.52	0.52	0.36	0.54	0.47
13	Und	Und	Und	0.62	0.62	0.45	0.52	0.24	0.59	0.67
14	Und	Und	Und	0.62	0.55	0.44	0.51	0.29	0.39	0.25
15	Und	Und	Und	0.63	0.55	0.49	0.44	0.28	0.09	VL

VL: Model with very low NSE

$M6_y$ (see the last model in Table 5.3) which uses previous five days measurements in addition to the prediction day's streamflow measurements at all three neighboring stations to predict Yenicegoruce streamflow provides the best NSE for the validation phase. For $M6_y$, as can be seen in Tables 5.4 and 5.5, for the models with a comparatively low cluster radius, cluster centers are chosen too close to each other, as they are selected amongst the most frequently observed data points. Hence, the firing degrees for the data points corresponding to extreme events are very low for all rules, so they are rounded to zero, and a division by zero error occurs. Outputs of such models are marked as "Und" to represent undefined in Tables 5.4 and 5.5. In Table 5.4, as the number of cluster centers increases, better NSE values are obtained as expected. Since the increase in the number of cluster centers results in a higher dimensional model, the prediction performance of the FRB increases for the training period. However, for the validation period (see Table 5.5), an increase in the number of cluster centers results in lower NSE performance due to overfitting. This effect is most obvious for cluster radii of 0.35, 0.4, 0.45, and 0.5 (see last four columns of Tables 5.4 and 5.5). The change in NSE with the increase of the number of cluster centers for $M6_Y$ for training and validation data sets for each different cluster radii are given in Figure 5.2. Legend information and axis titles of graphs in Figure 5.2 are presented at the bottom right corner of the figure. To clearly demonstrate the overfitting point, the number of cluster centers is increased up to 20. Furthermore, the number of cluster centers where the validation performance decreases (i.e., overfitting occurs) is different for different cluster radius, as can be seen from Figure 5.2. For instance, for r_a=0.2, the overfitting starts around fifteen cluster centers; while, for r_a=0.35, the overfitting starts around nine cluster centers. The selection of the cluster radius is a critical, yet an unresolved issue. One commonly used approach is to carry out runs for different combinations; thus, to conduct a trial-and-error procedure as applied in this study. Overfitting might result in very low (below zero) NSE values for the validation phase. The details about the models with very low NSE referred to as "VL" in the tables (see Table 5.5), are given in the following sections.

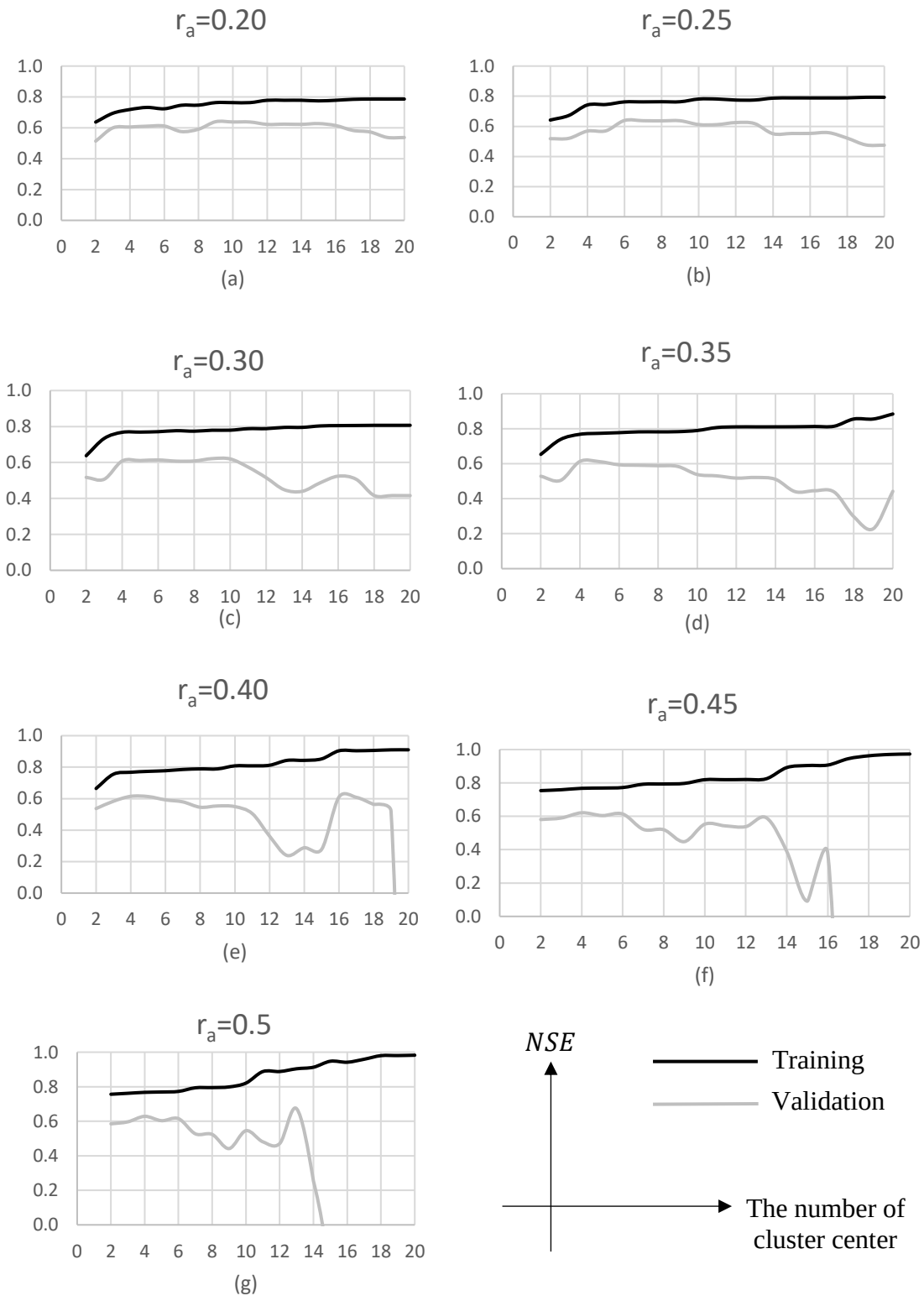

Figure 5.2. Change in NSE according to number of cluster center for $M6_Y$ with various cluster centers

An increase in the cluster radius causes cluster centers to be more distant from each other; thus, events other than usual have better chances to be identified as cluster centers and the data points corresponding to extreme events have higher chances to fire these rules. This may cause the model performance to increase in the training period, as presented in Table 5.4. However, if similar events to the identified unusual events as cluster centers are not observed, the performance of the validation period does not improve. In other words, if unusual events of the training and validation data sets are not similar, the trained model performs poorly for the unusual data points of the validation period since the model has not adjusted/trained properly. Thus, increasing the cluster radius increases the performance for the training period but not necessarily for the validation period.

$M1_Y$ is the simplest FRB Model that uses only prediction day's discharges at the three neighboring stations, and it has unsatisfactory prediction performance for NSE and R^2. As explained at the beginning of this section, the drainage area of the modeled basin is very large and the travel time of streamflow from Inanli to Yenicegoruce streamgage is generally more than three days. Thus, when streamflow observations of the previous couple of days are included into the model as inputs, the performance of the model improves. This shows that analysis of the streamflow data leads to better understanding of the hydrologic response of the studied catchment and provides valuable information for the soft computing method-based model development (i.e., SC-based TS_FRB Model in this study).

FRB model with one cluster centers corresponds to MLR; while investigating effect of the clustering parameters on model performance, the comparison between linear model (i.e., MLR) and non-linear model (i.e., FRB with more than one cluster centers in this study) is carried out as well. The coefficients of the regression equation are obtained by recursive least square algorithm (see Equations 3.7 and 3.8). Coefficients obtained by using the recursive least square algorithm are compared to those obtained using Excel Regression tool. For, $M1_Y$, the regression equation obtained by Excel Regression tool is $Q_{Y,t} = -0.123(Q_{I,t}) + 0.029(Q_{L,t}) + 3.429(Q_{H,t}) + 14.860$.

Exactly same equation is obtained from the FRB model with one rule as well. For example for $r_a = 0.25$ (see Tables 5.4 and 5.5), while linear model (i.e., MLR equivalent) provides NSE values of 0.63 and 0.52 for training and validation periods, respectively, FRB model with eight cluster centers results in 0.76 and 0.64 for these periods. As can be seen from Table 5.4 and 5.5, most of the FRB model outperformed the linear model.

5.1.1.2. Predictions for Yenicegoruce with the test data

The predictions of $M6_Y$ together with the observations for Yenigoruce streamgage for the training period are presented in Figure 5.3. The goodness of fit measures shown in Table 5.1 indicate that the performance of the model is " Very Good". The model results follow the general trend in the observation for the training period as shown in Figure 5.3 and provides reasonable estimates for the peaks on December 28, 2001 (i.e., 554 m^3/s) and on February 8, 2003 (i.e., 576 m^3/s); on the other hand, the model significantly underestimates the peaks on December 8, 1998 (i.e., 857 m3/s) and February 11, 1999 (i.e., 909 m3/s). However, although the peaks on December 8, 1998 and February 11, 1999 are higher than the peak on December 28, 2001 and on February 8, 2003, the model's predictions for the peaks on December 8, 1998 and February 11, 1999 are considerably lower than that of the peak on December 28, 2001 and on February 8, 2003. It indicates that in addition to the magnitude of the data to be predicted, input variables in addition to the selected cluster centers has an important influence on the model performance for extreme events.

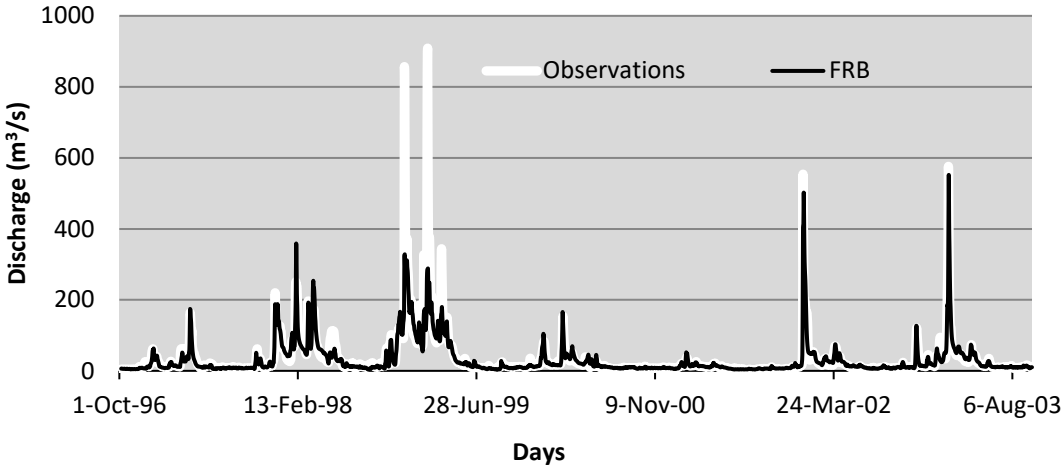

Figure 5.3. Hydrographs obtained from FRB for Yenicegoruce streamgage for the training period

Hydrographs obtained from $M6_Y$ for Yenicegoruce streamgage together with the observations for the validation period are given in Figure 5.4. The graph indicates that predictions of the model follow the general trend in the observations. The largest peak is 184 m^3/s and observed on February 2, 2004. This peak is reasonably well estimated by the model. The peak on February 17, 2005, which is 147 m^3/s, is correctly predicted as 145 m^3/s with two days lag (February 19, 2005). These results indicate that the model has seen similar behavior during the training period and devised appropriate rules to represent these cases. For the peak February 17, 2005 (i.e., 147 m^3/s), $M6_y$ which uses previous five days streamflow measurements in addition to the prediction day's discharges at all three neighboring stations provide nearly exact prediction in terms of the amount of discharge with two days lag. This causes low NSE values for the validation period (see Table 5.5). Thus, lagged inputs which are aimed to represent the travel times (see Figure 5.1) in the basin requires improvement or additional variables need to be added as inputs to the model. Selection of the lagged inputs is challenging because drainage area of Yenicegoruce (i.e., 10402.1 km^2) is much greater than the drainage areas of Luleburgaz, Hayrabolu, and Inanlı (i.e., 2794.5 km^2, 1389.8 km^2, and 1405.1 km^2, respectively); thus the

travel times are large and vary with respect to basin characteristics (i.e., initial moisture content, vegetation, etc.) among the study streamgages. Moreover, discharges and abstractions due to industrial facilities and irrigation purposes are significant in the basin and no input variables are used to quantify these anthropogenic effects on the discharges (Mesta et al., 2019; Gunes and Taninli, 2013; Sungur et al., 2014).

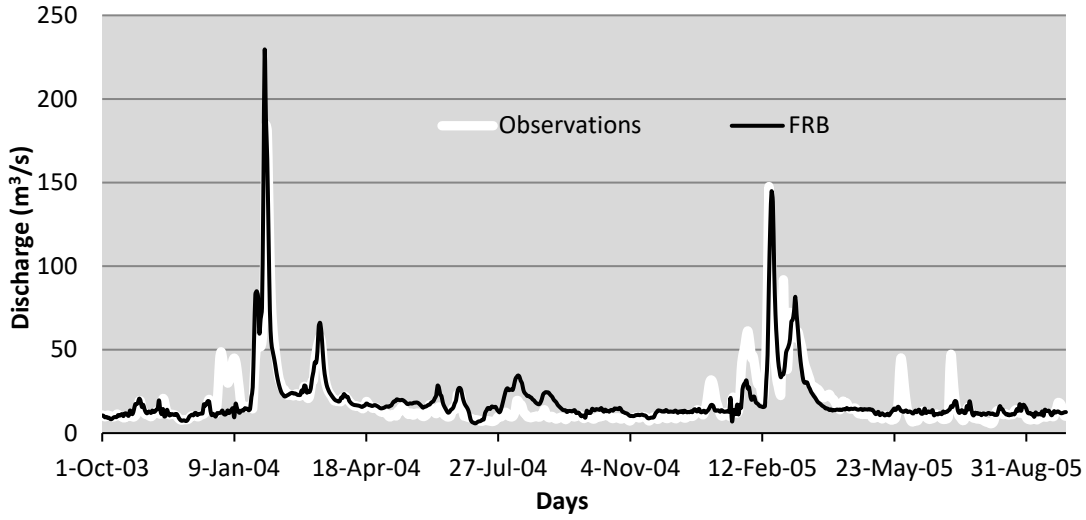

Figure 5.4. Hydrographs obtained from FRB for Yenicegoruce streamgage for the validation period

$M6_y$ amongst all sub-models is the best model based on performance for the validation period for Yenicegoruce. The performance of $M6_y$ for the testing period is given in Table 5.6. According to Table 5.6, $M6_y$ has "Unsatisfactory" performance based on all statistical measures. For Yenicegoruce, mean, maximum and the standard deviation values for the validation period are 18.51 m^3/s, 184 m^3/s, and 18.49 m^3/s, respectively. On the other hand, for testing period, mean, maximum and standard deviation values are 65.56 m^3/s, 701 m^3/s, and 84.03 m^3/s. It clearly shows that the streamflow at Yenicegoruce has very different behavior for the validation and the testing periods. Therefore, since the FRB is selected based on its performance

for the validation period, “Unsatisfactory" predictions for this streamgage is obtained for the testing period.

Table 5.6. Model performances for daily streamflow predictions of Yenicegoruce Streamgage for the testing period

	Test			
Yenicegoruce	R	R^2	NSE	$PBIAS$
$M6_Y$ $(c = 8, r_a = 0.25)$	0.67	0.45	0.24	49.5

Hydrographs obtained from $M6_Y$ for Yenicegoruce streamgage together with the observations for the testing period, are given in Figure 5.5. The graph indicates that the model considerably underestimates the observations. Similar to the training period, there are large peaks in the testing period and these peaks are poorly estimated by the FRB model. Since the number of large peaks is higher in the testing period the performance of the model is poor compared to the training period. The biggest peak (i.e., 701 m^3/s) observed on February 6, 2015 is estimated by the model as 121 m^3/s. On the other hand, on February 5, 2015 (one day before February 6, 2015) the model estimate 245 m^3/s streamflow where the observation is 572 m^3/s. This might be the underestimated prediction of the highest peak with one day lag. These results indicate that travel times from upstream streamgages to downstream ones varies, may be due to current basin characteristics such as vegetation, initial moisture content, etc. and also meteorological conditions. Since only streamflow observations of neighboring gages are used as inputs for the FRB models, such effects are not considered. Thus, although introduction of lagged streamflow observations improves the performance of the FRB model for the validation period, it does not have the same effect for the testing period. This might be due to overfitting of the higher dimensional FRB model.

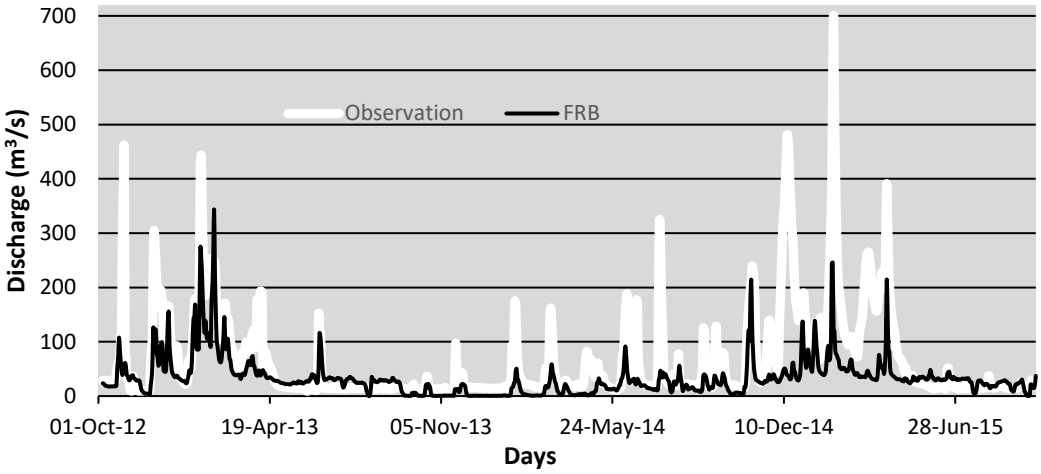

Figure 5.5. Hydrographs obtained from FRB for Yenicegoruce streamgage for the testing period

5.1.2. Inanli Streamgage

5.1.2.1.Analysis on the number of cluster center and the cluster radius

Similar to the procedure followed for Yenicegoruce, Inanli streamgage is assumed to be the subsequently ungauged location as Luleburgaz, Hayrabolu, and Yenicegoruce streamgages are used to predict Inanli's streamflow. Initially, the first type of the model, the base model, $M1_I$ is developed where streamflow records at time t at Luleburgaz ($Q_{L,t}$), Hayrabolu ($Q_{H,t}$) and Yenicegoruce ($Q_{Y,t}$) to predict streamflow at Inanli streamgage at time t ($Q_{I,t}$) (see Table 5.7). As shown in Figure 4.1, Inanlı streamgage is located at the upstream of Luleburgaz streamgage, which is located at the upstream of Yenicegoruce streamgage. Hayrabolu is located at the upstream of Yenicegoruce but on a different tributary. Therefore, to include the effect of the travel times between streamgages, other than $M1_I$, five other types of FRB models are developed to predict $Q_{I,t}$. The architectures of these models are given in Table 5.7.

Table 5.7. Model architectures used for Inanli streamflow predictions

Type of Model	Input Parameters	Output
$M1_I$	$Q_{L,t}, Q_{H,t}, Q_{Y,t}$	$Q_{I,t}$
$M2_I$	$Q_{L,t}, Q_{H,t}, Q_{Y,t}, Q_{Y,t+1}, Q_{Y,t+2}, Q_{Y,t+3}$	$Q_{I,t}$
$M3_I$	$Q_{L,t}, Q_{H,t}, Q_{H,t+1}, Q_{Y,t}, Q_{Y,t+1}, Q_{Y,t+2}, Q_{Y,t+3}$	$Q_{I,t}$
$M4_I$	$Q_{L,t}, Q_{L,t+1}, Q_{H,t}, Q_{H,t+1}, Q_{Y,t}, Q_{Y,t+1}, Q_{Y,t+2}, Q_{Y,t+3}$	$Q_{I,t}$
$M5_I$	$Q_{L,t}, Q_{L,t+1}, Q_{H,t}, , Q_{Y,t+2}, Q_{Y,t+3}$	$Q_{I,t}$
$M6_I$	$Q_{L,t}, Q_{H,t+1}, Q_{Y,t}$	$Q_{I,t}$

Similar to the Yenicegoruce, training, validation, and testing phases are conducted for Inanli streamgage and results are presented in the following paragraphs.

For each type of model, the performances of the selected models are represented in Table 5.8 for training and validation periods. As shown in Table 5.8, $M6_I$ (see the last row of Table 5.8) that uses streamflow measurement at t at Luleburgaz ($Q_{L,t}$) and Yenicegoruce ($Q_{Y,t}$), and $t+1$ at Hayrabolu ($Q_{H,t+1}$) to predict streamflow at t at Inanlı ($Q_{I,t}$), is the best type of model so the results of all of its sub-models for training and validation periods are given in Table 5.9 and 5.10, respectively. As can be seen from Table 5.10, $M6_I$, the model that provides the best validation performance, has 6 cluster centers and the cluster radius is 0.4 (see the last row of Table 5.8). According to Table 5.8, the model has "Satisfactory" performance in terms of NSE, "Good" performance in terms of R^2 and "Unsatisfactory" performance in terms of $PBIAS$ for the validation phase. The model also provides similar performances in terms of all goodness of fit measures for the training phase.

Table 5.8. Model performances of selected models for daily streamflow predictions of Inanli Streamgage for training and validation periods.

	Training				**Validation**			
Inanli	R	R^2	NSE	$PBIAS$	R	R^2	NSE	$PBIAS$
Selected Model								
$M1_I$ $(c = 11, r_a = 0.25)$	0.86	0.74	0.72	8.23	0.87	0.76	0.63	39.89
$M2_I$ $(c = 3, r_a = 0.20)$	0.76	0.57	0.52	6.12	0.86	0.74	0.59	42.51
$M3_I$ $(c = 5, r_a = 0.45)$	0.85	0.72	0.72	7.78	0.85	0.73	0.63	40.29
$M4_I$ $(c = 8, r_a = 0.40)$	0.87	0.75	0.75	7.15	0.83	0.68	0.59	39.68
$M5_I$ $(c = 10, r_a = 0.25)$	0.85	0.73	0.72	7.44	0.84	0.71	0.59	39.98
$M6_I$ $(c = 6, r_a = 0.40)$	0.84	0.70	0.69	8.43	0.89	0.79	0.68	39.87

The results of the sub-models other than $M6_I$ are given in Appendix B. As can be seen from Table 5.9 and 5.10, $M6_I$ provides 0.69 NSE value with 6 cluster center and 0.40 cluster radius. For Inanlı streamgage, the mean flow is 7.76 m^3/s, the maximum flow is 280 m^3/s, and the standard deviation is 17.22 m^3/s for the training phase as presented in Table 4.4. On the other hand, $M6_Y$ provides 0.78 NSE value with 6 cluster center and 0.4 cluster radius for Yenicegoruce streamgage which has 34.36 m^3/s as the mean flow, 909 m^3/s as the maximum flow, and 62.97 m^3/s as the standard deviation for the training phase (see Table 4.4). The reason that FRB provides better NSE with the same number of cluster centers and cluster radius for Yenicegoruce which has more severe extreme events in comparison to Inanlı for the training phase, may be that input pattern of $M6_Y$ provides more degrees of freedom than $M6_I$ to FRB (i.e., a total of 18 and 3 input variables are used for $M6_Y$ and $M6_I$, respectively).

Clusters are formed based on their potential for the SC algorithm. After the first cluster center is assigned having the highest potential amongst all data points, the potentials of the data points are updated to assign the next cluster center. In the potential updating process, the potential of the data point decays exponentially with the square of the distance between that data point and the most previously assigned cluster center (see Equation 3.2). Furthermore, the potential of the current cluster center is updated to zero so that it will not be selected as the next cluster center as well. However, when r_b which is proportional to r_a, increases, the potentials of the data points decay so much that the potentials of the data points become negative. Hence, having zero potential, previous cluster center becomes the data with the highest potential and it is assigned as the next cluster center. This problem repeats while identifying new cluster centers since all the potentials are negative except the one that belongs to the previous cluster center. In other words, the same cluster center is selected as the next cluster center repeatedly. Since, using the same cluster center more than once does not bring any additional information into the model, the performance of the model stays almost the same. Due to the same cluster center being identified repeatedly, for the cluster radius of 0.4, the performance of the model changes very slightly in the training period and validation period as can be seen in Tables 5.9 and 5.10. The models with repeated cluster centers for $M6_I$ with the cluster radius of 0.4 are shaded with grey for demonstration purposes in Tables 9 and 10. In all the other tables instead of gray shade, these kind of models are marked as "RCC" to represent Repeated Cluster Center.

Table 5.9. NSE values of $M6_I$ for training phase computed with different number of c and r_a

$M6_I$ (Training)	r_a									
number of c	**0.05**	**0.10**	**0.15**	**0.20**	**0.25**	**0.30**	**0.35**	**0.40**	**0.45**	**0.50**
1	Und	0.42	0.42	0.42	0.42	0.42	0.42	0.42	0.42	0.42
2	Und	0.41	0.45	0.43	0.49	0.49	0.49	0.49	0.49	0.50
3	Und	0.47	0.49	0.49	0.50	0.52	0.57	0.60	0.62	0.67
4	Und	0.48	0.49	0.48	0.50	0.66	0.59	0.63	0.68	0.69
5	Und	0.46	0.49	0.47	0.53	0.66	0.69	0.69	0.70	0.69
6	Und	0.47	0.49	0.50	0.62	0.66	0.71	**0.69**	0.72	RCC
7	Und	0.51	0.49	0.54	0.63	0.66	0.70	0.69	0.72	RCC
8	Und	0.51	0.50	0.59	0.68	0.69	0.71	0.71	RCC	RCC
9	Und	0.51	0.53	0.59	0.68	0.71	0.72	0.71	RCC	RCC
10	Und	0.50	0.56	0.59	0.70	0.76	0.77	0.72	RCC	RCC
11	Und	0.50	0.56	0.69	0.70	0.78	0.77	0.72	RCC	RCC
12	Und	0.50	0.55	0.69	0.72	0.80	0.76	0.72	RCC	RCC
13	Und	0.50	0.59	0.69	0.72	0.80	0.80	0.72	RCC	RCC
14	Und	0.50	0.59	0.70	0.74	0.82	0.80	0.73	RCC	RCC
15	Und	0.52	0.61	0.70	0.75	0.84	RCC	0.73	RCC	RCC

RCC: Repeated Cluster Centers

Table 5.10. NSE values of $M6_I$ for validation phase computed with different number of c and r_a

$M6_I$ (Validation)	r_a									
number of c	**0.05**	**0.10**	**0.15**	**0.20**	**0.25**	**0.30**	**0.35**	**0.40**	**0.45**	**0.50**
1	Und	0.59	0.59	0.59	0.59	0.59	0.59	0.59	0.59	0.59
2	Und	0.60	0.58	0.59	0.58	0.58	0.58	0.58	0.58	0.58
3	Und	0.59	0.59	0.59	0.57	0.56	0.56	0.57	0.56	0.59
4	Und	0.58	0.59	0.59	0.57	0.58	0.58	0.60	0.64	0.63
5	Und	0.58	0.59	0.59	0.60	0.59	0.63	0.68	0.66	0.63
6	Und	0.58	0.59	0.57	0.55	0.59	0.64	**0.68**	0.67	RCC
7	Und	0.58	0.59	0.56	0.57	0.62	0.66	0.68	0.64	RCC
8	Und	0.58	0.57	0.56	0.62	0.67	0.66	0.67	RCC	RCC
9	Und	0.58	0.56	0.57	0.62	0.67	0.63	0.67	RCC	RCC
10	Und	0.58	0.59	0.57	0.60	0.66	0.43	0.67	RCC	RCC
11	Und	0.58	0.59	0.59	0.59	0.52	0.55	0.67	RCC	RCC
12	Und	0.57	0.59	0.59	0.64	0.32	0.53	0.67	RCC	RCC
13	Und	0.57	0.56	0.56	0.64	0.26	0.43	0.67	RCC	RCC
14	Und	0.57	0.56	0.54	0.66	0.03	0.33	0.66	RCC	RCC
15	Und	0.56	0.52	0.54	0.66	VL	RCC	0.66	RCC	RCC

The rule-base of $M6_I$ is presented in Table 5.11. The membership functions of each fuzzy rule are given in Figure 5.6. As the number of cluster centers increases, the data points corresponding to extreme events have higher chances of becoming cluster centers. For example, while the first cluster center consists of lower streamflow measurements, the sixth cluster center consists of much higher streamflow values, as presented in Table 5.11 and Figure 5.6. If similar behavior to the ones identified by the higher number of cluster centers are observed during the training and testing periods the performance of the model improves. However, it is observed that generally utilization of only streamflow observations of neighboring gages is not sufficient to model system behavior (i.e., rainfall-runoff relationship). One remedy for this may be adding other input variables – demonstrating existing basin characteristics such as vegetation, initial moisture content, etc. – and meteorological conditions – season, previous rainfall events, etc. – to the FRB model.

Table 5.11. The cluster centers (fuzzy rules) for $M6_I$

	#	Year	Month	Day	Cluster Centers (in m^3/s)			
					Antecedent Part of the Fuzzy Rules			Output
					$Q_{L,t}$	$Q_{H,t+1}$	$Q_{Y,t}$	$Q_{I,t}$
Original	1	1999	7	31	4.51	1.14	9.58	2.90
	2	2003	2	20	14.80	11.80	64.70	10.40
	3	2003	2	11	46.40	33.60	222.00	31.30
	4	2003	4	14	12.30	6.59	69.30	8.41
	5	2003	2	3	171.00	39.20	112.00	135.00
	6	1998	12	12	84.50	72.60	293.00	115.00
Normalized	1	1999	7	31	0.10	0.14	0.33	0.14
	2	2003	2	20	0.29	0.51	0.60	0.36
	3	2003	2	11	0.49	0.72	0.79	0.57
	4	2003	4	14	0.26	0.40	0.61	0.32
	5	2003	2	3	0.72	0.76	0.69	0.85
	6	1998	12	12	0.60	0.88	0.83	0.82

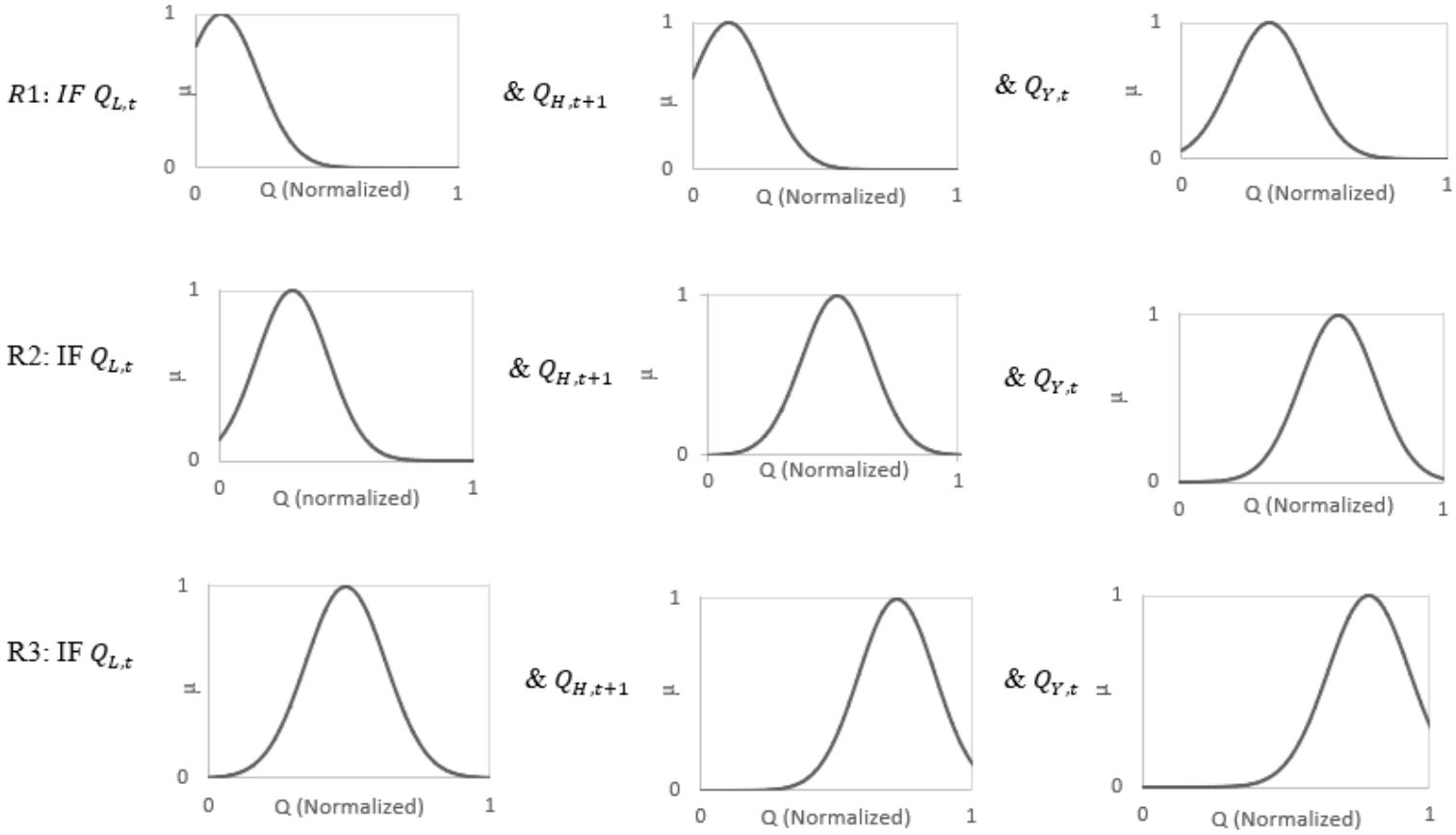

Figure 5.6. Membership functions of the Fuzzy Rules for $M6_I$

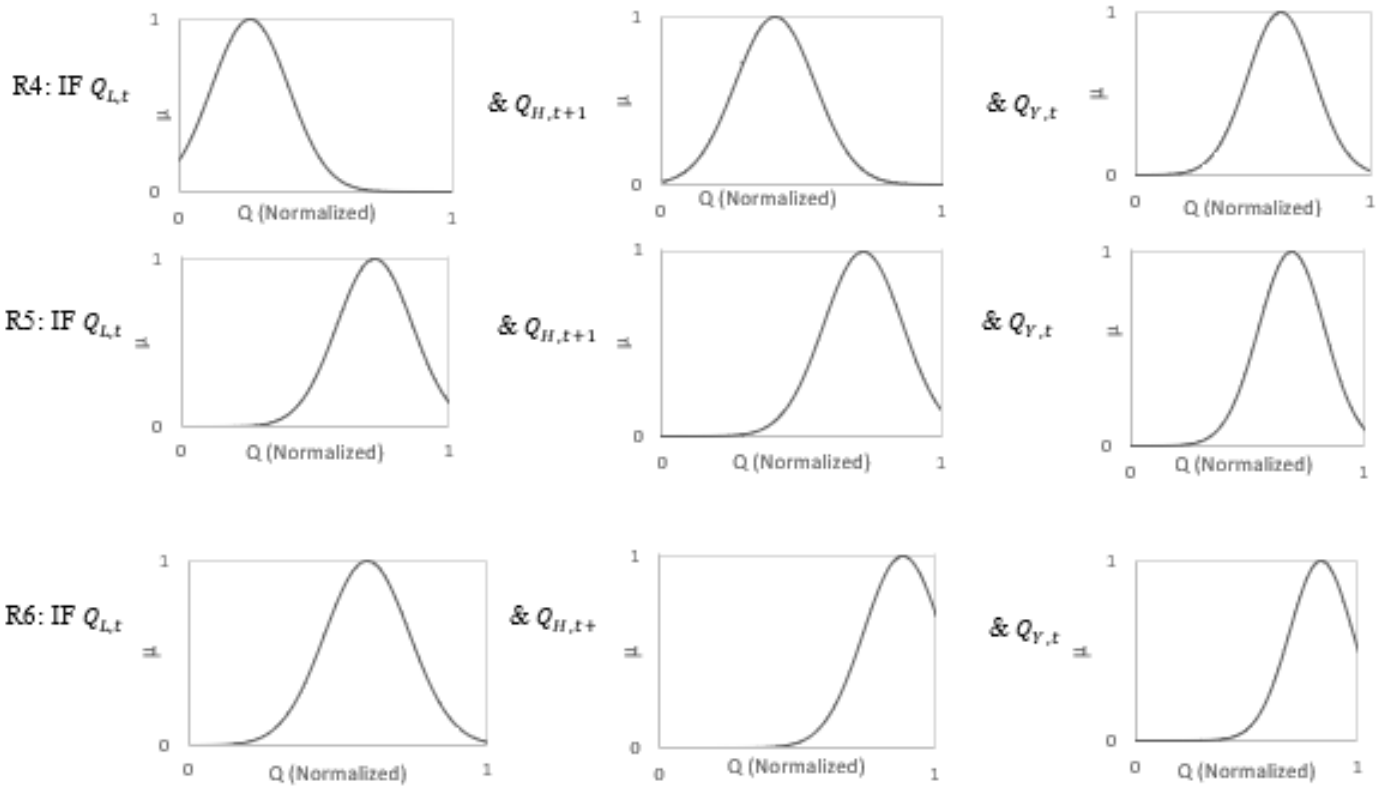

Figure 5.6. Antecedent Part of the Fuzzy Rules for $M6_I$ (Cont'd)

5.1.2.2.Predictions for Inanli with the test data

The predictions obtained from $M6_I$ together with the observations for Inanli streamflow for the training period are presented in Figure 5.7. Although the model results follow the trend in observations for the training phase on Inanli, the peak flows are not reasonably predicted. The reason for this may be insufficient representation of extreme events in the rule-base. As can be seen from Table 5.11, the largest streamflow for Inanlı corresponds to the fifth fuzzy rule and it is 135 m^3/s. Thus, prediction of higher streamflow values with the rule-base given in Table 5.11 is limited. "Good" predictions of high streamflow values at Inanlı can only be generated with streamflow patterns that are similar to the ones given in the fifth fuzzy rule in Table 5.11. Different streamflow patters which may result from different rainfall patterns in the basin may generate high streamflow values at Inanlı, but there are not any rules in the rule-base to represent these cases. Moreover, basin conditions are not included in the FRB model at all and they may affect rainfall-runoff response as well. As can be seen from Table 5.9, the model provides NSE values up to 0.84 for the training period for Inanli streamgage. However, this model provides very low NSE values for the validation period.

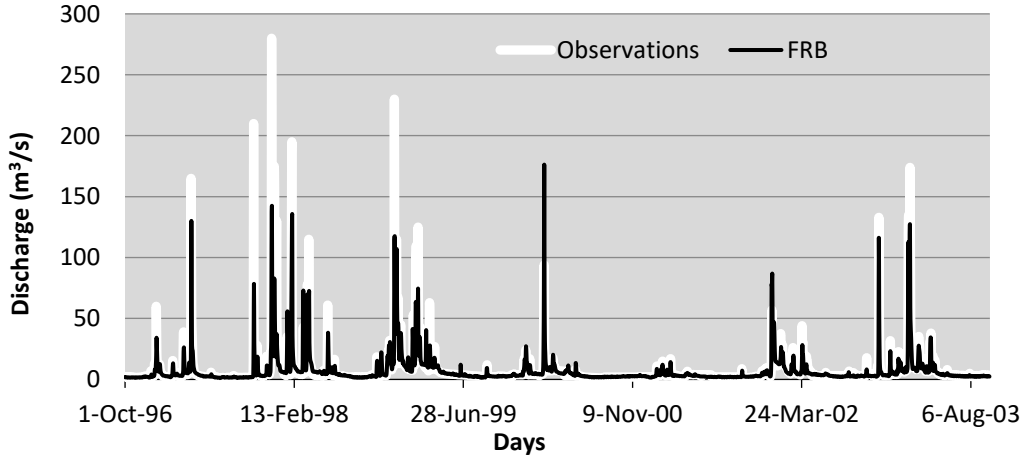

Figure 5.7. Hydrographs obtained from FRB for Inanli streamgage for the training period

Hydrographs obtained from $M6_I$ for Inanli streamflow for the validation period are presented in Figure 5.8. According to these hydrographs, the model follows the general trend in the observations. Both peaks, which are 153 m^3/s observed on January 30, 2004 and 120 m^3/s observed on January 23, 2004 are reasonably well predicted by the model. However, as can be seen from Figure 5.8, for the period from February 2004 to July 2004, although the model can simulate the trend in observations, predicted values are less than the observations. This might be due to the problem of external discharges (i.e., discharges of industrial facilities) or malfunctioning of the gage during this period.

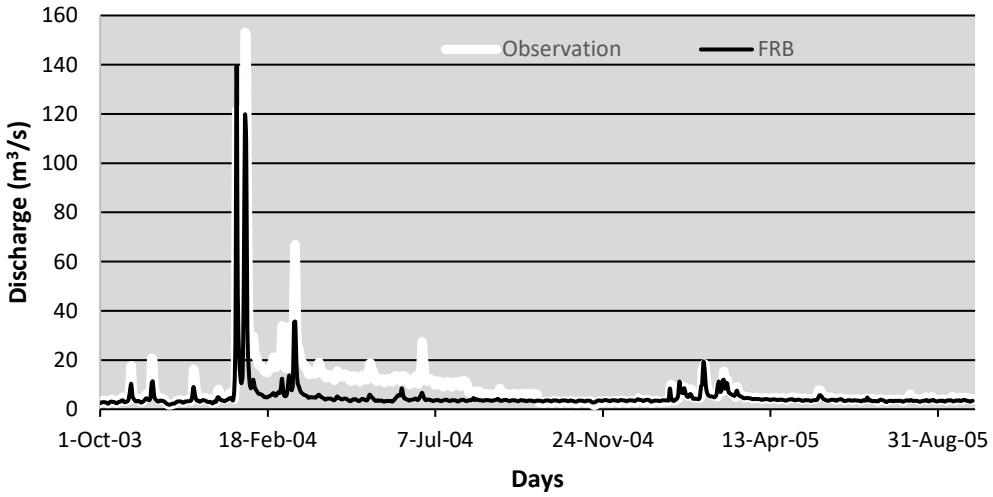

Figure 5.8. Hydrographs obtained from FRB for Inanli streamgage for the validation period

$M6_I$ amongst all sub-models provides the highest NSE value for the validation period for Inanli streamgage. The predictions using $M6_I$ are obtained and the performance of the model for the testing period is presented in Table 5.12. According to Table 5.12., the $M6_I$ provides "Satisfactory" performance in terms of R^2,

"Satisfactory (almost Good)" performance in terms of NSE and "Good" performance in terms of $PBIAS$ for the testing period. The reason for this may be the fact that the validation and the test period have similar flow behavior so that the model provides "Satisfactory" estimations for the testing period.

Table 5.12. Model performances for daily streamflow predictions of Inanli Streamgage for the testing period

	Test			
Inanli	R	R^2	NSE	$PBIAS$
$M6_I$ $(c = 6, r_a = 0.40)$	0.84	0.70	0.69	7.67

Hydrographs obtained from $M6_I$ and observations for Inanli streamflow for the testing period are presented in Figure 5.9. The model reasonably estimated the peak flows for the testing period. The reason is that similar streamflow behavior that are presented by the rule-base given in Table 5.11 occurred in the testing period. In addition to Table 5.12, Figure 5.9 also indicates that the model has been adequately trained and can provide "Good" estimations.

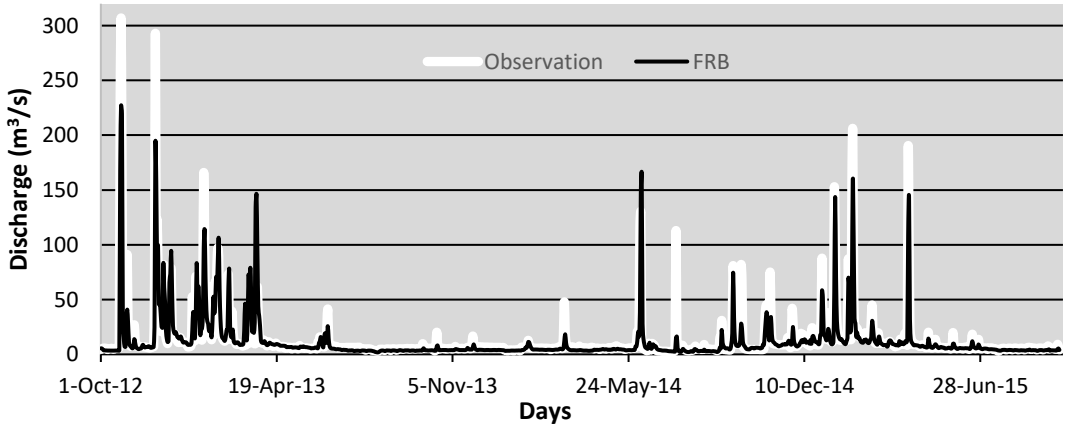

Figure 5.9. Hydrographs obtained from FRB for Inanli streamgage for the testing period

As can be seen in Table 5.10, some the number of cluster center and radius combinations result in very low NSE values. For example, NSE value provided by $M6_I$ with 15 cluster centers and cluster radius of 0.3 is -0.88 (see last row of Table 5.10) as "VL". This model is an example of an overtrained model. The hydrograph obtained from the overtrained (OT) FRB ($M6_I$ with 15 cluster centers and cluster radius of 0.3) for Inanlı for the validation phase is given in Figure 5.10. The OT FRB follows the general trend in the observation similar to $M6_I$ as presented in Figure 5.10. However, two streamflow observations 48.3 m^3/s observed on January 29, 2004 and 153 m^3/s observed on January 30, 2004 are predicted by the OT FRB as 391.3 m^3/s and 322.5 m^3/s, respectively. Due to overtraining, these streamflow observations are overestimated by the OT FRB which results in very low NSE.

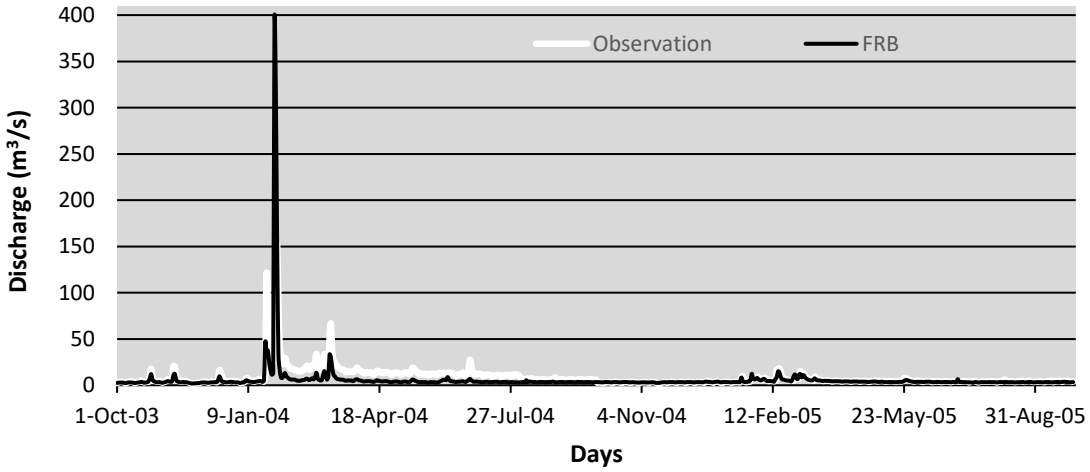

Figure 5.10. Hydrographs obtained from the overtrained FRB model ($M6_I$ with $c = 15, \quad r_a = 0.30$) for Inanli streamgage for the validation period

5.1.3. Luleburgaz streamgage

5.1.3.1. Analysis of the number of cluster center and the cluster radius

Similar to Yenicegoruce and Inanlı streamgages, Luleburgaz is assumed to be the subsequently ungauged location and Inanli, Hayrabolu, and Yenicegoruce streamgages are used to predict Luleburgaz's streamflow. The first type of the model, the base model $M1_L$, which uses streamflow records at time t at Inanli ($Q_{I,t}$), Hayrabolu ($Q_{H,t}$) and Yenicegoruce ($Q_{Y,t}$) to predict streamflow at Luleburgaz streamgage at time t ($Q_{L,t}$) is developed initially. Similar to Yenicegoruce and Inanli, considering different travel times, four other types of FRB models, in addition to the base model are built to make predictions at Luleburgaz streamgage. The architectures of these models are presented in Table 5.13.

Table 5.13. Model architectures used for Luleburgaz streamflow predictions

Type of Model	Input Parameters	Output
$M1_L$	$Q_{I,t}, Q_{H,t}, Q_{Y,t}$	$Q_{L,t}$
$M2_L$	$Q_{I,t}, Q_{H,t}, Q_{Y,t}, Q_{Y,t+1}, Q_{Y,t+2}, Q_{Y,t+3}$	$Q_{L,t}$
$M3_L$	$Q_{I,t-1}, Q_{I,t}, Q_{H,t}, Q_{Y,t}, Q_{Y,t+1}, Q_{Y,t+2}, Q_{Y,t+3}$	$Q_{L,t}$
$M4_L$	$Q_{I,t-1}, Q_{I,t}, Q_{H,t}, , Q_{H,t+1}, Q_{Y,t}, Q_{Y,t+1}, Q_{Y,t+2}, Q_{Y,t+3}$	$Q_{L,t}$
$M5_L$	$Q_{I,t}, Q_{H,t}, Q_{Y,t+3}$	$Q_{L,t}$

Similar to Yenicegoruce and Inanli, training, validation and testing is performed for Luleburgaz streamgage and presented in the following paragraphs.

For each type of model, the performances of the selected models are represented in Table 5.14 for the training and validation periods. The model with 5 cluster centers

and the cluster radius of 0.15 (see the last row of Table 5.14) provides the best validation performance; thus, the results of all of its sub-models for training and validation periods are given in Tables 5.15 and 5.16, respectively. The model with 11 cluster centers and 0.1 radius provides an NSE of 0.83 for the validation period as shown in Table 5.16. This is only slightly better than the performance of the model with 5 cluster centers and radius of 0.15. Thus, it is considered that introduction of six additional cluster centers is not justified, so the model with five cluster centers is identified as the best model. $M5_L$ which uses streamflow measurement at time t at Inanli ($Q_{I,t}$) and Hayrabolu ($Q_{H,t}$), and at time $t+3$ at Yenicegoruce to predict streamflow at time t at Luleburgaz is the best model. The results of other sub-models for Luleburgaz streamgage are given in Appendix C.

Table 5.14. Model performances of selected for daily streamflow predictions of Luleburgaz Streamgage for training and validation periods

	Training				**Validation**			
Luleburgaz	R	R^2	NSE	$PBIAS$	R	R^2	NSE	$PBIAS$
Selected Model								
$M1_L$ $(c=5, r_a=0.20)$	0.73	0.53	0.50	10.34	0.91	0.83	0.80	-22.78
$M2_L$ $(c=2, r_a=0.25)$	0.78	0.61	0.56	10.14	0.85	0.71	0.69	-21.00
$M3_L$ $(c=2, r_a=0.15)$	0.78	0.61	0.55	10.44	0.81	0.66	0.60	-26.56
$M4_L$ $(c=2, r_a=0.15)$	0.78	0.60	0.54	10.56	0.81	0.65	0.59	-26.94
$M5_L$ $(c=5, r_a=0.15)$	0.75	0.56	0.52	10.04	0.92	0.84	0.82	-19.35

According to Table 5.14, the model has "Very Good" performance in terms of NSE, "Good" performance in terms of R^2 and "Unsatisfactory" performance in terms of

PBIAS for the validation period. However, for the training period, the model has lower prediction performance compared to its prediction performance in the validation period. This is because of the differences between the frequency and magnitude of the extreme event of the training and validation periods, as presented in Table 4.4. While Luleburgaz streamgage has 12.13 m^3/s as the mean flow, 32.20 m^3/s as the standard deviation, and 800 m^3/s as its maximum flow for the training period, it has 7.88 m^3/s as the mean flow, 10.61 m^3/s as the standard deviation, and 211 m^3/s as its maximum flow for the validation period. This indicates that the training period has examples of all types of flow behaviors found in the validation period; thus, the model is trained well to predict the streamflows of the validation period.

Table 5.15. NSE values of $M5_L$ for training phase computed with different number of c and r_a

$M5_L$ (Training)	r_a									
number of c	**0.05**	**0.10**	**0.15**	**0.20**	**0.25**	**0.30**	**0.35**	**0.40**	**0.45**	**0.50**
1	Und	Und	0.49	0.49	0.49	0.49	0.49	0.49	0.49	0.49
2	Und	0.50	0.50	0.50	0.51	0.51	0.52	0.52	0.52	0.52
3	Und	0.52	0.51	0.51	0.52	0.53	0.52	0.52	0.51	0.51
4	Und	0.52	0.51	0.52	0.52	0.53	0.52	0.52	0.51	0.52
5	Und	0.51	**0.52**	0.52	0.53	0.52	0.52	0.52	0.53	0.54
6	Und	0.51	0.52	0.52	0.53	0.52	0.52	0.53	0.54	RCC
7	Und	0.52	0.53	0.53	0.53	0.53	0.53	0.54	0.61	RCC
8	Und	0.53	0.53	0.53	0.52	0.53	0.59	RCC	RCC	RCC
9	Und	0.52	0.55	0.53	0.52	0.60	0.59	RCC	RCC	RCC
10	Und	0.52	0.53	0.52	0.52	0.61	0.58	RCC	RCC	RCC
11	Und	0.53	0.53	0.52	0.56	0.61	0.63	RCC	RCC	RCC
12	Und	0.53	0.53	0.52	0.61	0.61	RCC	RCC	RCC	RCC
13	Und	0.52	0.53	0.52	0.63	0.61	RCC	RCC	RCC	RCC
14	Und	0.53	0.53	0.52	0.63	0.62	RCC	RCC	RCC	RCC
15	Und	0.55	0.52	0.53	0.63	0.65	RCC	RCC	RCC	RCC

Table 5.16. NSE values of $M5_L$ for validation phase computed with different number of c and r_a

$M5_L$ (Validation)	r_a									
number of c	**0.05**	**0.10**	**0.15**	**0.20**	**0.25**	**0.30**	**0.35**	**0.40**	**0.45**	**0.50**
1	Und	Und	0.76	0.76	0.76	0.76	0.76	0.76	0.76	0.76
2	Und	0.78	0.79	0.79	0.80	0.81	0.80	0.80	0.80	0.79
3	Und	0.79	0.79	0.79	0.78	0.77	0.76	0.75	0.75	0.74
4	Und	0.78	0.79	0.78	0.75	0.77	0.75	0.73	0.71	0.70
5	Und	0.78	**0.82**	0.78	0.76	0.76	0.73	0.71	0.67	0.66
6	Und	0.78	0.80	0.77	0.76	0.76	0.74	0.64	0.52	RCC
7	Und	0.77	0.77	0.73	0.78	0.74	0.72	0.57	0.45	RCC
8	Und	0.81	0.76	0.76	0.77	0.74	0.63	RCC	RCC	RCC
9	Und	0.81	0.74	0.77	0.76	0.60	0.68	RCC	RCC	RCC
10	Und	0.81	0.73	0.77	0.75	0.53	0.70	RCC	RCC	RCC
11	Und	0.83	0.73	0.76	0.67	0.54	0.70	RCC	RCC	RCC
12	Und	0.83	0.73	0.76	0.59	0.53	RCC	RCC	RCC	RCC
13	Und	0.80	0.75	0.77	0.44	0.51	RCC	RCC	RCC	RCC
14	Und	0.78	0.79	0.77	0.44	0.52	RCC	RCC	RCC	RCC
15	Und	0.76	0.78	0.75	0.44	0.55	RCC	RCC	RCC	RCC

5.1.3.2. Predictions for Luleburgaz with the test data

The hydrographs obtained from $M5_L$ together with the observations are given for the training period in Figure 5.11. The model underestimates all the peak flows observed during the training period. It indicates that the number of cluster centers and cluster radius used to build the model, are not capable of predicting streamflow at Luleburgaz.

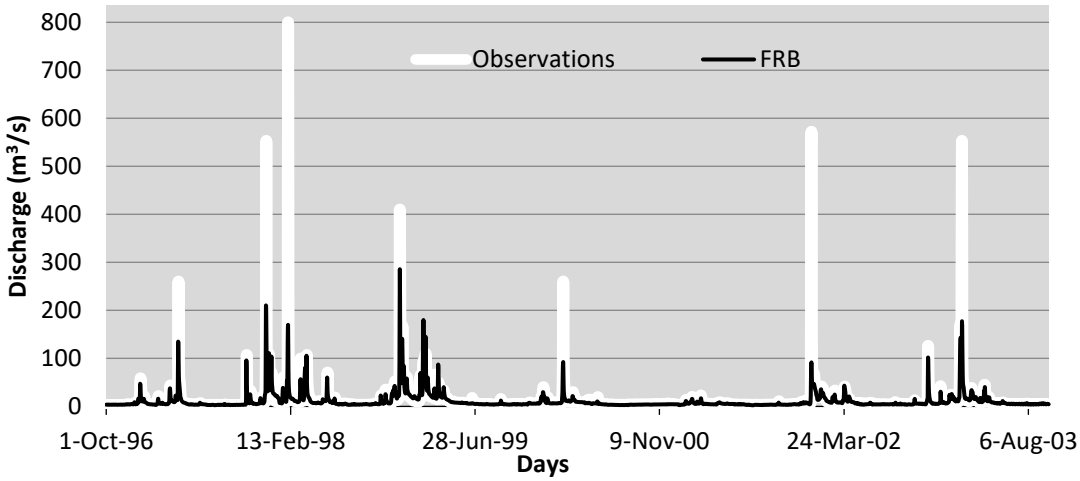

Figure 5.11. Hydrographs obtained from FRB for Luleburgaz streamgage for the training period

The hydrographs obtained from $M5_L$ and observations for the validation period are given in Figure 5.12. The peak flow, which is 89.3 m^3/s and observed on January 23, 2004, is reasonably predicted by the model; however, the other peak flow, which is 211 m^3/s and observed on January 30, 2004, is underestimated by the model. It indicates that the model has seen similar discharges to the discharges to the one observed on January 23, 2004; however, discharges observed on January 30, result from a different meteorological condition and basin characteristics combination from what the FRB is trained for.

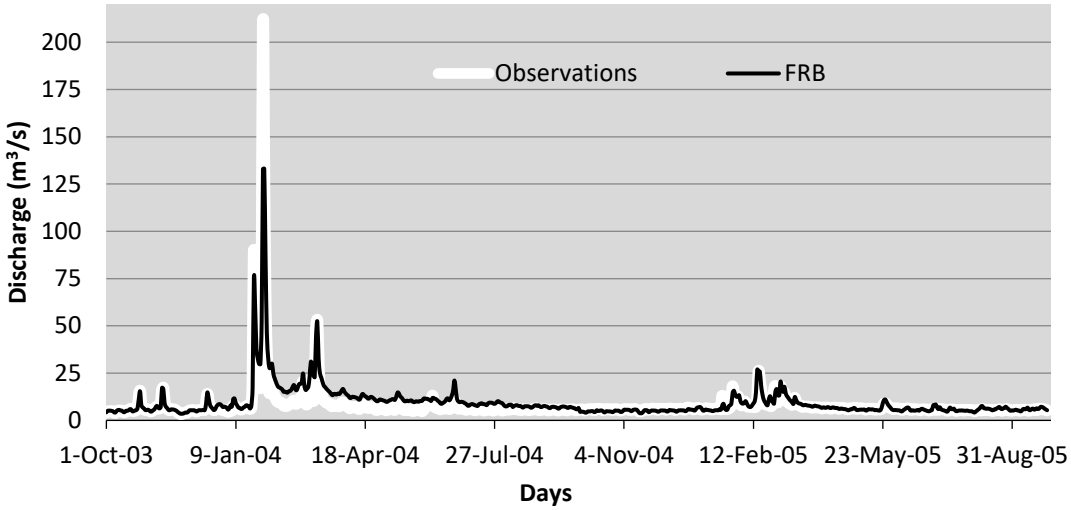

Figure 5.12. Hydrographs obtained from FRB for Luleburgaz streamgage for the validation period

$M5_L$ providing the highest NSE for the validation period is selected as the best type of model for Luleburgaz. The predictions for the testing period are obtained by using $M5_L$. The performance of the model for the testing period is presented in Table 5.17. According to Table 5.17, FRB provides "Satisfactory (almost "Good")" performance in terms of R^2 and NSE, and "Good" performance in terms of $PBIAS$. It indicates that FRB is trained and validated efficiently. Trial-and-error procedure to determine the number of cluster centers and the cluster radius provides satisfactory results for Luleburgaz streamgage.

Table 5.17. Model performances for daily streamflow predictions of Luleburgaz Streamgage for the testing period

	Test			
Luleburgaz	R	R^2	NSE	$PBIAS$
$M5_L$ $(c = 5, r_a = 0.15)$	0.86	0.73	0.69	9.65

The hydrographs obtained from the $M5_L$ are given for the testing period in Figure 5.13. According to the hydrographs, the model follows the general trend in the observations for the testing period. Considering that the peak flows observed on the testing period are more extreme and occur more frequently compared to the ones observed in the validation period, the model provides reasonable estimations for these peak flows. The highest peak, which is 376 m^3/s observed on December 2, 2012 is estimated by FRB as 245 m^3/s. The other peak flow which is 365 m^3/s and observed on February 3, 2015 is estimated by FRB as 255 m^3/s, which are acceptable estimates.

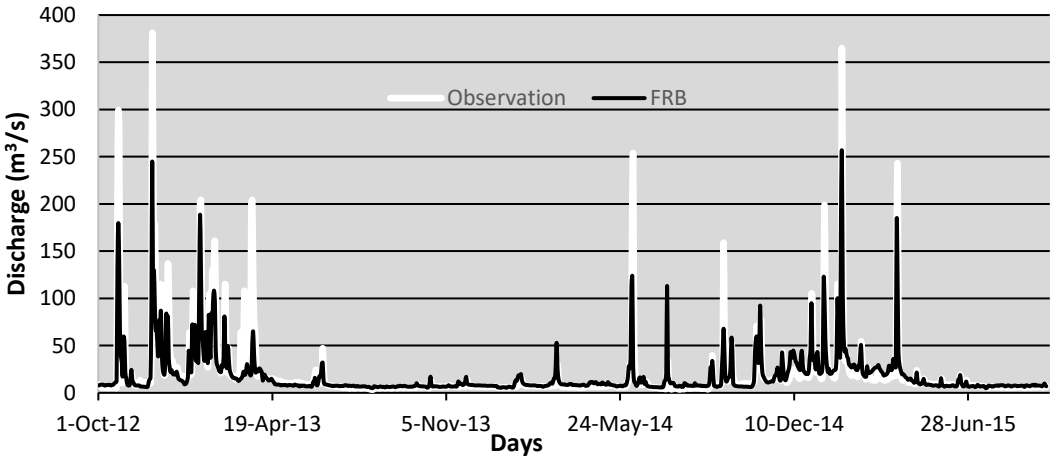

Figure 5.13. Hydrographs obtained from FRB for Luleburgaz streamgage for the testing period

5.1.4. Hayrabolu Streamgage

5.1.4.1. Analysis of the number of cluster center and the cluster radius

Similar to the procedure followed for Yenicegoruce, Inanli and Luleburgaz, Hayrabolu is assumed to be subsequently ungaged location as records of Inanli, Luleburgaz and Yenicegoruce streamgages are used to predict streamflow at Hayrabolu. Initially, the first type of the model, the base model $M1_H$, is developed by using the streamflow records at time t at Inanli ($Q_{I,t}$), Luleburgaz ($Q_{L,t}$) and Yenicegoruce ($Q_{Y,t}$) to predict streamflow at Hayrabolu streamgage at time t ($Q_{H,t}$). Considering the travel time of streamflow between subbasins, in addition to the base model, four different type of models are built to predict $Q_{H,t}$. The architectures of these models are given in Table 5.18.

Table 5.18. Model performances for daily streamflow predictions of Hayrabolu Streamgage

Type of Model	Input Parameters	Output
$M1_H$	$Q_{I,t}, Q_{L,t}, Q_{Y,t}$	$Q_{H,t}$
$M2_H$	$Q_{I,t}, Q_{L,t}, Q_{Y,t}, Q_{Y,t+1}, Q_{Y,t+2}, Q_{Y,t+3}$	$Q_{H,t}$
$M3_H$	$Q_{I,t-1}, Q_{I,t}, Q_{L,t}, Q_{Y,t}, Q_{Y,t+1}, Q_{Y,t+2}, Q_{Y,t+3}$	$Q_{H,t}$
$M4_H$	$Q_{I,t-1}, Q_{I,t}, Q_{L,t-1}, Q_{L,t}, Q_{Y,t}, Q_{Y,t+1}, Q_{Y,t+2}, Q_{Y,t+3}$	$Q_{H,t}$
$M5_H$	$Q_{I,t}, Q_{L,t-1}, Q_{L,t}, Q_{Y,t}, Q_{Y,t+1}, Q_{Y,t+2}$	$Q_{H,t}$

Similar to the Yenicegoruce, Inanli, and Luleburgaz, training, validation and testing is carried out for Hayrabolu streamgage and results are presented below.

For each type of model, the performances provided by the selected model for both training and validation periods are given in Table 5.19 for Hayrabolu. As presented in Table 5.19, $M3_H$ (see the third row of Table 5.19) that uses streamflow records at Inanli at time t, $t-1$ ($Q_{I,t-1}, Q_{I,t}$), at Luleburgaz at time t ($Q_{L,t}$) and at Yenicegoruce at time $t, t+1, t+2, t+3$ ($Q_{Y,t}, Q_{Y,t+1}, Q_{Y,t+2}, Q_{Y,t+3}$) is selected as the best type of model; therefore, the results of its sub-models for training and the validation periods are presented in Tables 5.20 and 5.21, respectively. Although, $M5_H$ provides slightly higher performance than $M3_H$, $M3_H$ is selected as the best model, since the large number of cluster centers used in $M5_H$ makes the model computationally expensive and introduces risk of overfitting without significant improvement in the goodness of fit measures. According to Table 5.19, $M3_H$ has "Satisfactory" performance in terms of R^2 and NSE, and "Unsatisfactory" performance in terms of "$PBIAS$" for the validation period. On the other hand, the model has "Very good" performance in terms of NSE and "Good" performance in terms of R^2 and $PBIAS$ for the training period. In comparison, the other models presented in table 5.19, better performance of $M3_H$ with a relatively low number of cluster centers on the training period might be because of the relatively higher cluster radius, which allows the model to select the extreme events as cluster centers.

Table 5.19. Model performances of selected models for daily streamflow predictions of Hayrabolu Streamgage

	Training				**Validation**			
Hayrabolu	R	R^2	NSE	$PBIAS$	R	R^2	NSE	$PBIAS$
Selected Model								
$M1_H\ (c = 7, r_a = 0.25)$	0.83	0.68	0.68	13.69	0.66	0.43	0.42	8.77
$M2_H\ (c = 13, r_a = 0.30)$	0.92	0.84	0.84	9.04	0.79	0.63	0.56	16.30
$M3_H\ (c = 6, r_a = 0.45)$	0.91	0.82	0.82	9.89	0.79	0.63	0.55	16.33
$M4_H\ (c = 8, r_a = 0.30)$	0.90	0.80	0.80	8.24	0.74	0.54	0.49	15.58
$M5_H\ (c = 7, r_a = 0.50)$	0.90	0.81	0.81	9.52	0.76	0.60	0.54	14.93

For relatively low number of cluster centers and cluster radii, the NSE values provided by the model for validation and training phase are low, as can be seen from Table 5.20 and Table 5.21. The results of the other sub-models of other types of models for Hayrabolu streamgage are given in Appendix D.

Table 5.20. NSE values of $M3_H$ for the training phase with different number of c and r_a

$M3_H$ (Training)	r_a									
number of c	**0.05**	**0.10**	**0.15**	**0.20**	**0.25**	**0.30**	**0.35**	**0.40**	**0.45**	**0.50**
1	Und	Und	0.70	0.70	0.70	0.70	0.70	0.70	0.70	0.70
2	Und	Und	0.69	0.64	0.64	0.64	0.64	0.64	0.65	0.65
3	Und	Und	0.65	0.64	0.63	0.63	0.61	0.62	0.65	0.63
4	Und	Und	0.64	0.65	0.69	0.65	0.75	0.76	0.76	0.77
5	Und	Und	0.64	0.59	0.69	0.75	0.72	0.77	0.81	0.79
6	Und	Und	0.65	0.60	0.61	0.76	0.77	0.79	**0.82**	0.83
7	Und	Und	0.62	0.64	0.77	0.76	0.80	0.82	0.84	0.84
8	Und	Und	0.62	0.65	0.78	0.79	0.83	0.82	0.86	0.86
9	Und	Und	0.62	0.66	0.78	0.83	0.83	0.85	0.87	0.87
10	Und	Und	0.63	0.71	0.81	0.83	0.85	0.86	0.87	0.87
11	Und	Und	0.64	0.75	0.82	0.85	0.86	0.87	0.88	0.87
12	Und	0.63	0.65	0.75	0.82	0.86	0.87	0.87	0.90	RCC
13	Und	0.63	0.69	0.75	0.82	0.87	0.87	0.87	0.89	RCC
14	Und	0.61	0.74	0.75	0.82	0.88	0.86	0.89	0.91	RCC
15	Und	0.61	0.73	0.75	0.82	0.87	0.87	0.89	0.92	RCC

Table 5.21. NSE values of $M3_H$ for the validation phase with different number of c and r_a

$M3_H$ (Validation)	r_a									
number of c	**0.05**	**0.10**	**0.15**	**0.20**	**0.25**	**0.30**	**0.35**	**0.40**	**0.45**	**0.50**
1	Und	Und	0.39	0.39	0.39	0.39	0.39	0.39	0.39	0.39
2	Und	Und	0.41	0.43	0.43	0.43	0.44	0.44	0.44	0.44
3	Und	Und	0.43	0.43	0.44	0.43	0.44	0.44	0.44	0.44
4	Und	Und	0.43	0.43	0.45	0.38	0.46	0.50	0.46	0.47
5	Und	Und	0.43	0.43	0.45	0.45	0.43	0.46	0.52	0.50
6	Und	Und	0.43	0.43	0.36	0.47	0.41	0.46	**0.55**	0.52
7	Und	Und	0.43	0.43	0.46	0.47	0.43	0.46	0.50	0.48
8	Und	Und	0.43	0.43	0.43	0.45	0.44	0.48	0.51	0.52
9	Und	Und	0.43	0.36	0.44	0.44	0.44	0.47	0.50	0.44
10	Und	Und	0.42	0.37	0.45	0.44	0.46	0.45	VL	0.44
11	Und	Und	0.42	0.43	0.44	0.53	0.47	0.42	VL	0.41
12	Und	0.43	0.35	0.43	0.44	0.54	0.44	0.40	VL	RCC
13	Und	0.43	0.36	0.44	0.44	0.42	0.43	0.60	0.34	RCC
14	Und	0.43	0.42	0.43	0.44	0.40	0.41	VL	VL	RCC
15	Und	0.43	0.39	0.43	0.44	0.59	0.45	VL	VL	RCC

5.1.4.2. Predictions for Hayrabolu with the test data

The predictions obtained from the $M3_H$ and observations for Hayrabolu are given in Figure 5.14 for the training period. Most of the peak flows observed in the training period are reasonably estimated by the model.

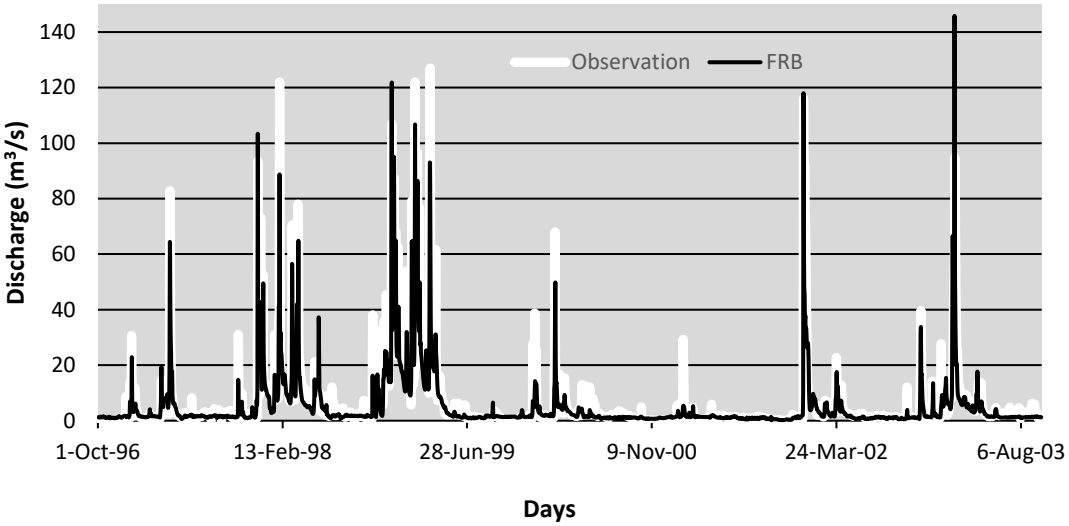

Figure 5.14. Hydrographs obtained from FRB for Hayrabolu streamgage for the training period

The predictions obtained from $M3_H$ and observations for Hayrabolu for the validation period are given in Figure 5.15. The peak flow, which is 143 m^3/s and observed on January 30, 2004, and another peak flow, which is 103 m^3/s and observed on February 15, 2005, are significantly underestimated by the model. The maximum observed flow at Hayrabolu during the training period is 127 m^3/s. Therefore, the model has failed to predict the peak flow, which has higher magnitude (i.e., 143 m^3/s) for the validation period compared the maximum flow observed in the training period (i.e., 127 m^3/s). The vital problem about using black-box models (FRB in this study) to analyze natural phenomenon is that they are only capable of performing what they have been trained for.

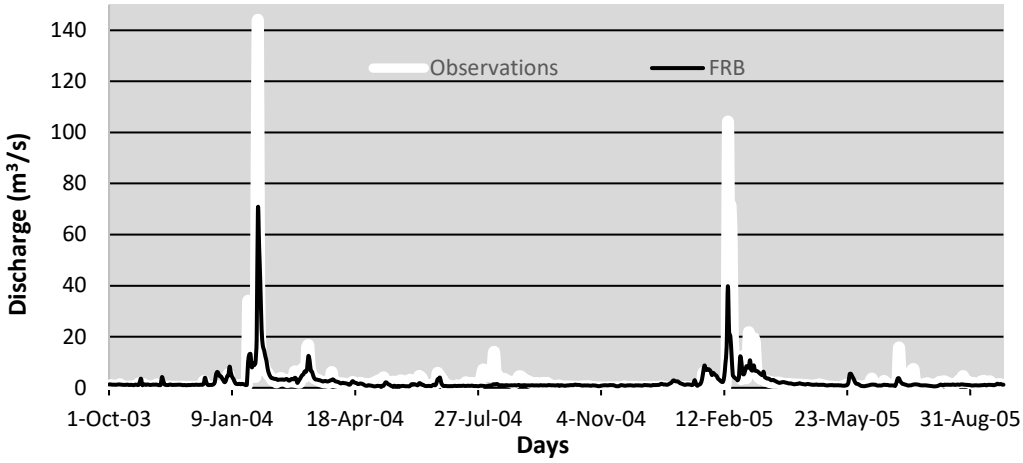

Figure 5.15. Hydrographs obtained from FRB for Hayrabolu streamgage for the validation period

$M3_H$ providing the highest NSE value for the validation period on Hayrabolu streamgage amongst all sub-models is the best type of model. The daily streamflow predictions are obtained by using $M3_H$ for the testing period at Hayrabolu. The performance measures of the model for the testing period is presented in Table 5.22. According to Table 5.22, the $M3_H$ has "Unsatisfactory" performance in terms of all statistical measures. The statistical measures for the validation and the testing periods are quite different from each other for Hayrabolu as shown in Table 4.4. This may be an indicator of different flow behavior in these two periods and the reason for poor model performance.

Table 5.22. Model performances for daily streamflow predictions of Hayrabolu Streamgage for the testing period

	Test			
Hayrabolu	R	R^2	NSE	$PBIAS$
$M3_H$ $(c = 6, r_a = 0.45)$	0.58	0.34	0.12	-54.19

Hydrographs obtained from $M3_H$ for Hayrabolu streamgage, together with the observations for the testing period, are given in Figure 5.16. According to the hydrographs, the model could be evaluated as unsuccessful in following the trends in observations. Most of the peak flows are either over or underestimated.

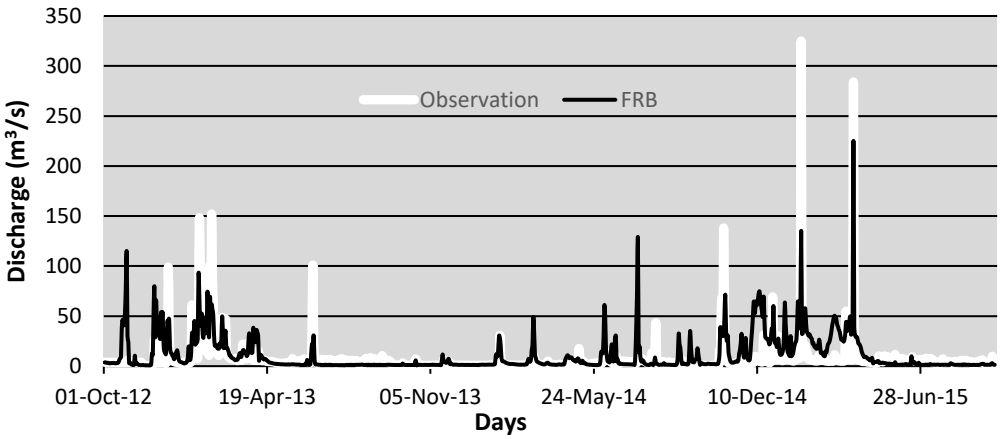

Figure 5.16. Hydrographs obtained from FRB for Hayrabolu streamgage for the testing period

5.1.5. Prediction of Luleburgaz with Fuzzy Rule-Based Extreme Model

The FRB model only takes streamflow observations of the surrounding gages as input. Based on these observations, one can expect to predict high or low streamflow at the ungaged location. To test the use of this idea, a new FRB model for Luleburgaz streamgage, called FRB-Extreme, is developed and trained only for the high flow periods since the FRB models experience difficulties in estimating especially high flows. Streamflow observations of the nearest streamgage to Luleburgaz, namely Inanli streamgage is used to select high flow periods, and streamflow data of the selected periods are used to train FRB-Extreme. Streamflow observations higher than 15 m^3/s which corresponds to 90^{th} percentile of the Inanli dataset is used for training $M5_L$ (with $c = 5, r_a = 0.15$). Then, the trained model is used to estimate only high flows of the testing period. The results are demonstrated in Figure 5.17 for

the testing period. FRB-Extreme predicts the largest two flows which are 376 m^3/s and 365 m^3/s better than the FRB ($M5_L$) model; however, the improvement is not significant. The main reason for this is the fact that there is a very limited number of high flow values that are used in the training of the FRB-Extreme model. It is expected to have better model performances when longer streamflow data is available for training purposes.

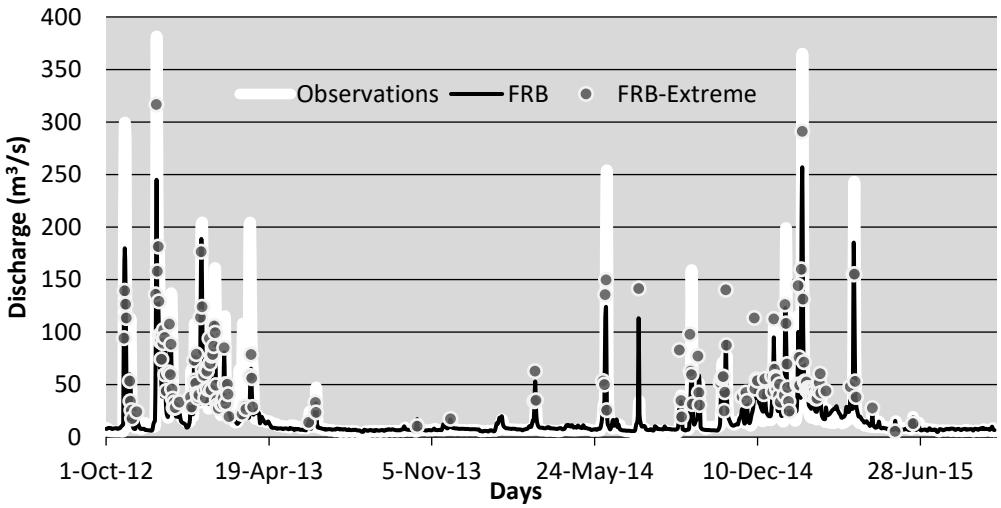

Figure 5.17. Hydrographs obtained from FRB and FRB-Extreme for Luleburgaz streamgage for the testing period

5.1.6. Effect of Input Parameter Selection on Model Performance

As can be seen in Figure 4.1, Inanli and Luleburgaz streamgages are located close to each other and the best model performances are achieved for these two gages. To investigate the effect of input parameters on model performance, some of the input parameter are removed from the best models' set up. For example, for Inanli, the best model is $M6_I$ which uses streamflow measurement at t at Luleburgaz ($Q_{L,t}$) and Yenicegoruce ($Q_{Y,t}$), and $t+1$ at Hayrabolu ($Q_{H,t+1}$) to predict streamflow at t at

Inanlı ($Q_{I,t}$). Streamflow measurement at Hayrabolu and Yenicegoruce are removed individually and together from $M6_I$ and $M7_I$ (without Hayrabolu, $Q_{H,t+1}$), $M8_I$ (without Yenicegoruce, $Q_{Y,t}$) and $M9_I$ (without both Hayrabolu and Yenicegoruce) are obtained. The architectures and the performances of these additional models are presented in Table 5.23 and Table 5.24, respectively.

Table 5.23. Additional model architectures used for Inanli streamflow predictions

Type of Model	**Input Parameters**	**Output**
$M7_I$	$Q_{L,t}, Q_{Y,t}$	$Q_{I,t}$
$M8_I$	$Q_{L,t}$, $Q_{H,t+1}$	$Q_{I,t}$
$M9_I$	$Q_{L,t}$	$Q_{I,t}$

Table 5.24. The best model and additional models performances used for Inanli streamflow predictions

	Training (1996-2003)			**Validation (2004-2005)**			**Testing (2013-2015)**		
	R^2	NSE	$PBIAS$	R^2	NSE	$PBIAS$	R^2	NSE	$PBIAS$
The Best Model									
$M6_I$ $(c = 6, r_a = 0.40)$	0.70	0.69	8.43	0.79	0.68	39.87	0.70	0.69	7.67
The Additional Models									
$M7_I$ $(c = 6, r_a = 0.40)$	0.69	0.68	9.32	0.85	0.67	41.17	0.63	0.63	10.30
$M8_I$ $(c = 6, r_a = 0.40)$	0.70	0.69	9.00	0.82	0.59	42.90	0.63	0.62	12.88
$M9_I$ $(c = 6, r_a = 0.40)$	0.70	0.69	9.02	0.85	0.62	42.52	0.50	0.49	7.01

As can be seen from Table 5.24, $M7_I$ and $M8_I$ provides similar performances for training and testing, and outperformed by $M6_I$. It indicates that although model performances are similar to that of the best model (i.e., $M6_I$) for the training period, the value of the information coming from streamflow measurement at time $t+1$ at Hayrabolu and at time t at Yenicegoruce is revealed in the performance of the testing period. Thus, the set of inputs used in the best model results in the best performance.

For Luleburgaz, the same procedure is applied and new models referred to as $M6_L$, $M7_L$ and $M8_L$ are formulated (see Table 5.25). The performances of these additional models are presented in Table 5.26.

Table 5.25. Additional model architectures used for Luleburgaz streamflow predictions

Type of Model	Input Parameters	Output
$M6_L$	$Q_{I,t}, Q_{Y,t+3}$	$Q_{L,t}$
$M7_L$	$Q_{I,t}, Q_{H,t}$	$Q_{L,t}$
$M8_L$	$Q_{I,t}$	$Q_{L,t}$

Table 5.26. The best model and the additional model performances used for Luleburgaz streamflow predictions

	Training (1996-2003)			**Validation (2004-2005)**			**Testing (2013-2015)**		
	R^2	NSE	$PBIAS$	R^2	NSE	$PBIAS$	R^2	NSE	$PBIAS$
The Best Model									
$M5_L$ $(c = 5, r_a = 0.15)$	0.56	0.52	10.04	0.84	0.82	-19.35	0.73	0.69	9.65
The Additional Models									
$M6_L$ $(c = 5, r_a = 0.15)$	0.58	0.54	9.33	0.86	0.85	-13.64	0.71	0.69	9.04
$M7_L$ $(c = 5, r_a = 0.15)$	0.53	0.50	10.94	0.84	0.75	-34.07	0.67	0.60	19.53
$M8_L$ $(c = 5, r_a = 0.15)$	0.51	0.48	11.56	0.69	0.44	-52.20	0.74	0.68	14.87

As can be seen from Table 5.26, $M6_L$ and $M5_L$ provides similar performances for training, validation and testing periods. It indicates streamflow measurement at time t at Hayrabolu does not provide additional information to the FRB model, thus can be removed from the input parameter set of the FRB model. On the other hand, removing the streamflow measurement at time $t + 3$ at Yenicegoruce worsen the performance of the model.

5.1.7. Effect of Validation Period Selection on the Model Performance

In previous sections, FRB models are trained using the daily streamflow records of 1997-2003 water years. Afterward, the model performances are evaluated to identify the best number of cluster center and cluster radius combination using streamflow records of 2004-2005 water years (i.e., the validation period) and the best performing model (i.e., the best combination of the number of the cluster center and the cluster radius) is selected (referred to as the selected model). The selected model (trained and validated) is used to make predictions for 2013-2015 water years (i.e., the testing period). Thus, the data is divided into three pieces as follows: i) training composed of streamflow observations of 1997-2003 water years, ii) validation composed of streamflow observations of 2004-2005 water years, and iii) testing composed of streamflow observations of 2013-2105 water years. Predictions are made for all four streamgages.

In this section, to investigate the effect of the validation period selection on the model performance, the test period and validation period are interchanged as follows: i) training composed of streamflow observations of 1997-2003 water years, ii) validation composed of streamflow observations of 2013-2015 water years, and iii) testing composed of streamflow observations of 2004-2005 water years. Again, predictions are made for all four streamgages. This set of calculations are referred to as Case 2 from here after. The results are summarized for Case 2 in Table 5.27.

As can be seen in Table 5.27, the FRB models provide "Good" performance for Luleburgaz, "Satisfactory" performance for Inanli and Yenicegoruce, and "Unsatisfactory" performance for Hayrabolu in terms of NSE for Case 2. The hydrographs obtained from the models for all streamgages, together with the observations for Case 2 are given in Figures 5.18, 5.19, 5.20, 5.21 for Yenicegoruce, Inanli, Luleburgaz and Hayrabolu, respectively.

Table 5.27. Model performances of selected models for daily streamflow predictions of all Streamgages for Training and Test periods for Case 2

		Training (1996-2003)				Test (2004-2005)			
	Selected Model	R	R^2	NSE	$PBIAS$	R	R^2	NSE	$PBIAS$
Yenicegoruce	$M1_Y$ $(c = 7, r_a = 0.25)$	0.74	0.55	0.53	13.24	0.62	0.38	0.15	-6.87
	$M2_Y$ $(c = 7, r_a = 0.15)$	0.78	0.61	0.61	8.55	0.66	0.43	0.01	-14.62
	$M3_Y$ $(c = 7, r_a = 0.20)$	0.86	0.73	0.73	6.04	0.73	0.53	0.25	-10.42
	$M4_Y$ $(c = 4, r_a = 0.35)$	0.87	0.76	0.76	4.61	0.79	0.62	0.41	-6.02
	$M5_Y$ $(c = 4, r_a = 0.45)$	0.88	0.77	0.76	5.71	0.83	0.69	0.61	-5.73
	$M6_Y$ $(c = 7, r_a = 0.40)$	0.89	0.79	0.79	5.47	0.81	0.65	0.58	-6.20
Inanli	$M1_I$ $(c = 6, r_a = 0.20)$	0.77	0.59	0.57	7.11	0.83	0.70	0.57	41.89
	$M2_I$ $(c = 6, r_a = 0.30)$	0.78	0.61	0.59	6.92	0.80	0.64	0.56	39.48
	$M3_I$ $(c = 8, r_a = 0.20)$	0.79	0.62	0.61	7.13	0.79	0.63	0.54	39.77
	$M4_I$ $(c = 4, r_a = 0.25)$	0.81	0.66	0.65	6.80	0.85	0.72	0.53	42.61
	$M5_I$ $(c = 6, r_a = 0.15)$	0.79	0.63	0.62	6.44	0.84	0.70	0.52	43.70
	$M6_I$ $(c = 6, r_a = 0.20)$	0.74	0.55	0.50	6.89	0.88	0.78	0.57	42.18
Luleburgaz	$M1_L$ $(c = 6, r_a = 0.20)$	0.73	0.53	0.50	10.17	0.90	0.80	0.76	-23.46
	$M2_L$ $(c = 5, r_a = 0.35)$	0.78	0.61	0.61	7.09	0.78	0.60	0.49	-19.81
	$M3_L$ $(c = 5, r_a = 0.30)$	0.81	0.66	0.64	6.68	0.78	0.61	0.43	-24.00
	$M4_L$ $(c = 5, r_a = 0.40)$	0.81	0.65	0.64	6.25	0.76	0.58	0.28	-25.69
	$M5_L$ $(c = 4, r_a = 0.45)$	0.74	0.55	0.51	9.84	0.86	0.74	0.71	-23.35
Hayrabolu	$M1_H$ $(c = 12, r_a = 0.25)$	0.86	0.74	0.73	13.49	0.60	0.36	0.36	-5.38
	$M2_H$ $(c = 6, r_a = 0.25)$	0.83	0.70	0.68	9.91	0.68	0.46	0.40	14.52
	$M3_H$ $(c = 6, r_a = 0.25)$	0.82	0.67	0.61	8.39	0.61	0.38	0.36	16.73
	$M4_H$ $(c = 7, r_a = 0.25)$	0.88	0.77	0.77	8.72	0.67	0.45	0.36	-39.08
	$M5_H$ $(c = 8, r_a = 0.20)$	0.82	0.67	0.62	8.76	0.69	0.47	0.39	13.91

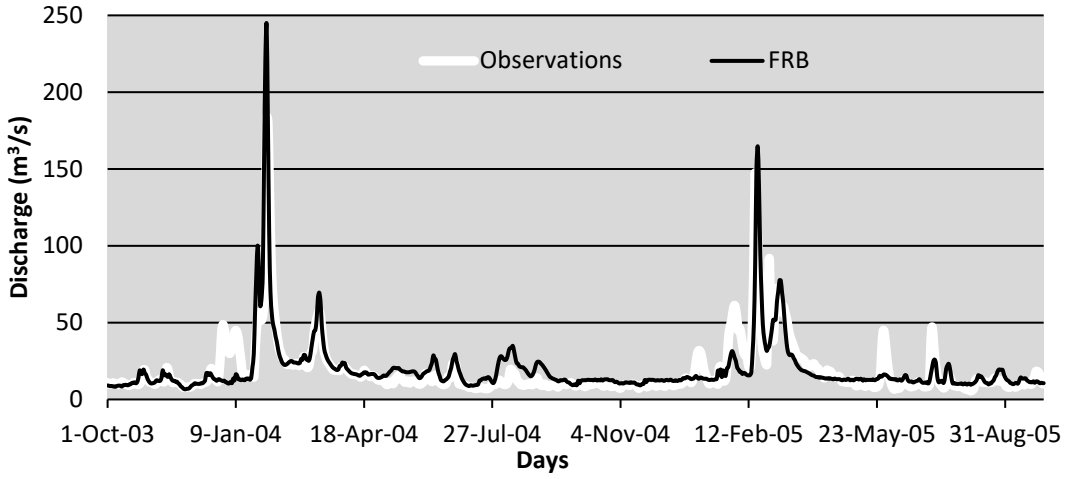

Figure 5.18. Hydrographs obtained from FRB for Yenicegoruce streamgage for Case 2

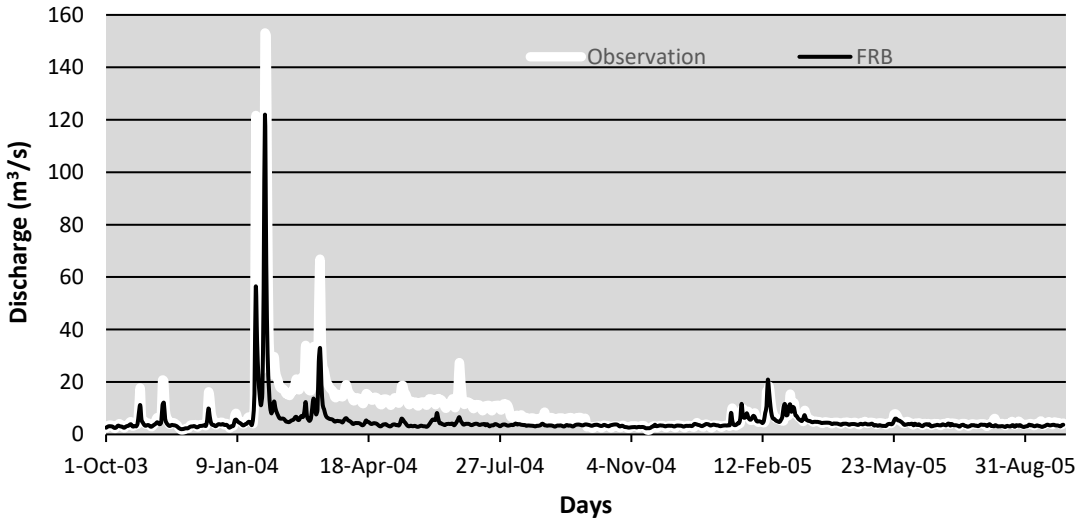

Figure 5.19. Hydrographs obtained from FRB for Inanli streamgage for Case 2

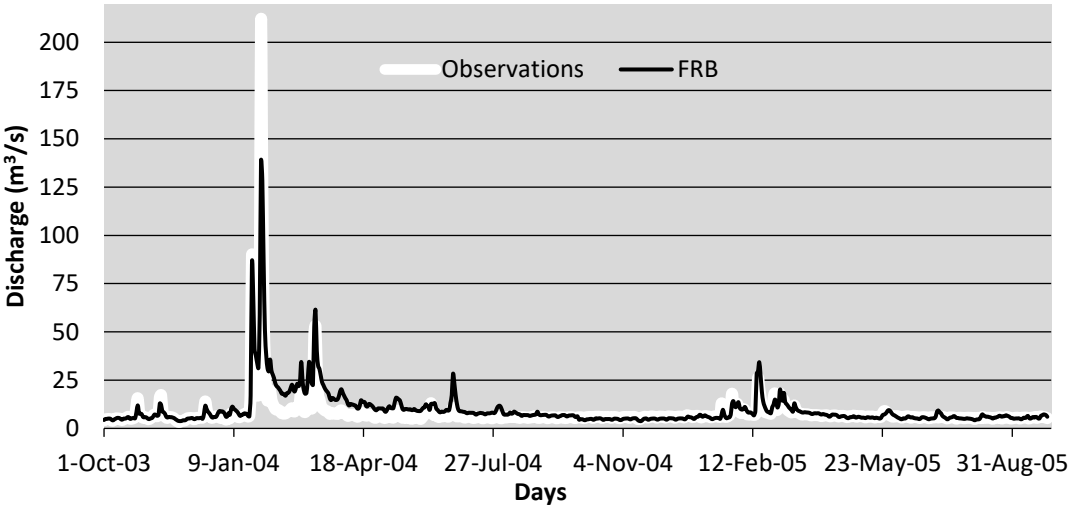

Figure 5.20. Hydrographs obtained from FRB for Luleburgaz streamgage for Case 2

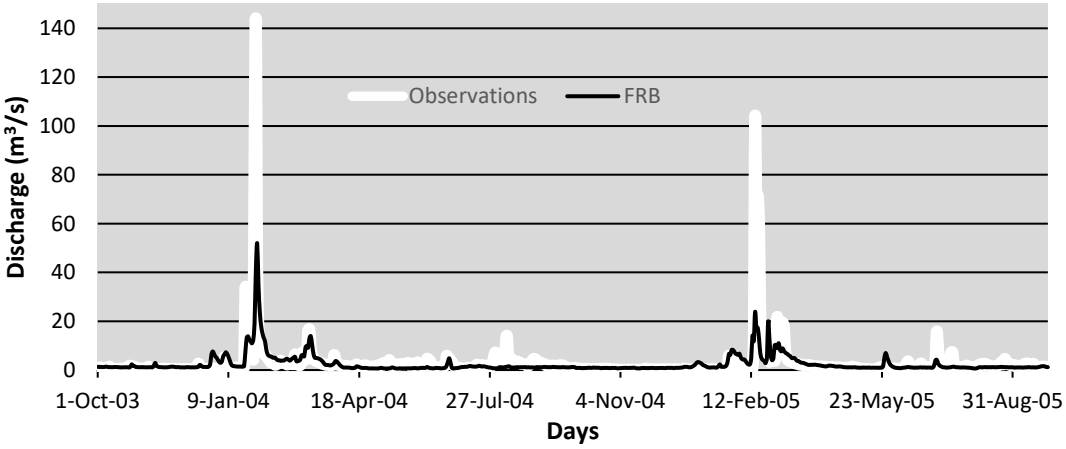

Figure 5.21. Hydrographs obtained from FRB for Hayrabolu streamgage for Case 2

As shown in Figures 5.18, 5.19, and 5.20, the models follow the general trend in observation and reasonably predict peak flows at Yenicegoruce, Inanli and Luleburgaz for Case 2. On the other hand, at Hayrabolu, although the model follows

the general trend in observations, it underestimates the peak flow as shown in Figure 5.21 for Case 2.

5.1.8. Summary of Results

In this study, in order to investigate the effect of clustering parameters, namely the number of the cluster center and the cluster radius on model performance, the models with various number of cluster centers and cluster radii are built. Furthermore, models with different input parameters are built to include the effect of travel time of water between streamgages. All the models are trained and validated, then, validated models are used to make predictions for the testing period. To investigate the effect of the selection of the validation period on the model performance for the testing period, a second case, Case 2 is designed where validation and testing periods are changed. For all the models, the performance of the best models for both cases are Summarized in Table 5.28.

Table 5.28. Model performances of the best models for daily streamflow predictions of all streamgages

	Testing period: 2013-2015				**Testing Period: 2004-2005**			
Streamgage	R	R^2	NSE	$PBIAS$	R	R^2	NSE	$PBIAS$
Yenicegoruce	0.67	0.45	0.24	49.5	0.83	0.69	0.61	-5.73
Inanli	0.84	0.7	0.69	7.67	0.88	0.78	0.57	42.18
Luleburgaz	0.86	0.73	0.69	9.65	0.89	0.80	0.76	-23.46
Hayrabolu	0.58	0.34	0.12	-54.19	0.68	0.46	0.40	14.52

Except for Inanli, the best models validated by using the period between 2013-2015 outperform the best models validated by using the period between 2004-2005. For Inanli, best models of both cases provide similar performances for test periods as presented in Table 5.28. Statistical measures in Table 4.4 indicate that higher flows are observed on the testing period (2013-2015) compared to the validation period (2004-2005). This might be due to various reasons such as change in rainfall regime and increase in snow-melt due to global warming. Therefore, the models selected based on the validation period of Case 2 which contain higher flow data, resulted in better performances for the testing period. This indicates that utilization of a time period with higher streamflow observations as the validation period results in identification of a better model (i.e., model performing better in the testing period).

CHAPTER 6

CONCLUSION

Missing long time series of streamflow observations is filled using streamflow observations of neighboring catchments through SC-based TS_FRB models in this study. Daily streamflow values for extended periods are estimated for streamgages that become inoperative after a period of data collection using FRB models. In developing countries, such as Turkey, continuous time series of streamflow data is not available most of the time, and this hinders water resources planning studies. Similar to the case at Meric-Ergene Basin, water extractions and discharges from rivers are not monitored and recorded sufficiently, and this makes the calibration of hydrological models challenging. Many industrial establishments withdraw their process water from groundwater wells and discharge their effluents to rivers without licenses or permissions. To lessen the effects and visibility of their contaminated discharges, some of these facilities release their effluents to waterways, especially during massive rainfall events. Such practices result in unexpected oscillations (i.e., different than the natural rainfall-runoff response of the basin) in streamflow and make it very hard to calibrate hydrological models. The impact of such anthropogenic effects is embedded in the streamflow observations of sub-catchments of a basin and it may be possible to capture these effects through utilization of data-driven methods. With this aim, in this study, streamflow observations of neighboring catchments are used to predict missing streamflow data using data-driven models (FRB in this study).

The following conclusions are reached:

- SC is used to build the rule-base of the FRB. Selection of the clustering parameters, namely the number of the cluster center and cluster radius, is critical since they affect the architecture of the data-driven model. The goal is to identify the best architecture that is capable of representing the system's behavior adequately. In this study, to determine the best number of the cluster center and the cluster radius combination, a large number of FRB models are built and trained. The performances of these sub-models for the validation period are evaluated to identify the best combination of the number of the cluster center and the cluster radius. Then the performance of the best model is tested for a completely different time interval. When small cluster radius is used, cluster centers are formed close to each other and low and average flows are selected as cluster centers. FRB model having low and average flows as fuzzy rules, can successfully predicts the regular flow, while it fails to predicts extreme values. Therefore, for smaller cluster radius, many cluster centers should be chosen to avoid rule-base being composed of just low flows. However, choosing a large number of cluster centers might result in overfitting. On the other hand, for bigger cluster radius, the cluster centers are formed far from each other. In other words, the data points corresponding to high flows have a chance to be selected as a cluster center. However, if the radius is too high, the data points corresponding to extreme events of the training period might be assigned as cluster centers. If similar extreme events are not observed in the testing period, the performance of the model decreases. These observations are made in this study and can be used as guiding principles, however devising a methodology for the identification of the best cluster radius and the number of cluster center combination still remains a challenge.
- In this study, a comparison between linear and non-linear models is carried out as well. The FRB model with one cluster center is equivalent to MLR. For all streamgages, FRB outperformed MLR. This indicates that the non-

linear models (i.e., FRB with multiple rules) provide better predictions compared to the linear model (i.e., MLR) in the study area.

- In this study, FRB models with different input variables, representing the lagged streamflows at neighboring basins, are trained and tested as well. As explained in Section 4 in detail, due to variation in the areas of subbasins, the distances between streamgages are different from each other; and it takes time for water to travel from a streamgage to another. To include this effect, lagged time series of streamflows are used. Including lagged time series of streamflow to models, enhances the model for Yenicegoruce at most, because Yenicegoruce, which is located at the outlet of the basin, has the biggest subbasin area amongst other stations. However, this introduces the risk of overfitting as well. Thus, the training performance increases however the prediction performance does not improve. For Luleburgaz and Inanli, including the lagged time series of streamflows to models slightly enhances the model performance. Flow characteristics (i.e., rainfall-runoff response) being similar in training, validation and testing periods improves development of better performing models.
- The performance of the FRB models trained solely by using neighboring streamgages, can be considered as "Good" in estimating daily streamflow values at the subsequently ungaged location for closely spaced streamgages such as Inanli and Luleburgaz gages. Thus, with relatively less site-specific data, daily streamflow estimations for long data gaps is achieved by the FRB model. The proposed model can be used to generate continuous streamflow time series that can be used in hydrodynamic and water quality assessment studies for closely spaced streamgages. On the other hand, for Yenicegoruce and Hayrabolu streamgages, the FRB models failed to generate "Satisfactory" prediction. Yenicegoruce is located at the outlet of the basin and has much larger drainage area compared to others; thus is located far away from the closest neighboring streamgage. On the other hand, Hayrabolu streamgage is located at a different tributary than Inanli, Luleburgaz and

Yenicegoruce. Thus, hydrological responses of Yenicegoruce and Hayrabolu basins are not properly represented using the responses of other three basins. It is not possible to sufficiently represent basin characteristics like current vegetation and initial moisture content, current meteorological conditions affecting the rainfall-runoff responses and travel times between the streamgages in the FRB model solely by the streamflow observations of other streamgages. Inclusion of additional inputs such as indicators of basin characteristics or meteorological conditions may improve the performances of the FRB models.

- Similar to hydrological models, the general trend in streamflow measurements is reasonably predicted by FRB models, but both models experiences difficulties in predicting peak flows. The possibility of developing separate models for low and high flow periods using a FRB approach is investigated in this study as well. Training is carried out using the same dataset. However, selection of the best FRB models is performed by using two separate datasets namely, low flow period and high flow period. FRB models selected according to the high flow period provides significantly better performance compared to FRB models selected by using the low flow period. The reason for this is that the rule-base of FRB models selected by using low flow period, is not capable of predicting high flow events. On the other hand, rules devised according to the high flow events, have good representation capability for low flow events as well.
- The variety of FRB models with different rule-bases (i.e., the number of the cluster center and the cluster radius combinations) are build and trained. Then, the models' performances are evaluated (validated) to select the best performing model amongst all trained models. Finally, trained and validated models are used to make predictions for the test period. To test the robustness of the FRB models, the best models are identified by using two different validation periods (i.e., swapping the validation and test periods). For Inanli and Luleburgaz, NSE values changes from 0.57 to 0.69 and 0.69 to 0.76,

respectively. It shows that the FRB models built for Inanli and Luleburgaz are robust models. On the other hand, for Yenicegoruce and Hayrabolu, NSE values vary significantly. This indicates that FRB models for Yenicegoruce and Hayrabolu are not robust and their performance highly depends on flow behaviors of training and validation periods. For these streamgages addition of new inputs which may act as indicators of basin characteristics and meteorological conditions seems to be necessary to improve the performance of the models.

Remark for future research.

- A wider range of inputs (i.e., catchment characteristics, meteorological data) may improve the performance of the FRB. Especially, for streamgages that are separated from each other with larger distances, then better models can be calibrated.
- Currently, selection of the best cluster radius and the number of cluster centers combination is a challenging task. Development of a robust methodology for the identification of the best combination will be very useful for data-driven model development.

REFERENCES

Aissia, M. A. B., Chebana, F., & Ouarda, T. B. (2017). Multivariate missing data in hydrology–Review and applications. Advances in Water Resources, 110, 299-309.

Akgun, O. B., & Kentel, E. Estimation of Streamflow using Takagi-Sugeno Fuzzy Rule-Based Model, in Goffredo La Loggia, Gabriele Freni, Valeria Puleo and Mauro De Marchis (editors). HIC 2018. 13th International Conference on Hydroinformatics, 3, 18-25

Akkemik, U., D'Arrigo, R., Cherubini, P., Kose, N., Jacoby, G. C. (2008). Tree-ring reconstructions of precipitation and streamflow for north-western Turkey. International Journal of Climatology, 28(2), 173-183.

Allen, E. B., Rittenour, T. M., DeRose, R. J., Bekker, M. F., Kjelgren, R., Buckley, B. M. (2013). A tree-ring based reconstruction of Logan River streamflow, northern Utah. Water Resources Research, 49(12), 8579-8588.

Angelov, P. (2004). An approach for fuzzy rule-base adaptation using on-line clustering. International Journal of Approximate Reasoning, 35(3), 275-289.

Angelov, P. P., & Filev, D. P. (2004). An approach to online identification of Takagi-Sugeno fuzzy models. *IEEE Transactions on Systems, Man, and Cybernetics, Part B (Cybernetics)*, *34*(1), 484-498.

Angelov, P., & Yager, R. (2013). Density-based averaging–a new operator for data fusion. *Information Sciences*, *222*, 163-174.

Angelov, P. (2014). Outside the box: an alternative data analytics framework. Journal of Automation Mobile Robotics and Intelligent Systems, 8(2), 29-35.

Archfield, S. A., Vogel, R. M. (2010) Map correlation method: Selection of a reference streamgage to estimate daily streamflow at ungaged catchments. Water Resources Research, 46(10), W10513.

Asquith, W. H., Roussel, M. C., Vrabel, J. (2006). Statewide analysis of the drainage-area ratio method for 34 streamflow percentile ranges in Texas (No. 2006-5286). US Geological Survey.

Ayvaz, M. T., Tezel, U., Kentel, E., & Goktas, R. K. (2018). Weekly flow prediction of Ergene River using an artificial neural network based solution approach, in Goffredo La Loggia, Gabriele Freni, Valeria Puleo and Mauro De Marchis (editors). HIC 2018. 13th International Conference on Hydroinformatics, vol 3, pages 155--161

Banakar, A., & Azeem, M. F. (2006). Input selection for TSK fuzzy model based on modified mountain clustering. In 2006 3rd International IEEE Conference Intelligent Systems (pp. 295-299). IEEE.

Batistakis Y., Halkidi, M., & Vazirgiannis, M. (2001). "On clustering validation techniques." Journal of intelligent information systems, 17(2), 107-145.

Beauchamp, J.J., Downing, D.J., Railsback, S.F. (1989) Comparison of regression and time series methods for synthesizing missing streamflow records, Water Resources Bulletin, 25(5), 961-975.

Bekker, M. F., Justin DeRose, R., Buckley, B. M., Kjelgren, R. K., Gill, N. S. (2014). A 576-year Weber River streamflow reconstruction from tree rings for water resource risk assessment in the Wasatch Front, Utah. JAWRA Journal of the American Water Resources Association, 50(5), 1338-1348.

Boakye, P.G. & Schultz, G.A. (1994) Filling gaps in runoff time series in west Africa, Hydrological Sciences Journal, 39(6), 621-636.

Chiu, S. L. (1994). Fuzzy model identification based on cluster estimation. Journal of Intelligent & fuzzy systems, 2(3), 267-278.

Cigizoglu, H.K. (2003) Estimation, forecasting and extrapolation of river flows by artificial neural networks, Hydrological Sciences Journal, 48(3), 349-361.

Dastorani, M. T., Moghadamnia, A., Piri, J., & Rico-Ramirez, M. (2010). Application of ANN and ANFIS models for reconstructing missing flow data. *Environmental monitoring and assessment*, *166*(1-4), 421-434.

Demirli, K., & Muthukumaran, P. (2000). Higher order fuzzy system identification using subtractive clustering. Journal of Intelligent & Fuzzy Systems, 9(3, 4), 129-158.

Demirli, K., Cheng, S. X., & Muthukumaran, P. (2003). Subtractive clustering based modeling of job sequencing with parametric search. *Fuzzy Sets and Systems*, *137*(2), 235-270.

Dogulu, N., & E. Kentel (2017), Clustering of hydrological data: A review of methods for runoff predictions in ungauged basins, in EGU General Assembly Conference, edited, p. 12005.

Elshorbagy, A., Simonovic S.P., Panu, U.S. (2002) Estimation of missing streamflow data using principles of chaos theory, Journal of Hydrology, 255, 123-133.

Ergen, K., Kentel, E. (2016) An integrated map correlation method and multiple-source sites drainage-area ratio method for estimating streamflows at ungauged catchments: A case study of the Western Black Sea Region, Turkey, Journal of Environmental Management, 166, 309-320.

Freeze, R. A. (1982). "Hydrogeological Concepts in Stochastic and Deterministic Rainfall–Runoff Predictions." Geological Society of America Special Papers, 189, 63-80.

Harvey, C., Dixon, H., & Hannafor, J. (2012) An appraisal of the performance of data-infilling methods for application to daily mean river flow records in UK, Hydrology Research, 43(5), 618-636.

Hirsch, R. M. (1979). An evaluation of some record reconstruction techniques. Water resources research, 15(6), 1781-1790.

Kahraman A.C., Özkul M. (2018) Ergene Basin Conservation Action Plan Follow-up Report II, Marmara Union of Municipalities Department of Environmental Management Coordination, Istanbul, Turkey (in Turkish).

Kamwaga, S., Mulungu, D. M., Valimba, P. (2018). Assessment of empirical and regression methods for infilling missing streamflow data in Little Ruaha catchment Tanzania. Physics and Chemistry of the Earth, 106, 17-28

Kentel, E. (2006). Uncertainty modeling health risk assessment and groundwater resources management (Doctoral Dissertation). Retreieved from: https://smartech.gatech.edu/bitstream/handle/1853/11584/kentel_elcin_200608_phd.pdf

Kentel, E. (2009). Estimation of river flow by artificial neural networks and identification of input vectors susceptible to producing unreliable flow estimates. Journal of hydrology, 375(3-4), 481-488.

Khalil, M., Panu, U. S., & Lennox, W. C. (2001). Groups and neural networks based streamflow data infilling procedures. Journal of Hydrology, 241(3-4), 153-176.

Kisi, O., Shiri, J., & Nikoofar, B. (2012). Forecasting daily lake levels using artificial intelligence approaches. Computers & Geosciences, 41, 169-180.

Krasnogorskaya, N., Belozerova, E., Longobardi, A., Nafikova, E. (2019) The map-correlation method for ungauged catchments streamflow prediction in the Ufa River, Russian Federation. International Journal of Hydrology Science and Technology, 9(6). https://doi.org/10.1504/IJHST.2019.103440

Kriegel, H. P., Kröger, P., Sander, J., & Zimek, A. (2011). “Density-based clustering.” Wiley Interdisciplinary Reviews: Data Mining and Knowledge Discovery, 1(3), 231-240.

Lara, A., Urrutia, R., Villalba, R., Luckman, B. H., Soto, D., Aravena, J. C., Mc Phee J., Wolodarsky A., Peoza L., León, J. (2005). The potential use of tree-rings to reconstruct streamflow and estuarine salinity in the Valdivian Rainforest eco-region, Chile. Dendrochronologia, 22(3), 155-161.

Lettenmaier, D. P. (1980). Intervention analysis with missing data. Water Resources Research, 16(1), 159-171.

Lohani, A. K., Goel, N. K., & Bhatia, K. K. S. (2014). Improving real time flood forecasting using fuzzy inference system. Journal of hydrology, 509, 25-41.

Meko, D. M., Therrell, M. D., Baisan, C. H., Hughes, M. K. (2001). Sacramento River flow Reconstructed to AD 869 from Tree Rings 1. JAWRA Journal of the American Water Resources Association, 37(4), 1029-1039.

Mesta, B., Kargı, P.G., Tezyapar, I., Ayvaz, M.T., Goktas, R.K., Kentel, E., & Tezel, U. (2018) Identification of Rainfall-Runoff Relationship at Yenigoruce Basin Using HEC-HMS Hydrologic Model. International Symposium on Urban Water and Wastewater Management, October 25-27, 2018, Denizli, Turkey (in Turkish).

Mesta, B., Kargi, P. G., Tezyapar, I., Ayvaz, M. T., Goktas, R. K., Kentel, E., & Tezel, U. (2019) Determination of rainfall-runoff relationship in Yenicegoruce Basin with HEC-HMS hydrologic model. Yenicegörüce Havzası'ndaki yağış-akış ilişkisinin HEC-HMS hidrolojik modeli ile belirlenmesi. Pamukkale University Journal of Engineering Sciences, Special Issue Article (in Turkish), 25(8), 949-955, doi:10.5505/pajes.2019.75133

Ministry of Environment and Forestry (MoEF) (2008) Meric-Ergene Basin Protection Action Plan, MoEF General Directorate of Environmental Management, Ankara, Turkey (in Turkish).

Ministry of Environment and Urbanization (MoEU) (2015) Ergene Basin Water Quality Monitoring Report for Spring – Summer Season, MoEU General Directorate of Environmental Impact Assessment Permitting and Auditing Department of Laboratory Analysis and Monitoring, Ankara, Turkey (in Turkish).

Ministry of Environment and Urbanization (MoEU) (2020, April 8) Completed Projects. Retrieved from: https://www.tarimorman.gov.tr/SYGM/Belgeler/PROJELER/Tamamlanan%20projeleri%20(3)-converted%20(1).pdf

Moriasi, D. N., Gitau, M. W., Pai, N., & Daggupati, P. (2015). Hydrologic and water quality models: Performance measures and evaluation criteria. Transactions of the ASABE, 58(6), 1763-1785.

Mwale, F. D., Adeloye, A. J., Rustum, R. (2012). Infilling of missing rainfall and streamflow data in the Shire River basin, Malawi–A self organizing map approach. Physics and Chemistry of the Earth, Parts A/B/C, 50, 34-43.

Nayak, P. C., Sudheer, K. P., & Ramasastri, K. S. (2005). Fuzzy computing based rainfall–runoff model for real time flood forecasting. Hydrological Processes: An International Journal, 19(4), 955-968.

Nayak, P. C., & Sudheer, K. P. (2008). Fuzzy model identification based on cluster estimation for reservoir inflow forecasting. Hydrological Processes: An International Journal, 22(6), 827-841.

Ng, W. W., Panu, U. S., & Lennox, W. C. (2009). Comparative studies in problems of missing extreme daily streamflow records. Journal of Hydrologic Engineering, 14(1), 91-100.

Jacquin, A. P., & Shamseldin, A. Y. (2009). Review of the application of fuzzy inference systems in river flow forecasting. Journal of hydroinformatics, 11(3-4), 202-210.

Jain, A. K., Murty, M. N., & Flynn, P. J. (1999). “Data clustering: a review.” ACM Computing Surveys, 31(3), 264-323.

Jang, J. S. (1993). ANFIS: adaptive-network-based fuzzy inference system. IEEE transactions on systems, man, and cybernetics, 23(3), 665-685.

Ross, T. J. (2004). Fuzzy logic with engineering applications (Vol. 2). New York: Wiley.

Shah, S. K., Bhattacharyya, A., Shekhar, M. (2013). Reconstructing discharge of Beas river basin, Kullu valley, western Himalaya, based on tree-ring data. Quaternary international, 286, 138-147.

Shiau, J. T., & Hsu, H. T. (2016). Suitability of ANN-based daily streamflow extension models: a case study of Gaoping River basin, Taiwan. Water resources management, 30(4), 1499-1513.

Strachan, S., Biondi, F., Leising, J. (2011). 550-Year reconstruction of streamflow variability in Spring Valley, Nevada. Journal of Water Resources Planning and Management, 138(4), 326-333.

Takagi, T., & Sugeno, M. (1985). Fuzzy identification of systems and its applications to modeling and control. IEEE Transactions on Systems, Man, and Cybernetics, (1), 116132.

Tencaliec, P., Favre, A.-C., Prieur, C., and Mathevel, T. (2015) Reconstruction of missing daily streamflow data using dynamic regression models, Water Resources Research, 51, 9447-9463, doi:10.1002/2015WR017399.

Tezel, U., Ayvaz, M.T., Balcıoğlu, I., Gölge, M., Göktaş, R.K., Hanedar, A., Kentel, E., Sandıkkaya, M.T. ve Kaynak Tezel, B., Development of a geographical information systems based decision-making tool for water quality management of Ergene watershed using pollutant fingerprints, 115Y064 numbered TÜBİTAK Project Final Report, Ankara, 2019.

Valipour, M., Banihabib, M. E., & Behbahani, S. M. R. (2013). Comparison of the ARMA, ARIMA, and the autoregressive artificial neural network models in forecasting the monthly inflow of Dez dam reservoir. Journal of hydrology, 476, 433-441.

Vernieuwe, H., Georgieva, O., De Baets, B., Pauwels, V. R., Verhoest, N. E., & De Troch, F. P. (2005). Comparison of data-driven Takagi–Sugeno models of rainfall–discharge dynamics. Journal of Hydrology, 302(1-4), 173-186.

Walker, A., & Braglia, L. (2018). Package 'openxlsx'.

Woodhouse, C. A., Lukas, J. J. (2006). Multi-century tree-ring reconstructions of Colorado streamflow for water resource planning. Climatic Change, 78(2-4), 293-315.

Young, K. C. (1994). Reconstructing streamflow time series in central Arizona using monthly precipitation and tree ring records. Journal of climate, 7(3), 361-374.

Yozgatligil, C., Aslan, S., Iyigun, C., Batmaz, I. (2013). Comparison of missing value imputation methods in time series: the case of Turkish meteorological data. Theoretical and applied climatology, 112(1-2),

Xiong, L., Shamseldin, A. Y., & O'connor, K. M. (2001). A non-linear combination of the forecasts of rainfall-runoff models by the first-order Takagi–Sugeno fuzzy system. Journal of hydrology, 245(1-4), 196-217.

Zadeh, L. A. (1965). Fuzzy sets. Information and control, 8(3), 338-353.

Zadeh, L. A. (1975). The concept of a linguistic variable and its application to approximate reasoning—I. *Information sciences*, *8*(3), 199-249.

Zadeh, L. A. (1994). "The role of fuzzy logic in modeling, identification and control." Modeling Identification and Control, 15(3), 191-203.

APPENDICES

A. The results of sub-models for Yenicegoruce Streamgage

A.1. NSE values of $M1_Y$ for training phase computed with different number of c and r_a

$M1_Y$ (training)	r_a									
number of c	**0.05**	**0.10**	**0.15**	**0.20**	**0.25**	**0.30**	**0.35**	**0.40**	**0.45**	**0.50**
1	Und	Und	VL	VL	VL	VL	VL	VL	VL	VL
2	Und	Und	0.04	0.34	0.44	0.47	0.48	0.49	0.49	0.49
3	Und	Und	0.47	0.48	0.49	0.50	0.52	0.53	0.53	0.53
4	Und	Und	0.47	0.48	0.49	0.53	0.52	0.53	0.54	0.56
5	Und	0.36	0.48	0.51	0.52	0.53	0.54	0.54	0.56	0.58
6	Und	0.37	0.48	0.51	0.52	0.55	0.54	0.55	0.56	0.58
7	Und	0.47	0.48	0.51	0.53	0.55	0.57	0.58	RCC	0.59
8	Und	0.48	0.48	0.53	0.55	0.57	0.58	0.59	RCC	RCC
9	Und	0.48	0.49	0.54	0.55	0.58	0.60	0.59	RCC	RCC
10	Und	0.48	0.51	0.54	0.56	0.62	0.61	RCC	RCC	RCC
11	Und	0.48	0.51	0.54	0.55	0.61	0.62	RCC	RCC	RCC
12	Und	0.48	0.52	0.54	0.57	0.62	0.62	RCC	RCC	RCC
13	Und	0.48	0.52	0.55	0.58	0.62	0.63	RCC	RCC	RCC
14	Und	0.51	0.52	0.55	0.62	0.62	0.62	RCC	RCC	RCC
15	Und	0.51	0.53	0.56	0.62	0.63	RCC	RCC	RCC	RCC

A.2. NSE values of $M1_Y$ for validation phase computed with different number of c and r_a

$M1_Y$ (validation)	r_a									
number of c	**0.05**	**0.10**	**0.15**	**0.20**	**0.25**	**0.30**	**0.35**	**0.40**	**0.45**	**0.50**
1	Und	Und	VL	VL	VL	VL	VL	VL	VL	VL
2	Und	Und	VL	VL	VL	VL	0.04	0.09	0.11	0.12
3	Und	Und	VL	VL	0.16	0.25	0.15	0.13	0.12	0.17
4	Und	Und	VL	0.04	0.17	0.25	0.11	0.11	0.17	0.32
5	Und	VL	VL	0.22	0.11	0.26	0.26	0.29	0.08	0.14
6	Und	VL	0.09	0.24	0.11	0.30	0.27	0.31	0.12	0.17
7	Und	VL	0.13	0.24	0.15	0.29	0.40	0.25	RCC	0.07
8	Und	VL	0.13	0.29	0.28	0.25	0.31	0.21	RCC	RCC
9	Und	VL	0.19	0.30	0.30	0.24	0.09	0.30	RCC	RCC
10	Und	0.00	0.19	0.22	0.31	VL	0.19	RCC	RCC	RCC
11	Und	0.00	0.20	0.22	0.32	0.15	0.23	RCC	RCC	RCC
12	Und	0.11	0.20	0.24	0.33	0.13	0.24	RCC	RCC	RCC
13	Und	0.12	0.20	0.33	0.30	0.20	0.18	RCC	RCC	RCC
14	Und	0.06	0.20	0.33	0.03	0.23	0.12	RCC	RCC	RCC
15	Und	0.16	0.27	0.36	VL	VL	0.14	RCC	RCC	RCC

A.3. NSE values of $M2_Y$ for training phase computed with different number of c and r_a

$M2_Y$ (training)	r_a									
number of c	**0.05**	**0.10**	**0.15**	**0.20**	**0.25**	**0.30**	**0.35**	**0.40**	**0.45**	**0.50**
1	Und	Und	VL	VL	VL	VL	VL	VL	VL	VL
2	Und	Und	VL	0.28	0.34	0.42	0.58	0.60	0.61	0.62
3	Und	Und	0.59	0.31	0.55	0.61	0.59	0.65	0.66	0.67
4	Und	Und	0.62	0.55	0.57	0.61	0.63	0.65	0.67	0.68
5	Und	Und	0.46	0.61	0.61	0.62	0.64	0.68	0.67	0.68
6	Und	Und	0.59	0.62	0.62	0.66	0.68	0.68	0.68	0.70
7	Und	Und	0.61	0.62	0.63	0.66	0.67	0.68	0.71	0.69
8	Und	Und	0.61	0.63	0.64	0.67	0.68	0.69	0.72	0.70
9	Und	Und	0.61	0.63	0.66	0.68	0.70	0.71	0.75	0.70
10	Und	Und	0.63	0.64	0.66	0.70	0.70	0.73	0.76	0.75
11	Und	Und	0.63	0.66	0.68	0.70	0.72	0.74	0.76	0.76
12	Und	Und	0.63	0.66	0.68	0.70	0.73	0.75	0.80	RCC
13	Und	Und	0.63	0.66	0.68	0.70	0.73	0.75	0.81	RCC
14	Und	Und	0.66	0.66	0.68	0.70	0.80	0.76	0.81	RCC
15	Und	Und	0.66	0.66	0.68	0.72	0.82	0.78	0.81	RCC

A.4. NSE values of $M2_Y$ for validation phase computed with different number of c and r_a

$M2_Y$ (validation)	r_a									
number of c	**0.05**	**0.10**	**0.15**	**0.20**	**0.25**	**0.30**	**0.35**	**0.40**	**0.45**	**0.50**
1	Und	Und	VL	VL	VL	VL	VL	VL	VL	VL
2	Und	Und	VL	VL	VL	VL	VL	VL	0.04	0.06
3	Und	Und	0.02	VL	VL	0.06	VL	0.22	0.16	0.12
4	Und	Und	0.15	VL	VL	0.06	0.17	0.23	0.08	0.03
5	Und	Und	VL	0.00	0.01	0.10	0.20	0.26	0.08	0.03
6	Und	Und	VL	0.09	0.11	0.16	0.01	0.23	0.06	VL
7	Und	Und	0.01	0.09	0.21	0.16	VL	0.19	VL	0.06
8	Und	Und	0.02	0.21	0.10	0.05	VL	VL	0.29	VL
9	Und	Und	0.08	0.20	0.13	0.07	0.17	VL	0.13	VL
10	Und	Und	0.21	0.10	0.05	0.18	0.15	VL	0.09	VL
11	Und	Und	0.21	0.13	0.37	0.17	VL	VL	VL	VL
12	Und	Und	0.21	0.12	0.38	VL	VL	VL	VL	VL/RCC
13	Und	Und	0.21	0.13	0.36	VL	0.04	VL	VL	VL/RCC
14	Und	Und	0.16	0.07	0.04	VL	VL	VL	VL	VL/RCC
15	Und	Und	0.13	0.05	0.05	0.20	VL	0.39	VL	VL/RCC

A.5. NSE values of $M3_Y$ for training phase computed with different number of c and r_a

$M3_Y$ (training)	r_a									
number of c	**0.05**	**0.10**	**0.15**	**0.20**	**0.25**	**0.30**	**0.35**	**0.40**	**0.45**	**0.50**
1	Und	Und	Und	0.09	0.09	0.09	0.09	0.09	0.09	0.09
2	Und	Und	Und	0.14	0.16	0.61	0.64	0.68	0.73	0.73
3	Und	Und	Und	0.63	0.59	0.71	0.72	0.73	0.74	0.74
4	Und	Und	Und	0.66	0.69	0.71	0.74	0.73	0.74	0.74
5	Und	Und	0.64	0.67	0.73	0.73	0.75	0.75	0.74	0.76
6	Und	Und	0.72	0.73	0.74	0.74	0.75	0.75	0.76	0.76
7	Und	Und	0.72	0.73	0.74	0.74	0.75	0.75	0.76	0.77
8	Und	Und	0.72	0.74	0.74	0.74	0.74	0.77	0.77	0.79
9	Und	Und	0.73	0.73	0.74	0.76	0.76	0.77	0.79	0.80
10	Und	Und	0.73	0.73	0.74	0.76	0.76	0.77	0.80	0.80
11	Und	Und	0.73	0.74	0.75	0.77	0.76	0.81	0.80	0.85
12	Und	Und	0.73	0.76	0.75	0.77	0.77	0.86	0.81	0.86
13	Und	Und	0.73	0.75	0.76	0.77	0.78	0.86	0.82	0.88
14	Und	Und	0.74	0.75	0.76	0.78	0.78	0.83	0.82	0.89
15	Und	Und	0.74	0.76	0.77	0.78	0.80	0.83	0.83	0.89

A.6. NSE values of $M3_Y$ for validation phase computed with different number of c and r_a

$M3_Y$ (validation)	r_a									
number of c	**0.05**	**0.10**	**0.15**	**0.20**	**0.25**	**0.30**	**0.35**	**0.40**	**0.45**	**0.50**
1	Und	Und	Und	VL	VL	VL	VL	VL	VL	VL
2	Und	Und	Und	VL	VL	VL	VL	VL	0.17	0.18
3	Und	Und	Und	VL	VL	0.09	0.15	0.24	0.27	0.27
4	Und	Und	Und	VL	0.00	0.12	0.20	0.24	0.27	0.28
5	Und	Und	VL	VL	0.24	0.23	0.23	0.25	0.24	0.28
6	Und	Und	0.10	0.23	0.25	0.26	0.24	0.24	0.21	0.28
7	Und	Und	0.14	0.25	0.27	0.26	0.24	0.17	0.20	0.48
8	Und	Und	0.15	0.24	0.25	0.25	0.22	0.22	0.42	0.26
9	Und	Und	0.25	0.28	0.25	0.18	0.27	0.21	0.21	0.53
10	Und	Und	0.25	0.27	0.24	0.15	0.26	0.42	0.18	VL
11	Und	Und	0.25	0.24	0.15	0.25	0.25	VL	0.17	VL
12	Und	Und	0.25	0.23	0.15	0.26	0.39	VL	VL	VL
13	Und	Und	0.25	0.15	0.17	0.10	0.40	VL	VL	VL
14	Und	Und	0.13	0.15	0.14	0.07	0.39	VL	VL	VL
15	Und	Und	0.27	0.18	0.28	0.08	0.08	0.36	VL	VL

A.7. NSE values of $M4_Y$ for training phase computed with different number of c and r_a

$M4_Y$ (training)	r_a									
number of c	**0.05**	**0.10**	**0.15**	**0.20**	**0.25**	**0.30**	**0.35**	**0.40**	**0.45**	**0.50**
1	Und	Und	Und	0.44	0.44	0.44	0.44	0.44	0.44	0.44
2	Und	Und	Und	0.45	0.45	0.47	0.68	0.72	0.75	0.76
3	Und	Und	Und	0.71	0.65	0.73	0.75	0.76	0.76	0.76
4	Und	Und	Und	0.72	0.76	0.76	0.75	0.77	0.76	0.77
5	Und	Und	Und	0.73	0.76	0.76	0.76	0.78	0.76	0.77
6	Und	Und	Und	0.76	0.76	0.77	0.76	0.78	0.77	0.79
7	Und	Und	Und	0.76	0.76	0.77	0.77	0.78	0.79	0.80
8	Und	Und	Und	0.76	0.77	0.77	0.78	0.78	0.79	0.80
9	Und	Und	Und	0.76	0.77	0.77	0.79	0.79	0.82	0.83
10	Und	Und	Und	0.77	0.77	0.78	0.80	0.80	0.82	0.84
11	Und	Und	Und	0.77	0.78	0.79	0.81	0.81	0.84	0.85
12	Und	Und	0.76	0.77	0.78	0.79	0.81	0.81	0.84	0.85
13	Und	Und	0.76	0.77	0.79	0.79	0.81	0.81	0.84	0.92
14	Und	Und	0.76	0.77	0.79	0.80	0.82	0.81	0.85	0.93
15	Und	Und	0.78	0.77	0.79	0.80	0.82	0.85	0.87	0.94

A.8. NSE values of $M4_Y$ for validation phase computed with different number of c and r_a

$M4_Y$ (validation)	r_a									
number of c	**0.05**	**0.10**	**0.15**	**0.20**	**0.25**	**0.30**	**0.35**	**0.40**	**0.45**	**0.50**
1	Und	Und	Und	0.11	0.11	0.11	0.11	0.11	0.11	0.11
2	Und	Und	Und	0.07	0.08	0.10	0.20	0.29	0.39	0.42
3	Und	Und	Und	0.28	0.12	0.31	0.40	0.44	0.43	0.45
4	Und	Und	Und	0.32	0.41	0.41	0.41	0.42	0.43	0.47
5	Und	Und	Und	0.31	0.42	0.42	0.49	0.42	0.44	0.43
6	Und	Und	Und	0.42	0.46	0.46	0.47	0.40	0.42	0.46
7	Und	Und	Und	0.48	0.46	0.46	0.45	0.40	0.35	0.41
8	Und	Und	Und	0.48	0.45	0.42	0.42	0.32	0.31	0.40
9	Und	Und	Und	0.48	0.45	0.42	0.33	0.32	0.48	0.24
10	Und	Und	Und	0.39	0.45	0.37	0.21	0.39	0.42	0.51
11	Und	Und	Und	0.45	0.42	0.31	0.31	0.47	0.01	0.56
12	Und	Und	0.48	0.46	0.39	0.30	0.28	0.47	0.01	0.59
13	Und	Und	0.47	0.46	0.27	0.23	0.21	0.46	0.01	0.18
14	Und	Und	0.47	0.46	0.27	0.22	0.32	0.48	VL	VL
15	Und	Und	0.41	0.40	VL	0.21	0.31	0.10	VL	VL

A.9. NSE values of $M5_Y$ for training phase computed with different number of c and r_a

$M5_Y$ (training)	r_a									
number of c	**0.05**	**0.10**	**0.15**	**0.20**	**0.25**	**0.30**	**0.35**	**0.40**	**0.45**	**0.50**
1	Und	Und	Und	Und	0.57	0.57	0.57	0.57	0.57	0.57
2	Und	Und	Und	0.58	0.59	0.60	0.61	0.74	0.75	0.76
3	Und	Und	Und	0.62	0.73	0.71	0.74	0.75	0.76	0.77
4	Und	Und	Und	0.68	0.75	0.76	0.76	0.76	0.76	0.77
5	Und	Und	Und	0.74	0.76	0.77	0.77	0.77	0.77	0.79
6	Und	Und	Und	0.76	0.76	0.77	0.77	0.78	0.77	0.79
7	Und	Und	Und	0.76	0.75	0.77	0.78	0.78	0.79	0.79
8	Und	Und	Und	0.77	0.78	0.77	0.78	0.78	0.79	0.80
9	Und	Und	Und	0.76	0.77	0.78	0.79	0.80	0.79	0.82
10	Und	Und	Und	0.76	0.77	0.78	0.80	0.80	0.82	0.87
11	Und	Und	Und	0.76	0.78	0.79	0.80	0.80	0.83	0.88
12	Und	Und	Und	0.76	0.78	0.80	0.80	0.83	0.83	0.88
13	Und	Und	Und	0.78	0.78	0.80	0.80	0.83	0.83	0.89
14	Und	Und	Und	0.77	0.79	0.80	0.80	0.83	0.88	0.91
15	Und	Und	0.77	0.77	0.79	0.80	0.82	0.89	0.89	0.91

A.10. NSE values of $M5_Y$ for validation phase computed with different number of c and r_a

$M5_Y$ (validation)	r_a									
number of c	**0.05**	**0.10**	**0.15**	**0.20**	**0.25**	**0.30**	**0.35**	**0.40**	**0.45**	**0.50**
1	Und	Und	Und	Und	0.48	0.48	0.48	0.48	0.48	0.48
2	Und	Und	Und	0.47	0.47	0.48	0.49	0.55	0.56	0.58
3	Und	Und	Und	0.46	0.54	0.44	0.56	0.57	0.58	0.56
4	Und	Und	Und	0.57	0.57	0.59	0.59	0.60	0.61	0.57
5	Und	Und	Und	0.54	0.57	0.57	0.59	0.58	0.57	0.49
6	Und	Und	Und	0.31	0.62	0.59	0.57	0.55	0.56	0.51
7	Und	Und	Und	0.37	0.62	0.61	0.56	0.55	0.49	0.51
8	Und	Und	Und	0.41	0.58	0.61	0.56	0.54	0.48	0.47
9	Und	Und	Und	0.62	0.60	0.56	0.52	0.50	0.45	0.57
10	Und	Und	Und	0.62	0.60	0.54	0.51	0.50	0.55	0.34
11	Und	Und	Und	0.62	0.55	0.45	0.49	0.52	0.61	VL
12	Und	Und	Und	0.63	0.50	0.42	0.38	0.57	0.60	VL
13	Und	Und	Und	0.58	0.53	0.41	0.40	0.55	0.61	VL
14	Und	Und	Und	0.60	0.48	0.45	0.40	0.55	0.41	VL
15	Und	Und	0.59	0.58	0.21	0.10	0.44	0.40	VL	VL

B. The results of the sub-models for Inanli Streamgage

B.1. NSE values of $M1_I$ for training phase computed with different number of c and r_a

$M1_I$ (training)	r_a									
number of c	**0.05**	**0.10**	**0.15**	**0.20**	**0.25**	**0.30**	**0.35**	**0.40**	**0.45**	**0.50**
1	Und	Und	0.42	0.42	0.42	0.42	0.42	0.42	0.42	0.42
2	Und	0.41	0.45	0.46	0.48	0.49	0.49	0.49	0.50	0.50
3	Und	0.49	0.50	0.50	0.50	0.52	0.60	0.64	0.64	0.68
4	Und	0.50	0.50	0.47	0.50	0.67	0.62	0.64	0.69	0.69
5	Und	0.47	0.51	0.56	0.62	0.67	0.70	0.66	0.70	0.73
6	Und	0.47	0.48	0.57	0.62	0.68	0.69	0.70	0.72	0.77
7	Und	0.51	0.50	0.57	0.64	0.71	0.69	0.72	RCC	0.78
8	Und	0.51	0.50	0.61	0.69	0.71	0.70	0.74	RCC	RCC
9	Und	0.49	0.50	0.63	0.70	0.72	0.78	0.79	RCC	RCC
10	Und	0.49	0.55	0.67	0.72	0.81	0.80	RCC	RCC	RCC
11	Und	0.49	0.55	0.67	0.72	0.81	0.83	RCC	RCC	RCC
12	Und	0.49	0.61	0.68	0.75	0.82	0.86	RCC	RCC	RCC
13	Und	0.49	0.62	0.69	0.75	0.83	0.87	RCC	RCC	RCC
14	Und	0.53	0.62	0.69	0.80	0.87	0.87	RCC	RCC	RCC
15	Und	0.54	0.64	0.71	0.81	0.87	RCC	RCC	RCC	RCC

B.2. NSE values of $M1_I$ for validation phase computed with different number of c and r_a

$M1_I$ (validation)	r_a									
number of c	**0.05**	**0.10**	**0.15**	**0.20**	**0.25**	**0.30**	**0.35**	**0.40**	**0.45**	**0.50**
1	Und	Und	0.61	0.61	0.61	0.61	0.61	0.61	0.61	0.61
2	Und	0.61	0.60	0.60	0.60	0.60	0.60	0.60	0.60	0.60
3	Und	0.60	0.60	0.60	0.60	0.58	0.57	0.58	0.59	0.60
4	Und	0.59	0.61	0.61	0.60	0.61	0.58	0.59	0.62	0.62
5	Und	0.60	0.60	0.57	0.58	0.61	0.60	0.59	0.64	0.67
6	Und	0.60	0.61	0.57	0.58	0.61	0.60	0.59	0.17	0.53
7	Und	0.60	0.60	0.57	0.58	0.60	0.61	0.61	RCC	0.55
8	Und	0.60	0.60	0.57	0.61	0.60	0.65	VL	RCC	RCC
9	Und	0.61	0.60	0.58	0.61	0.58	VL	0.53	RCC	RCC
10	Und	0.61	0.58	0.61	0.63	VL	VL	0.56	RCC	RCC
11	Und	0.61	0.58	0.61	0.63	VL	VL	0.59	RCC	RCC
12	Und	0.60	0.58	0.60	0.53	VL	VL	0.61	RCC	RCC
13	Und	0.60	0.58	0.60	0.63	VL	VL	0.63	RCC	RCC
14	Und	0.58	0.58	0.59	VL	VL	VL	0.64	RCC	RCC
15	Und	0.58	0.60	0.60	VL	VL	VL	0.65	RCC	RCC

B.3. NSE values of $M2_I$ for training phase computed with different number of c and r_a

$M2_I$ (training)	r_a									
number of c	**0.05**	**0.10**	**0.15**	**0.20**	**0.25**	**0.30**	**0.35**	**0.40**	**0.45**	**0.50**
1	Und	Und	0.48	0.48	0.48	0.48	0.48	0.48	0.48	0.48
2	Und	Und	0.48	0.52	0.52	0.53	0.54	0.56	0.57	0.57
3	Und	Und	0.52	0.52	0.56	0.57	0.57	0.56	0.57	0.57
4	Und	Und	0.52	0.53	0.60	0.58	0.60	0.58	0.58	0.60
5	Und	Und	0.55	0.56	0.60	0.59	0.62	0.69	0.62	0.64
6	Und	Und	0.56	0.56	0.62	0.59	0.76	0.71	0.75	0.77
7	Und	Und	0.56	0.60	0.63	0.67	0.76	0.71	0.75	0.79
8	Und	Und	0.56	0.61	0.63	0.68	0.75	0.76	0.75	0.79
9	Und	Und	0.56	0.61	0.68	0.69	0.75	0.76	0.79	0.85
10	Und	0.56	0.59	0.63	0.68	0.69	0.77	0.82	0.79	0.88
11	Und	0.56	0.61	0.63	0.70	0.78	0.79	0.87	RCC	RCC
12	Und	0.56	0.61	0.64	0.80	0.82	0.79	0.89	RCC	RCC
13	Und	0.56	0.63	0.65	0.80	0.82	0.80	0.91	RCC	RCC
14	Und	0.59	0.63	0.65	0.81	0.82	0.85	0.93	RCC	RCC
15	Und	0.59	0.63	0.65	0.82	0.80	0.89	0.94	RCC	RCC

B.4. NSE values of $M2_I$ for validation phase computed with different number of c and r_a

$M2_I$ (validation)	r_a									
number of c	**0.05**	**0.10**	**0.15**	**0.20**	**0.25**	**0.30**	**0.35**	**0.40**	**0.45**	**0.50**
1	Und	Und	0.59	0.59	0.59	0.59	0.59	0.59	0.59	0.59
2	Und	Und	0.59	0.59	0.59	0.59	0.59	0.58	0.58	0.57
3	Und	Und	0.59	0.59	0.58	0.56	0.55	0.58	0.57	0.56
4	Und	Und	0.59	0.59	0.54	0.53	0.51	0.52	0.50	0.51
5	Und	Und	0.59	0.58	0.54	0.56	0.53	0.58	0.54	0.51
6	Und	Und	0.58	0.58	0.53	0.56	0.55	0.43	0.56	0.52
7	Und	Und	0.58	0.54	0.50	0.55	0.55	0.43	0.45	0.51
8	Und	Und	0.58	0.57	0.50	0.57	0.48	0.49	0.45	0.44
9	Und	Und	0.58	0.52	0.52	0.53	0.47	0.37	VL	0.57
10	Und	0.59	0.55	0.51	0.52	0.53	0.46	VL	0.31	VL
11	Und	0.58	0.54	0.51	0.48	0.38	0.42	VL	RCC	VL/RCC
12	Und	0.58	0.53	0.51	0.34	0.39	0.34	VL	RCC	VL/RCC
13	Und	0.58	0.52	0.50	0.34	0.38	0.21	VL	RCC	VL/RCC
14	Und	0.56	0.52	0.50	0.37	0.36	VL	VL	RCC	VL/RCC
15	Und	0.56	0.50	0.50	0.38	0.37	VL	VL	RCC	VL/RCC

B.5. NSE values of $M3_I$ for training phase computed with different number of c and r_a

$M3_I$ (training)	r_a									
number of c	**0.05**	**0.10**	**0.15**	**0.20**	**0.25**	**0.30**	**0.35**	**0.40**	**0.45**	**0.50**
1	Und	Und	0.48	0.48	0.48	0.48	0.48	0.48	0.48	0.48
2	Und	Und	0.47	0.47	0.52	0.53	0.54	0.54	0.56	0.57
3	Und	Und	0.49	0.52	0.53	0.54	0.56	0.56	0.59	0.57
4	Und	Und	0.52	0.53	0.56	0.56	0.59	0.61	0.59	0.60
5	Und	Und	0.53	0.54	0.56	0.59	0.60	0.62	0.72	0.62
6	Und	Und	0.54	0.56	0.58	0.60	0.60	0.63	0.75	0.76
7	Und	Und	0.54	0.57	0.59	0.60	0.69	0.72	0.78	0.79
8	Und	Und	0.55	0.61	0.61	0.64	0.69	0.76	0.78	0.79
9	Und	Und	0.56	0.61	0.62	0.67	0.75	0.77	0.79	0.79
10	Und	Und	0.57	0.60	0.65	0.67	0.75	0.77	0.84	0.81
11	Und	Und	0.57	0.62	0.65	0.67	0.77	0.79	0.88	RCC
12	Und	Und	0.61	0.62	0.66	0.67	0.77	0.82	0.91	RCC
13	Und	Und	0.59	0.62	0.66	0.68	0.80	0.88	0.93	RCC
14	Und	Und	0.60	0.63	0.68	0.76	0.82	0.91	RCC	RCC
15	Und	Und	0.60	0.63	0.73	0.76	0.82	0.94	RCC	RCC

B.6. NSE values of $M3_I$ for validation phase computed with different number of c and r_a

$M3_I$ (validation)	r_a									
number of c	**0.05**	**0.10**	**0.15**	**0.20**	**0.25**	**0.30**	**0.35**	**0.40**	**0.45**	**0.50**
1	Und	Und	0.60	0.60	0.60	0.60	0.60	0.60	0.60	0.60
2	Und	Und	0.60	0.60	0.59	0.59	0.59	0.59	0.58	0.58
3	Und	Und	0.59	0.59	0.59	0.59	0.55	0.53	0.47	0.56
4	Und	Und	0.59	0.59	0.58	0.57	0.49	0.51	0.47	0.46
5	Und	Und	0.58	0.59	0.58	0.51	0.51	0.52	0.63	0.51
6	Und	Und	0.58	0.58	0.50	0.53	0.51	0.52	0.50	0.63
7	Und	Und	0.58	0.52	0.50	0.53	0.57	0.58	0.58	0.41
8	Und	Und	0.58	0.54	0.58	0.53	0.57	0.55	0.58	0.41
9	Und	Und	0.58	0.54	0.56	0.55	0.46	0.57	VL	0.41
10	Und	Und	0.52	0.50	0.50	0.55	0.52	0.61	VL	VL
11	Und	Und	0.52	0.48	0.50	0.55	0.50	0.53	VL	VL/RCC
12	Und	Und	0.54	0.48	0.49	0.55	0.50	0.40	VL	VL/RCC
13	Und	Und	0.49	0.48	0.49	0.55	0.46	VL	VL	VL/RCC
14	Und	Und	0.49	0.51	0.49	0.50	VL	VL	VL/RCC	VL/RCC
15	Und	Und	0.49	0.51	0.57	0.49	0.57	VL	VL/RCC	VL/RCC

B.7. NSE values of $M4_I$ for training phase computed with different number of c and r_a

$M4_I$ (training)	r_a									
number of c	**0.05**	**0.10**	**0.15**	**0.20**	**0.25**	**0.30**	**0.35**	**0.40**	**0.45**	**0.50**
1	Und	Und	0.62	0.62	0.62	0.62	0.62	0.62	0.62	0.62
2	Und	Und	0.62	0.62	0.63	0.64	0.64	0.64	0.65	0.66
3	Und	Und	0.63	0.63	0.65	0.65	0.66	0.66	0.66	0.66
4	Und	Und	0.63	0.63	0.65	0.66	0.67	0.67	0.66	0.66
5	Und	Und	0.66	0.68	0.65	0.67	0.67	0.68	0.69	0.68
6	Und	Und	0.66	0.65	0.67	0.68	0.67	0.69	0.77	0.77
7	Und	Und	0.65	0.66	0.68	0.69	0.73	0.74	0.79	0.77
8	Und	Und	0.65	0.66	0.68	0.69	0.73	0.75	0.86	0.76
9	Und	Und	0.65	0.66	0.68	0.70	0.73	0.80	0.90	0.80
10	Und	Und	0.65	0.68	0.68	0.71	0.79	0.84	0.92	0.85
11	Und	Und	0.66	0.69	0.68	0.76	0.80	0.87	0.93	0.89
12	Und	Und	0.66	0.68	0.68	0.76	0.80	0.88	0.93	0.90
13	Und	Und	0.67	0.68	0.68	0.78	0.81	0.90	0.94	0.92
14	Und	Und	0.69	0.69	0.69	0.83	0.85	0.95	0.96	0.94
15	Und	Und	0.69	0.69	0.75	0.83	0.86	0.95	0.97	RCC

B.8. NSE values of $M4_I$ for validation phase computed with different number of c and r_a

$M4_I$ (validation)	r_a									
number of c	**0.05**	**0.10**	**0.15**	**0.20**	**0.25**	**0.30**	**0.35**	**0.40**	**0.45**	**0.50**
1	Und	Und	0.53	0.53	0.53	0.53	0.53	0.53	0.53	0.53
2	Und	Und	0.53	0.53	0.52	0.52	0.52	0.52	0.52	0.52
3	Und	Und	0.52	0.52	0.53	0.53	0.53	0.53	0.53	0.52
4	Und	Und	0.52	0.52	0.53	0.52	0.52	0.52	0.53	0.51
5	Und	Und	0.52	0.52	0.53	0.52	0.52	0.51	0.51	0.51
6	Und	Und	0.52	0.53	0.53	0.53	0.52	0.51	0.55	0.56
7	Und	Und	0.52	0.52	0.52	0.52	0.54	0.56	0.52	0.56
8	Und	Und	0.52	0.52	0.53	0.52	0.56	0.59	0.38	0.48
9	Und	Und	0.53	0.52	0.52	0.52	0.55	0.46	VL	0.37
10	Und	Und	0.53	0.53	0.52	0.48	0.53	0.46	VL	0.34
11	Und	Und	0.52	0.53	0.52	0.51	0.51	0.06	VL	0.40
12	Und	Und	0.53	0.50	0.54	0.51	0.51	0.30	VL	0.35
13	Und	Und	0.52	0.50	0.54	0.42	0.52	0.34	VL	VL
14	Und	Und	0.53	0.51	0.51	0.28	0.56	VL	VL	VL
15	Und	Und	0.53	0.51	0.54	0.28	0.32	VL	VL	VL/RCC

B.9. NSE values of $M5_I$ for training phase computed with different number of c and r_a

$M5_I$ (training)	r_a									
number of c	**0.05**	**0.10**	**0.15**	**0.20**	**0.25**	**0.30**	**0.35**	**0.40**	**0.45**	**0.50**
1	Und	Und	0.59	0.59	0.59	0.59	0.59	0.59	0.59	0.59
2	Und	Und	0.60	0.60	0.61	0.62	0.63	0.63	0.63	0.63
3	Und	Und	0.60	0.61	0.64	0.65	0.65	0.65	0.66	0.68
4	Und	Und	0.61	0.63	0.64	0.65	0.71	0.72	0.67	0.72
5	Und	Und	0.61	0.65	0.64	0.68	0.71	0.72	0.74	0.76
6	Und	Und	0.62	0.65	0.64	0.69	0.71	0.72	0.78	0.79
7	Und	Und	0.62	0.64	0.65	0.70	0.71	0.72	0.80	RCC
8	Und	Und	0.62	0.64	0.71	0.73	0.79	0.77	0.84	RCC
9	Und	Und	0.64	0.67	0.71	0.73	0.80	0.79	0.87	RCC
10	Und	Und	0.65	0.67	0.72	0.78	0.81	0.81	0.90	RCC
11	Und	Und	0.65	0.70	0.72	0.84	0.83	0.86	RCC	RCC
12	Und	Und	0.65	0.70	0.74	0.84	0.87	0.88	RCC	RCC
13	Und	Und	0.65	0.71	0.74	0.84	0.91	0.89	RCC	RCC
14	Und	0.63	0.65	0.71	0.81	0.86	0.93	0.91	RCC	RCC
15	Und	0.63	0.65	0.71	0.83	0.90	0.94	0.92	RCC	RCC

B.10. NSE values of $M5_I$ for validation phase computed with different number of c and r_a

$M5_I$ (validation)	r_a									
number of c	**0.05**	**0.10**	**0.15**	**0.20**	**0.25**	**0.30**	**0.35**	**0.40**	**0.45**	**0.50**
1	Und	Und	0.53	0.53	0.53	0.53	0.53	0.53	0.53	0.53
2	Und	Und	0.52	0.52	0.52	0.52	0.52	0.52	0.52	0.52
3	Und	Und	0.52	0.52	0.53	0.53	0.52	0.53	0.54	0.54
4	Und	Und	0.52	0.52	0.53	0.53	0.56	0.57	0.53	0.56
5	Und	Und	0.52	0.53	0.53	0.54	0.56	0.57	0.57	0.46
6	Und	Und	0.52	0.53	0.53	0.54	0.56	0.57	0.55	0.49
7	Und	Und	0.51	0.52	0.54	0.54	0.56	0.58	0.28	RCC
8	Und	Und	0.51	0.52	0.56	0.56	0.50	0.50	VL	RCC
9	Und	Und	0.52	0.54	0.56	0.56	0.50	0.48	VL	RCC
10	Und	Und	0.51	0.54	0.59	0.24	0.51	0.32	0.14	RCC
11	Und	Und	0.52	0.56	0.59	0.43	0.31	VL	VL/RCC	RCC
12	Und	Und	0.53	0.56	0.59	0.31	VL	VL	VL/RCC	RCC
13	Und	Und	0.54	0.55	0.58	0.31	VL	VL	VL/RCC	RCC
14	Und	0.51	0.54	0.55	0.52	0.28	VL	0.02	VL/RCC	RCC
15	Und	0.51	0.54	0.58	0.40	VL	VL	VL	VL/RCC	RCC

C. The results of the sub-models for Luleburgaz Streamgage

C.1. NSE values of $M1_L$ for training phase computed with different number of c and r_a

$M1_L$ (training)	r_a									
number of c	**0.05**	**0.10**	**0.15**	**0.20**	**0.25**	**0.30**	**0.35**	**0.40**	**0.45**	**0.50**
1	Und	0.45	0.45	0.45	0.45	0.45	0.45	0.45	0.45	0.45
2	Und	0.46	0.47	0.47	0.48	0.48	0.48	0.49	0.49	0.49
3	Und	0.48	0.48	0.48	0.49	0.50	0.49	0.49	0.48	0.48
4	Und	0.48	0.48	0.49	0.49	0.49	0.49	0.49	0.48	0.48
5	Und	0.47	0.48	0.50	0.49	0.49	0.48	0.49	0.53	0.52
6	Und	0.47	0.49	0.50	0.49	0.51	0.48	0.49	0.53	0.61
7	Und	0.48	0.49	0.50	0.51	0.49	0.48	0.73	RCC	0.67
8	Und	0.48	0.49	0.50	0.48	0.73	0.73	0.75	RCC	RCC
9	Und	0.49	0.50	0.50	0.48	0.74	0.72	0.81	RCC	RCC
10	Und	0.49	0.50	0.51	0.48	0.75	0.75	RCC	RCC	RCC
11	Und	0.49	0.50	0.51	0.63	0.78	0.79	RCC	RCC	RCC
12	Und	0.49	0.50	0.51	0.63	0.78	0.89	RCC	RCC	RCC
13	Und	0.49	0.50	0.51	0.75	0.84	0.91	RCC	RCC	RCC
14	Und	0.51	0.50	0.51	0.80	0.88	0.90	RCC	RCC	RCC
15	Und	0.51	0.51	0.48	0.86	0.88	RCC	RCC	RCC	RCC

C.2. NSE values of $M1_L$ for validation phase computed with different number of c and r_a

$M1_L$ (validation)	r_a									
number of c	**0.05**	**0.10**	**0.15**	**0.20**	**0.25**	**0.30**	**0.35**	**0.40**	**0.45**	**0.50**
1	Und	0.68	0.68	0.68	0.68	0.68	0.68	0.68	0.68	0.68
2	Und	0.71	0.74	0.73	0.75	0.76	0.77	0.78	0.78	0.78
3	Und	0.66	0.73	0.73	0.77	0.80	0.80	0.80	0.80	0.81
4	Und	0.64	0.73	0.77	0.77	0.80	0.78	0.81	0.79	0.76
5	Und	0.74	0.73	0.80	0.79	0.81	0.79	0.76	0.79	0.78
6	Und	0.74	0.76	0.76	0.78	0.77	0.78	0.77	0.77	0.78
7	Und	0.74	0.77	0.76	0.76	0.82	0.79	0.35	RCC	0.78
8	Und	0.74	0.76	0.75	0.77	0.39	0.41	0.45	RCC	RCC
9	Und	0.75	0.76	0.76	0.77	0.40	0.58	0.63	RCC	RCC
10	Und	0.75	0.74	0.76	0.72	0.16	0.60	RCC	RCC	RCC
11	Und	0.75	0.74	0.76	0.51	0.02	0.64	RCC	RCC	RCC
12	Und	0.76	0.75	0.73	0.59	0.15	0.78	RCC	RCC	RCC
13	Und	0.77	0.75	0.74	0.46	0.53	VL	RCC	RCC	RCC
14	Und	0.78	0.75	0.76	0.27	VL	VL	RCC	RCC	RCC
15	Und	0.75	0.77	0.78	0.31	VL	VL/RCC	RCC	RCC	RCC

C.3. NSE values of $M2_L$ for training phase computed with different number of c and r_a

$M2_L$ (training)	r_a									
number of c	**0.05**	**0.10**	**0.15**	**0.20**	**0.25**	**0.30**	**0.35**	**0.40**	**0.45**	**0.50**
1	Und	Und	0.52	0.52	0.52	0.52	0.52	0.52	0.52	0.52
2	Und	Und	0.55	0.56	0.56	0.57	0.57	0.59	0.59	0.60
3	Und	Und	0.56	0.56	0.59	0.59	0.59	0.59	0.59	0.59
4	Und	Und	0.56	0.57	0.59	0.60	0.61	0.59	0.61	0.61
5	Und	Und	0.57	0.59	0.59	0.60	0.61	0.62	0.61	0.62
6	Und	Und	0.59	0.59	0.60	0.60	0.66	0.64	0.67	0.67
7	Und	Und	0.59	0.58	0.60	0.61	0.66	0.64	0.69	0.73
8	Und	Und	0.59	0.60	0.60	0.61	0.68	0.74	0.76	0.76
9	Und	Und	0.59	0.59	0.62	0.62	0.68	0.80	0.75	0.80
10	Und	Und	0.59	0.59	0.62	0.62	0.68	0.79	0.75	0.95
11	Und	0.59	0.59	0.59	0.62	0.73	0.73	0.79	RCC	RCC
12	Und	0.59	0.60	0.59	0.62	0.72	0.79	0.91	RCC	RCC
13	Und	0.59	0.60	0.60	0.72	0.72	0.87	0.93	RCC	RCC
14	Und	0.59	0.60	0.60	0.72	0.82	0.87	0.94	RCC	RCC
15	Und	0.59	0.60	0.60	0.72	0.85	0.88	0.96	RCC	RCC

C.4. NSE values of $M2_L$ for validation phase computed with different number of c and r_a

$M2_L$ (validation)	r_a									
number of c	**0.05**	**0.10**	**0.15**	**0.20**	**0.25**	**0.30**	**0.35**	**0.40**	**0.45**	**0.50**
1	Und	Und	0.67	0.67	0.67	0.67	0.67	0.67	0.67	0.67
2	Und	Und	0.54	0.69	0.69	0.69	0.69	0.67	0.67	0.66
3	Und	Und	0.68	0.69	0.66	0.65	0.64	0.66	0.66	0.66
4	Und	Und	0.68	0.68	0.62	0.56	0.52	0.58	0.53	0.51
5	Und	Und	0.68	0.67	0.62	0.52	0.49	0.44	0.49	0.49
6	Und	Und	0.66	0.67	0.59	0.52	0.40	0.44	0.36	0.40
7	Und	Und	0.66	0.64	0.52	0.45	0.39	0.44	0.34	0.42
8	Und	Und	0.66	0.58	0.55	0.43	0.35	0.43	0.31	0.62
9	Und	Und	0.66	0.54	0.49	0.46	0.35	0.40	0.31	0.53
10	Und	Und	0.63	0.54	0.49	0.46	0.35	0.04	VL	0.31
11	Und	0.67	0.59	0.57	0.49	0.42	0.45	0.13	RCC	RCC
12	Und	0.68	0.57	0.57	0.49	0.42	0.16	0.20	RCC	RCC
13	Und	0.69	0.57	0.53	0.42	0.43	0.16	VL	RCC	RCC
14	Und	0.68	0.60	0.53	0.43	0.44	VL	VL	RCC	VL/RCC
15	Und	0.68	0.58	0.53	0.42	0.44	VL	VL	RCC	VL/RCC

C.5. NSE values of $M3_L$ for training phase computed with different number of c and r_a

$M3_L$ (training)	r_a									
number of c	**0.05**	**0.10**	**0.15**	**0.20**	**0.25**	**0.30**	**0.35**	**0.40**	**0.45**	**0.50**
1	Und	Und	0.52	0.52	0.52	0.52	0.52	0.52	0.52	0.52
2	Und	Und	0.55	0.57	0.57	0.57	0.57	0.58	0.61	0.61
3	Und	Und	0.56	0.57	0.61	0.62	0.62	0.63	0.61	0.62
4	Und	Und	0.57	0.57	0.64	0.64	0.63	0.64	0.64	0.64
5	Und	Und	0.57	0.61	0.64	0.64	0.64	0.64	0.65	0.65
6	Und	Und	0.57	0.61	0.63	0.65	0.64	0.64	0.72	0.67
7	Und	Und	0.59	0.63	0.64	0.65	0.65	0.79	0.72	0.72
8	Und	Und	0.59	0.63	0.64	0.64	0.67	0.79	0.80	0.79
9	Und	Und	0.60	0.64	0.64	0.66	0.67	0.81	0.79	0.90
10	Und	Und	0.62	0.64	0.66	0.66	0.71	0.84	0.88	0.90
11	Und	Und	0.63	0.64	0.66	0.67	0.71	0.92	0.93	0.95
12	Und	Und	0.64	0.64	0.66	0.77	0.72	0.92	0.93	RCC
13	Und	Und	0.64	0.63	0.66	0.81	0.86	0.95	0.96	RCC
14	Und	Und	0.64	0.63	0.66	0.89	0.90	0.95	0.98	RCC
15	Und	Und	0.64	0.63	0.66	0.90	0.89	0.98	0.99	RCC

C.6. NSE values of $M3_L$ for validation phase computed with different number of c and r_a

$M3_L$ (validation)	r_a									
number of c	**0.05**	**0.10**	**0.15**	**0.20**	**0.25**	**0.30**	**0.35**	**0.40**	**0.45**	**0.50**
1	Und	Und	0.55	0.55	0.55	0.55	0.55	0.55	0.55	0.55
2	Und	Und	0.60	0.54	0.54	0.54	0.54	0.54	0.52	0.52
3	Und	Und	0.54	0.54	0.52	0.47	0.48	0.46	0.52	0.51
4	Und	Und	0.54	0.54	0.46	0.45	0.47	0.44	0.41	0.42
5	Und	Und	0.54	0.52	0.46	0.43	0.37	0.42	0.45	0.44
6	Und	Und	0.48	0.52	0.38	0.44	0.41	0.43	0.43	0.48
7	Und	Und	0.53	0.50	0.41	0.45	0.49	0.36	0.43	0.21
8	Und	Und	0.53	0.50	0.45	0.46	0.38	0.46	0.46	0.59
9	Und	Und	0.53	0.41	0.45	0.45	0.38	0.16	0.25	VL
10	Und	Und	0.49	0.41	0.45	0.45	0.27	0.10	VL	VL
11	Und	Und	0.50	0.44	0.44	0.47	0.27	0.33	VL	VL
12	Und	Und	0.43	0.45	0.44	0.47	0.26	0.35	VL	VL/RCC
13	Und	Und	0.42	0.45	0.44	0.35	0.32	0.25	VL	VL/RCC
14	Und	Und	0.42	0.45	0.43	0.39	VL	0.36	VL	VL/RCC
15	Und	Und	0.43	0.45	0.43	0.36	VL	VL	VL	VL/RCC

C.7. NSE values of $M4_L$ for training phase computed with different number of c and r_a

$M4_L$ (training)	r_a									
number of c	**0.05**	**0.10**	**0.15**	**0.20**	**0.25**	**0.30**	**0.35**	**0.40**	**0.45**	**0.50**
1	Und	Und	0.53	0.53	0.53	0.53	0.53	0.53	0.53	0.53
2	Und	Und	0.54	0.54	0.57	0.58	0.58	0.58	0.59	0.61
3	Und	Und	0.55	0.57	0.57	0.58	0.62	0.62	0.62	0.61
4	Und	Und	0.57	0.57	0.61	0.62	0.62	0.64	0.62	0.64
5	Und	Und	0.58	0.58	0.61	0.62	0.65	0.64	0.65	0.64
6	Und	Und	0.58	0.59	0.62	0.64	0.65	0.64	0.67	0.67
7	Und	Und	0.59	0.61	0.62	0.64	0.64	0.65	0.67	0.79
8	Und	Und	0.59	0.61	0.64	0.64	0.65	0.65	0.73	0.85
9	Und	Und	0.61	0.62	0.64	0.64	0.65	0.67	0.84	0.90
10	Und	Und	0.61	0.63	0.65	0.64	0.65	0.82	0.94	0.91
11	Und	Und	0.62	0.64	0.65	0.65	0.66	0.90	0.96	0.94
12	Und	Und	0.62	0.64	0.65	0.65	0.66	0.91	0.98	0.94
13	Und	Und	0.62	0.64	0.65	0.65	0.66	0.96	0.99	0.97
14	Und	Und	0.63	0.65	0.64	0.65	0.82	0.96	0.99	0.97
15	Und	Und	0.64	0.65	0.64	0.67	0.83	0.96	0.99	0.98

C.8. NSE values of $M4_L$ for validation phase computed with different number of c and r_a

$M4_L$ (validation)	r_a									
number of c	**0.05**	**0.10**	**0.15**	**0.20**	**0.25**	**0.30**	**0.35**	**0.40**	**0.45**	**0.50**
1	Und	Und	0.57	0.57	0.57	0.57	0.57	0.57	0.57	0.57
2	Und	Und	0.59	0.59	0.56	0.56	0.56	0.56	0.55	0.53
3	Und	Und	0.59	0.56	0.56	0.56	0.51	0.50	0.49	0.52
4	Und	Und	0.56	0.56	0.53	0.52	0.50	0.37	0.50	0.38
5	Und	Und	0.54	0.54	0.53	0.51	0.32	0.28	0.38	0.33
6	Und	Und	0.54	0.54	0.50	0.38	0.32	0.28	0.39	0.40
7	Und	Und	0.55	0.52	0.50	0.37	0.39	0.42	0.41	VL
8	Und	Und	0.56	0.52	0.42	0.38	0.47	0.46	VL	VL
9	Und	Und	0.53	0.49	0.41	0.39	0.46	0.37	0.03	VL
10	Und	Und	0.53	0.47	0.42	0.40	0.46	0.48	VL	VL
11	Und	Und	0.49	0.40	0.42	0.45	0.49	VL	VL	VL
12	Und	Und	0.50	0.40	0.42	0.45	0.49	VL	VL	VL
13	Und	Und	0.50	0.44	0.41	0.45	0.49	VL	VL	VL
14	Und	Und	0.44	0.44	0.44	0.44	0.49	VL	VL	VL
15	Und	Und	0.41	0.44	0.47	0.45	VL	VL	VL	VL

D. The results of the sub-models for Hayrabolu Streamgage

D.1. NSE values of $M1_H$ for training phase computed with different number of c and r_a

$M1_H$ (training)	r_a									
number of c	**0.05**	**0.10**	**0.15**	**0.20**	**0.25**	**0.30**	**0.35**	**0.40**	**0.45**	**0.50**
1	Und	0.60	0.60	0.60	0.60	0.60	0.60	0.60	0.60	0.60
2	Und	0.62	0.64	0.60	0.60	0.61	0.62	0.62	0.62	0.63
3	Und	0.59	0.60	0.60	0.65	0.66	0.67	0.67	0.68	0.68
4	Und	0.59	0.60	0.61	0.65	0.68	0.68	0.67	0.68	0.68
5	Und	0.63	0.60	0.63	0.65	0.68	0.69	0.69	0.70	0.71
6	Und	0.63	0.61	0.66	0.66	0.69	0.69	0.70	0.72	0.72
7	Und	0.64	0.65	0.66	0.68	0.71	0.70	0.71	RCC	0.74
8	Und	0.64	0.65	0.62	0.70	0.72	0.71	0.73	RCC	RCC
9	Und	0.60	0.65	0.63	0.70	0.72	0.73	0.74	RCC	RCC
10	Und	0.60	0.66	0.70	0.71	0.74	0.74	RCC	RCC	RCC
11	Und	0.60	0.66	0.70	0.71	0.75	0.74	RCC	RCC	RCC
12	Und	0.63	0.67	0.71	0.73	0.75	0.74	RCC	RCC	RCC
13	Und	0.63	0.67	0.72	0.72	0.75	0.75	RCC	RCC	RCC
14	Und	0.67	0.67	0.72	0.74	0.75	0.75	RCC	RCC	RCC
15	Und	0.67	0.65	0.73	0.75	0.76	RCC	RCC	RCC	RCC

D.2. NSE values of $M1_H$ for validation phase computed with different number of c and r_a

$M1_H$ (validation)	r_a									
number of c	**0.05**	**0.10**	**0.15**	**0.20**	**0.25**	**0.30**	**0.35**	**0.40**	**0.45**	**0.50**
1	Und	0.30	0.30	0.30	0.30	0.30	0.30	0.30	0.30	0.30
2	Und	0.32	0.27	0.32	0.32	0.32	0.32	0.32	0.32	0.32
3	Und	0.32	0.32	0.32	0.33	0.34	0.37	0.39	0.39	0.40
4	Und	0.32	0.32	0.32	0.33	0.40	0.40	0.40	0.40	0.38
5	Und	0.32	0.32	0.34	0.38	0.40	0.40	0.40	0.37	0.34
6	Und	0.32	0.32	0.35	0.38	0.44	0.40	0.40	0.34	0.34
7	Und	0.32	0.33	0.35	0.42	0.35	0.36	0.39	RCC	0.29
8	Und	0.32	0.32	0.39	0.35	0.34	0.38	0.35	RCC	RCC
9	Und	0.32	0.32	0.39	0.35	0.43	0.34	0.35	RCC	RCC
10	Und	0.32	0.37	0.37	0.35	0.37	0.36	RCC	RCC	RCC
11	Und	0.32	0.36	0.37	0.35	0.42	VL	RCC	RCC	RCC
12	Und	0.32	0.35	0.38	0.36	0.41	VL	RCC	RCC	RCC
13	Und	0.32	0.36	0.37	0.37	VL	VL	RCC	RCC	RCC
14	Und	0.36	0.36	0.37	0.35	VL	VL	RCC	RCC	RCC
15	Und	0.36	0.39	0.36	0.31	VL	VL/RCC	RCC	RCC	RCC

D.3. NSE values of $M2_H$ for training phase computed with different number of c and r_a

$M2_H$ (training)	r_a									
number of c	**0.05**	**0.10**	**0.15**	**0.20**	**0.25**	**0.30**	**0.35**	**0.40**	**0.45**	**0.50**
1	Und	Und	0.67	0.67	0.67	0.67	0.67	0.67	0.67	0.67
2	Und	Und	0.70	0.69	0.69	0.69	0.69	0.68	0.68	0.68
3	Und	Und	0.68	0.69	0.65	0.63	0.62	0.68	0.65	0.65
4	Und	Und	0.68	0.68	0.72	0.74	0.74	0.73	0.76	0.77
5	Und	Und	0.68	0.63	0.72	0.73	0.74	0.79	0.72	0.77
6	Und	Und	0.65	0.63	0.68	0.73	0.81	0.80	0.79	0.80
7	Und	Und	0.65	0.71	0.74	0.79	0.81	0.80	0.80	0.80
8	Und	Und	0.65	0.72	0.74	0.80	0.81	0.82	0.80	0.82
9	Und	Und	0.64	0.73	0.80	0.81	0.81	0.82	0.80	0.82
10	Und	0.66	0.65	0.73	0.80	0.81	0.81	0.84	0.84	0.85
11	Und	0.65	0.72	0.73	0.81	0.83	0.82	0.85	RCC	RCC
12	Und	0.65	0.72	0.74	0.83	0.84	0.84	0.85	RCC	RCC
13	Und	0.65	0.73	0.75	0.83	0.84	0.84	0.86	RCC	RCC
14	Und	0.65	0.73	0.75	0.83	0.84	0.85	0.88	RCC	RCC
15	Und	0.65	0.73	0.75	0.83	0.84	0.85	0.89	RCC	RCC

D.4. NSE values of $M2_H$ for validation phase computed with different number of c and r_a

$M2_H$ (validation)	r_a									
number of c	**0.05**	**0.10**	**0.15**	**0.20**	**0.25**	**0.30**	**0.35**	**0.40**	**0.45**	**0.50**
1	Und	Und	0.33	0.33	0.33	0.33	0.33	0.33	0.33	0.33
2	Und	Und	0.35	0.36	0.36	0.37	0.37	0.38	0.39	0.39
3	Und	Und	0.37	0.36	0.38	0.39	0.39	0.38	0.39	0.39
4	Und	Und	0.37	0.37	0.41	0.42	0.42	0.41	0.40	0.41
5	Und	Und	0.37	0.38	0.41	0.39	0.37	0.45	0.38	0.48
6	Und	Und	0.38	0.38	0.40	0.39	0.36	0.43	0.35	0.45
7	Und	Und	0.38	0.40	0.40	0.44	0.36	0.43	0.43	0.47
8	Und	Und	0.38	0.34	0.40	0.45	0.42	0.47	0.42	0.50
9	Und	Und	0.38	0.40	0.43	0.43	0.42	0.50	0.48	VL
10	Und	0.37	0.37	0.42	0.43	0.42	0.39	0.47	0.44	VL
11	Und	0.37	0.37	0.41	0.44	0.39	0.48	VL	RCC	VL/RCC
12	Und	0.37	0.40	0.43	0.40	0.51	0.49	VL	RCC	VL/RCC
13	Und	0.37	0.40	0.43	0.40	0.56	0.44	VL	RCC	VL/RCC
14	Und	0.36	0.40	0.43	0.38	0.51	0.42	VL	RCC	VL/RCC
15	Und	0.36	0.40	0.43	0.39	0.47	VL	VL	RCC	VL/RCC

D.5. NSE values of $M4_H$ for training phase computed with different number of c and r_a

$M4_H$ (training)	r_a									
number of c	**0.05**	**0.10**	**0.15**	**0.20**	**0.25**	**0.30**	**0.35**	**0.40**	**0.45**	**0.50**
1	Und	Und	0.69	0.69	0.69	0.69	0.69	0.69	0.69	0.69
2	Und	Und	0.67	0.60	0.60	0.61	0.60	0.61	0.62	0.63
3	Und	Und	0.62	0.60	0.60	0.61	0.59	0.59	0.65	0.60
4	Und	Und	0.62	0.59	0.68	0.66	0.72	0.74	0.69	0.77
5	Und	Und	0.61	0.58	0.68	0.73	0.75	0.79	0.80	0.79
6	Und	Und	0.62	0.57	0.61	0.75	0.77	0.83	0.80	0.83
7	Und	Und	0.63	0.61	0.77	0.75	0.83	0.84	0.82	0.84
8	Und	Und	0.56	0.61	0.77	0.80	0.84	0.84	0.82	0.86
9	Und	Und	0.56	0.67	0.77	0.80	0.84	0.86	0.85	0.87
10	Und	0.37	0.57	0.70	0.77	0.83	0.85	0.87	0.85	0.88
11	Und	0.37	0.61	0.72	0.77	0.84	0.85	0.89	0.87	0.89
12	Und	0.37	0.63	0.74	0.82	0.85	0.88	0.89	0.89	0.90
13	Und	0.37	0.69	0.74	0.83	0.86	0.89	0.90	0.89	0.90
14	Und	0.36	0.72	0.74	0.83	0.87	0.89	0.92	0.91	0.92
15	Und	0.36	0.72	0.76	0.83	0.88	0.90	0.93	0.91	0.93

D.6. NSE values of $M4_H$ for validation phase computed with different number of c and r_a

$M4_H$ (validation)	r_a									
number of c	**0.05**	**0.10**	**0.15**	**0.20**	**0.25**	**0.30**	**0.35**	**0.40**	**0.45**	**0.50**
1	Und	Und	0.40	0.40	0.40	0.40	0.40	0.40	0.40	0.40
2	Und	Und	0.42	0.44	0.45	0.45	0.45	0.45	0.45	0.45
3	Und	Und	0.44	0.44	0.45	0.44	0.45	0.45	0.44	0.45
4	Und	Und	0.44	0.44	0.45	0.41	0.47	0.48	0.44	0.48
5	Und	Und	0.44	0.44	0.45	0.41	0.43	0.46	0.51	0.51
6	Und	Und	0.44	0.44	0.37	0.47	0.45	0.44	0.49	0.48
7	Und	Und	0.44	0.43	0.44	0.46	0.45	0.43	0.49	0.50
8	Und	Und	0.44	0.43	0.42	0.49	0.46	0.47	0.45	0.45
9	Und	Und	0.44	0.39	0.42	0.49	0.46	0.42	0.46	0.48
10	Und	0.37	0.44	0.39	0.42	0.46	0.44	0.48	0.50	0.41
11	Und	0.37	0.42	0.40	0.43	0.46	0.42	0.45	VL	0.32
12	Und	0.37	0.42	0.41	0.42	0.47	0.45	0.22	VL	0.26
13	Und	0.37	0.38	0.41	0.43	0.48	0.49	VL	0.44	VL
14	Und	0.36	0.43	0.41	0.44	0.46	0.47	VL	VL	VL
15	Und	0.36	0.41	0.42	0.44	0.49	VL	VL	VL	VL

D.7. NSE values of $M5_H$ for training phase computed with different number of c and r_a

$M5_H$ (training)	r_a									
number of c	**0.05**	**0.10**	**0.15**	**0.20**	**0.25**	**0.30**	**0.35**	**0.40**	**0.45**	**0.50**
1	Und	Und	0.66	0.66	0.66	0.66	0.66	0.66	0.66	0.66
2	Und	Und	0.54	0.48	0.47	0.45	0.44	0.41	0.42	0.43
3	Und	Und	0.46	0.46	0.32	0.30	0.35	0.68	0.73	0.76
4	Und	Und	0.44	0.43	0.60	0.68	0.74	0.68	0.72	0.76
5	Und	Und	0.45	0.29	0.60	0.70	0.77	0.79	0.73	0.79
6	Und	Und	0.46	0.28	0.55	0.78	0.82	0.83	0.82	0.81
7	Und	Und	0.35	0.48	0.72	0.81	0.82	0.84	0.82	0.81
8	Und	Und	0.37	0.62	0.72	0.81	0.83	0.84	0.82	0.82
9	Und	Und	0.41	0.63	0.72	0.81	0.84	0.85	0.84	0.82
10	Und	Und	0.41	0.69	0.81	0.82	0.85	0.86	0.87	0.85
11	Und	Und	0.59	0.69	0.81	0.84	0.85	0.86	0.87	RCC
12	Und	Und	0.61	0.69	0.81	0.84	0.87	0.86	0.89	RCC
13	Und	0.34	0.61	0.70	0.82	0.84	0.87	0.88	0.90	RCC
14	Und	0.40	0.66	0.70	0.83	0.85	0.89	0.88	0.90	RCC
15	Und	0.40	0.67	0.65	0.83	0.85	0.90	0.90	0.90	RCC

D.8. NSE values of $M5_H$ for validation phase computed with different number of c and r_a

$M5_H$ (validation)	r_a									
number of c	**0.05**	**0.10**	**0.15**	**0.20**	**0.25**	**0.30**	**0.35**	**0.40**	**0.45**	**0.50**
1	Und	Und	0.38	0.38	0.38	0.38	0.38	0.38	0.38	0.38
2	Und	Und	0.41	0.41	0.42	0.42	0.42	0.42	0.43	0.43
3	Und	Und	0.41	0.42	0.42	0.42	0.42	0.42	0.42	0.44
4	Und	Und	0.42	0.42	0.42	0.43	0.44	0.43	0.43	0.46
5	Und	Und	0.42	0.42	0.42	0.39	0.45	0.47	0.43	0.53
6	Und	Und	0.42	0.42	0.40	0.41	0.46	0.46	0.45	0.53
7	Und	Und	0.42	0.40	0.46	0.46	0.45	0.48	0.38	0.54
8	Und	Und	0.42	0.39	0.45	0.46	0.44	0.49	0.39	0.49
9	Und	Und	0.41	0.40	0.45	0.47	0.44	0.41	0.38	0.53
10	Und	Und	0.41	0.40	0.44	0.44	0.44	VL	0.40	0.53
11	Und	Und	0.37	0.40	0.44	0.43	0.44	VL	0.30	RCC
12	Und	Und	0.37	0.39	0.44	0.39	0.35	VL	VL	RCC
13	Und	0.41	0.37	0.40	0.43	0.42	0.34	VL	VL	RCC
14	Und	0.40	0.40	0.40	0.44	0.40	0.21	VL	VL	RCC
15	Und	0.40	0.44	0.44	0.44	0.40	VL	VL	VL	RCC